

# **THE IMMOBILISATION OF ORGANIC WASTE BY GEOPOLYMERISATION**

by

**CHARLENE GOKHALE**

Thesis submitted in partial fulfilment of the requirements for the  
degree of

**MASTER OF SCIENCE IN ENGINEERING**



in the department of Chemical Engineering at the University of  
Stellenbosch

Supervisors: Prof. L. Lorenzen and Prof. JSJ van Deventer

Stellenbosch, December 2001

# DECLARATION

I, the undersigned, hereby declare that the work contained in this thesis is my own work and has not been submitted previously in its entirety or in part for a degree at any university.

**C. Gokhale:**

**Date:**

# SYNOPSIS

In excess of  $24 \times 10^6$  tons (1997, Eskom) of coal-derived fly ash is produced annually in South Africa for the production of electric power. A large quantity of this ash is disposed of as a solid waste in landfills, thus posing a serious environmental problem. Due to the shortage of landfill sites, new ways of utilising fly ash are needed. Recently several authors have shown that various combustion fly ashes can be converted into zeolites to obtain industrial products with applicability in environmental management. Geopolymerisation has emerged during the last few years as a possible solution to some waste stabilisation and solidification problems.

Phenolic compounds have been shown to be toxic to soil microorganisms at the parts-per-million level. Indeed several of the organic compounds classified by the U.S. Environmental Protection Agency as priority pollutants, are phenols. Immobilisation of phenols by adsorption on zeolites and encapsulation in a geopolymer appears to be a promising solution to this problem.

This thesis reports a technique for the production of a low-silica sodium zeolitic material from fly ash (zeolite NaP1), and its application for the stabilisation of phenols by adsorption and subsequent encapsulation in a geopolymer matrix. A commercial zeolite, clinoptilolite was also utilised as an adsorbent. Due to their uniform pore sizes and large surface areas, zeolitic materials are suitable for ion exchange and adsorption of certain organic substances. Adsorption data show that the commercial zeolite, clinoptilolite was an effective adsorbent for organics. Adsorption data showed that between 51.2ppm and 74.3ppm of chlorophenol or between 15.4ppm and 32.5ppm of phenol could be adsorbed. Physical encapsulation of the coated zeolite loaded with organic within a geopolymeric matrix increased the compressive strength of the matrix from 28.80 kN to 40.79 kN. Leaching data for the various geopolymer matrices with encapsulated and loaded zeolites show no organics being leached from the system at a detection level of 2ppm. According to the SABS these would have been acceptable organic concentrations within a waste water stream.

In utilising waste materials (fly ash and organic waste) and their reactive properties, it is now possible to create various geopolymers that are not only strong enough to be used as construction/building materials, but are also effective immobilisation systems for organic waste containment.

# OPSOMMING

Meer as  $24 \times 10^6$  tons (1997, Eskom) vlieg-as word jaarliks deur die verbranding van steenkool vir die produksie van elektrisiteit geproduseer. Dié as, wat tans in groot hoeveelhede as soliede afval in vaste-afval stortingsterreine gestort word, word gesien as 'n groeiende omgewingsprobleem.

'n Tekort aan geskikte stortingsterreine maak die ontwikkeling van nuwe gebruike vir die vlieg-as dringend nodsaaklik. Geopolimerisasie van vlieg-as materiale, 'n proses wat die laaste paar jaar ontwikkel is, blyk 'n potensiële oplossing te wees vir sommige afval stabilisering en solidifikasie toepassings.

Daar is bewyse dat fenoliese verbindings, selfs op 'n dele per miljoene (dpm) vlak, toksies is vir grondorganismes. Verskeie van die komponente wat deur die Amerikaanse Omgewingsbeskermingsagentskap (US EPA) as prioritats kontaminants geklassifiseer is, is ondermeer fenole. Die huidige werk ondersoek die adsorpsie van fenol op zeoliet NaPl en clinoptiloliet, gevolg deur fisiese omsluiting deur geopolimerisasie.

Verskeie outeurs het onlangs verwys na die omsetting van verskeie verbrandings vlieg-asse na zeoliete om bruikbare industriële produkte (vir gebruik in die omgewingsveld) te vorm. Die tesis rapporteer 'n metode vir die produksie van 'n lae silika natrium zeolitiese materiaal (zeoliet NaPl) uit vlieg-as en die gebruik daarvan in die stabilisering van fenole. 'n Kommersiële beskikbare zeoliet, clinoptiloliet, is ook gebruik as adsorbent. Uniforme porie groottes en hoë oppervlak areas maak zeolitiese materiale geskik vir ionuitruiling, asook die adsorpsie van verskeie organiese verbindings. Deur die fisiese omsluiting van die zeolitiese materiaal binne 'n geopolimeer matriks, kan materiale met beduidend hoë druksterktes, geproduseer word. Adsorpsie data het getoon data die kommersiële zeoliet, clinoptiloliet, 'n effektiewe adsorbent vir organiese stowwe is. Adsorpsie waardes het gewissel tussen 51.2dpm tot 74.3dpm vir chlorofenol en 15.4dpm tot 32.5dpm vir fenol. Fisiese enkalsulering van die behandelde zeoliet (coated fzeo) binne 'n geopolimeer matriks

het die saamdrukbaarheidsterkte van die betrokke matriks verhoog van 28.80 kN to 40.79 kN. Logingsdata verkry vir die onderskeie geopolimeer matrikse het getoon dat geen van die organiese stowwe uit dié matrikse vrygestel word nie. Indien die organiese stowwe wel vrygestel sou word, sou die waterfase konsentrasie onder 2 dpm, binne die aanvaarbare spesifikasie vir uitvloeisels volgens die SABS standard, gewees het.

Verskeie geopolimere, wat nie slegs sterk genoeg is om as konstruksie materiale te dien nie, maar addisioneel effektief as immobilisasie medium dien, kan dus uit die reaktiewe eienskappe van afval materiale (vlieg-as en organiese afval) vervaardig word.

# ACKNOWLEDGMENTS

To be able to produce anything of this magnitude, help from various people was essential. To show my sincere gratitude to all those who have helped me accomplish this momentous feat, a special thanks to the following:

**My supervisors** Prof L. Lorenzen and Prof JSJ van Deventer, for their help and support in every aspect of this project.

**My mom and dad** for their unconditional love and advice but most importantly for being the type of parents I would one day hope to be. *I did not forget mom.* Thank you **brother** for your sarcastic wit and ever loving nature.

The **staff** at the chemical engineering departments of the University of Stellenbosch and the University of Melbourne, Australia for all their hours of invaluable advice and assistance and especially to **Dr Feng** for his invaluable input.

To **Sean**, the man that loved and supported me through the good times and the bad.

To **Aunty Patsy and Uncle Derrick** for all their love and support.

**Dr. R. Kruger** for all his guidance, but more importantly a big thank you for introducing me to all the people whom have contributed to this project.

To my **special friends** in South Africa and in Australia: Johan, William, Morne, Linda, Grant, Luisa, Kelvin, David, Braam, Margot, Tyrone, Naven, and Niel. I thank you for not only being there for me when I needed you the most but also for all the special moments we spent together.

And lastly, to my **uncles, Harold and Raymond**. Thanking you seems so inappropriate for all that you have done for me. Hopefully one day I will be given the opportunity to show you my extreme gratitude.

# CONTENTS

	<b>PAGE</b>
<b>DECLARATION</b>	<b>ii</b>
<b>SYNOPSIS</b>	<b>iii</b>
<b>OPSOMMING</b>	<b>v</b>
<b>ACKNOWLEDGEMENTS</b>	<b>vii</b>
<b>CONTENTS</b>	<b>viii</b>
<b>LIST OF FIGURES</b>	<b>xiii</b>
<b>LIST OF TABLES</b>	<b>xvi</b>
<b>LIST OF SYMBOLS</b>	<b>xviii</b>
<b>CHAPTER 1</b>	<b>1</b>
<b>INTRODUCTION</b>	<b>1</b>
<b>CHAPTER 2</b>	<b>4</b>
<b>LITERATURE SURVEY</b>	<b>4</b>
2.1 Introduction	4
2.2 Waste immobilisation technologies	4
2.2.1 Portland cement based systems	5
2.2.2 Portland cement/soluble silicate process	6
2.2.3 Lime based processes	8
2.2.4 Portland cement/fly ash processes	9
2.2.5 Nonchemical processes and other systems	9
2.2.5.1 Inorganic processes	10
2.2.5.2 Organic processes	10
2.2.5.3 Nonchemical processes	11



	<b>PAGE</b>
2.3 Adsorbents for phenolic adsorption	11
2.4 Geopolymers	13
2.4.1 Fly ash	13
2.4.1.1 Fly ash composition	14
2.4.1.2 Fly ash physical properties	14
2.4.1.3 The pozzolanic reaction	15
2.4.2 Kaolin	16
2.4.3 Silica, silicate and aluminosilicate chemistry	17
2.4.3.1 Silicate structures	17
2.4.3.2 Surface acidity	18
2.4.3.3 Silica polymerisation	19
2.5 Summary	20
<b>CHAPTER 3</b>	<b>30</b>
<b>ORGANIC ENCAPSULATION AND GEOPOLYMERS</b>	<b>30</b>
3.1 Introduction	30
3.2 Organic encapsulation	30
3.2.1 Introduction	30
3.2.2 Reasons for organic waste encapsulation	31
3.2.3 Techniques for organic waste treatment	31
3.2.4 Organic reactions in a chemical fixation and solidification system	32
3.2.5 Commercial processes	34
3.3 Geopolymerisation	35
3.3.1 Introduction	35
3.3.2 Chemistry	35
3.3.3 Applications	37
3.4 Summary	39
<b>CHAPTER 4</b>	<b>48</b>
<b>EXPERIMENTAL AND RESEARCH METHODS</b>	<b>48</b>
4.1 Introduction	48
4.2 Experimental methods	49

4.2.1 Experimental materials	49
4.2.2 Preparation of geopolymer matrices	49
4.2.3 Zeolite synthesis	50
4.2.3.1 Acid treatment of zeolite NaP1	50
4.2.3.2 Dealumination of zeolite NaP1 and clinoptilolite	51
4.2.3.3 Ion exchange capacity	51
4.2.3 Dissolution experiments	51
4.2.4 Leaching tests	52
4.3 Methods of analysis	52
4.3.1 X-ray diffraction (XRD)	52
4.3.2 X-ray fluorescence spectroscopy (XRF)	53
4.3.3 Infrared spectroscopy (IR)	53
4.3.4 Scanning electron microscopy (SEM)	54
4.3.5 Inductively coupled plasma spectroscopy (ICP AES)	54
4.3.6 Compressive strength tests	54
4.3.7 Surface area analysis	55
4.3.8 Particle size distribution tests	55
4.3.9 Proton induced x-ray emission (PIXE)	55
4.3.10 Organic adsorption measurements	56
4.3.11 Zeta potential data	56
4.3.12 Atomic absorption spectroscopy (AA)	57
4.4 Summary	57
<b>CHAPTER 5</b>	<b>52</b>
<b>THE EFFECT OF ORGANIC ENCAPSULATION ON GEOPOLYMERS</b>	<b>61</b>
5.1 Background	61
5.2 Geopolymer matrices	62
5.2.1 Compressive strength	63
5.2.2 ICP analysis	63
5.2.3 Specific surface area analysis	64
5.2.4 X-ray diffraction analysis	65
5.2.5 Infrared analysis	65
5.2.6 Scanning electron microscopy	66
5.2.7 PIXE analysis	67
5.3 The effects of organics on geopolymerisation	68
5.3.1 Compressive strength	69
5.3.2 ICP analysis	69

	<b>PAGE</b>
5.3.3 Specific surface area analysis	69
5.3.4 X-ray diffraction analysis	70
5.3.5 Infrared analysis	70
5.3.6 Scanning electron microscopy	71
5.3.7 PIXE analysis	71
5.3.8. Immobilisation efficiencies	72
5.4 Summary	72
<b>CHAPTER 6</b>	<b>102</b>
<b>ZEOLITES</b>	<b>102</b>
6.1 Background	102
6.1.1 Previous studies	102
6.1.2 Types of zeolites	103
6.1.3 Inorganic/organic adsorption by zeolites	104
6.2 Zeolite synthesis	105
6.2.1 Zeolite synthesis	105
6.2.2 Influence of synthesis factors	106
6.3 Physical/chemical properties of zeolites	108
6.3.1 Physical properties	108
6.3.1.1 Particle size	108
6.3.1.2 Surface morphology	109
6.3.1.3 Density	109
6.3.1.4 Zeolite structure	109
6.3.1.5 Colour	110
6.3.2 Chemical properties	110
6.3.2.1 Zeolite chemical reactions	110
6.3.2.2 Zeolite reactions in solutions	111
6.4 Differences /similarities between zeolites and geopolymers	112
6.5 Summary	113

<b>CHAPTER 7</b>	118
<b>ZEOLITE INCORPORATION WITHIN GEOPOLYMERS</b>	118
7.1 Introduction	118
7.2 Organic adsorption by zeolites	119
7.2.1 Introduction	119
7.2.2 Zeolite synthesis	119
7.2.2.1 XRD analysis	120
7.2.2.2 Surface area changes	120
7.2.2.3 Cation exchange capacity	121
7.2.3 Adsorbed organics on zeolites	121
7.2.3.1 Types of zeolites	121
7.2.3.2 Organic adsorption experiments	121
7.2.3.3 Adsorption data	122
7.3 Zeolite encapsulation	123
7.4 The effect of zeolite encapsulation on geopolymerisation	123
7.4.1 Compressive strength results and specific surface area results	123
7.4.2 X-ray diffraction analysis	124
7.4.3. Infrared analysis	125
7.5 Leaching	126
7.5.1 Introduction	126
7.5.2 Previous studies	126
7.5.3. Factors affecting leaching	127
7.5.3.1 External factors	127
7.5.4 Leaching data	129
7.5.4.1 Silicon leaching	129
7.5.4.2 Aluminium leaching	130
7.5.4.3. Organic leaching	131
7.6 Summary	131
<b>CHAPTER 8</b>	161
<b>CONCLUSIONS</b>	161
<b>REFERENCES</b>	164

# LIST OF FIGURES

	<b>PAGE</b>
Figure 2.1: Hydrated silicate and aluminate compounds	25
Figure 2.2: The pozzolanic reaction	25
Figure 2.3: Structure of kaolinite	26
Figure 2.4: SiO <sub>4</sub> unit	26
Figure 2.5: Dehydration reactions of aluminium oxide	27
Figure 2.6: Condensation reactions for surface formation	27
Figure 2.7: Organic dehydration reactions	27
Figure 2.8: Surface modification reactions	28
Figure 2.9: Stages of silicon polymerisation	29
Figure 3.1: Hydrolysis reactions	44
Figure 3.2: Free radical reactions	45
Figure 3.3: Organic reduction reactions	46
Figure 3.4: A poly (sialate-siloxo) geopolymer	47
Figure 3.5: Geopolymer polycondensation reactions	47
Figure 4.1: Photograph of a cured geopolymer matrix.	60
Figure 5.1: XRD graph of Eskom fly ash	82
Figure 5.2: XRD graph of SASOL fly ash	83
Figure 5.3: XRD graph of 36 Eskom	84
Figure 5.4: XRD graph of 36 Sasol	85
Figure 5.5: IR graph of Eskom fly ash	86
Figure 5.6: IR graph of SASOL fly ash	87
Figure 5.7: IR graph of 36 Eskom	88
Figure 5.8: IR graph of 36 Sasol	89
Figure 5.9: SEM image of Eskom fly ash	89
Figure 5.10: SEM image of SASOL fly ash	89
Figure 5.11: SEM image of 36 Eskom	90
Figure 5.12: SEM image of 36 Sasol	90
Figure 5.13: XRD graph of 36 Sasol (PhOH)	91
Figure 5.14: XRD graph of 36 Sasol (Cl-PhOH)	92

Figure 5.14: XRD graph of 36 Eskom (PhOH)	93
Figure 5.15: XRD graph of 36 Eskom (Cl-PhOH)	94
Figure 5.17: IR graph of 36 Sasol (PhOH)	95
Figure 5.18: IR graph of 36 Sasol (Cl-PhOH)	96
Figure 5.19: IR graph of 36 Eskom (PhOH)	97
Figure 5.20: IR graph of 36 Eskom (Cl-PhOH)	98
Figure 5.21: SEM image of 36 Sasol (1% PhOH)	99
Figure 5.22: SEM image of 36 Eskom (1% PhOH)	99
Figure 5.23: SEM image of 36 Sasol (5% PhOH)	100
Figure 5.24: SEM image of 36 Sasol (5% Cl-PhOH)	100
Figure 5.25: SEM image of 36 Eskom (5% PhOH)	101
Figure 5.26: SEM image of 36 Eskom (5% Cl-PhOH)	101
Figure 6.1: Hydrothermal synthesis of zeolites	116
Figure 6.2: SEM image of fly ash	116
Figure 6.3: SEM image of zeolite NaP1	117
Figure 6.4: Gismondine structure	117
Figure 7.1: XRD graph of untreated fly ash	135
Figure 7.2: XRD graph of zeolite NaP1	135
Figure 7.3: Organic adsorption data	136
Figure 7.4: XRD graph of 36 Sasol (5% fzeo)	137
Figure 7.5: XRD graph of 36 Sasol (5% czeo)	138
Figure 7.6: XRD graph of 36 Sasol (5% zeo NaP1)	139
Figure 7.7: XRD graph of 36 Sasol (coated czeo)	140
Figure 7.8: IR graph of 36 Sasol	141
Figure 7.9: IR graph of 36 Sasol (5% fzeo)	142
Figure 7.10: IR graph of 36 Sasol (5% zeo NaP1)	143
Figure 7.11: IR graph of 36 Sasol (5% czeo)	144
Figure 7.12: IR graph of 36 Sasol (coated fzeo)	145
Figure 7.13: IR graph of 36 Sasol (coated czeo)	146
Figure 7.14: IR graph of 36 Sasol (coated zeo NaP1)	147
Figure 7.15: Leaching graphs of 36 Sasol [coated zeo NaP1 (PhOH)]	148

Figure 7.16: Leaching graphs of 36 Sasol [coated zeo NaP1 (Cl-PhOH)]	149
Figure 7.17: Leaching graphs of 36 Sasol [coated deal zeo NaP1 (Cl-PhOH)]	150
Figure 7.18: Leaching graphs of 36 Sasol [coated deal zeo NaP1 (PhOH)]	151
Figure 7.19: Leaching graphs of 36 Sasol [coated fzeo (Cl-PhOH)]	152
Figure 7.20: Leaching graphs of 36 Sasol [coated fzeo (PhOH)]	152
Figure 7.21: Leaching graphs of 36 Sasol [coated deal fzeo (Cl-PhOH)]	153
Figure 7.22: Leaching graphs of 36 Sasol [coated deal fzeo (PhOH)]	154
Figure 7.23: Leaching graphs of 36 Sasol [coated czeo (PhOH)]	155
Figure 7.24: Leaching graphs of 36 Sasol [coated czeo (Cl-PhOH)]	156
Figure 7.25: Leaching graphs of 36 Sasol	157
Figure 7.26: Leaching graphs of 36 Sasol (5% fzeo)	158
Figure 7.27: Leaching graphs of 36 Sasol (5% zeo NaP1)	159
Figure 7.28: Leaching graphs of 36 Sasol (5% czeo)	160

# LIST OF TABLES

	<b>PAGE</b>
Table 2.1: Basic hydration reactions	21
Table 2.2: Substances that negatively affect Portland cement reactions	21
Table 2.3: Compressive strength as a percent of control specimen	22
Table 2.4: Types of Portland cement	22
Table 2.5: Leaching of cement/fly ash vs other processes	23
Table 2.6: Long-term resistance of organic polymers used in solidification	23
Table 2.7: Characteristics of selected spill adsorbents	23
Table 2.8: Fly ash characteristics	24
Table 2.9: Composition of fly ash	24
Table 3.1: Organic-containing wastes	40
Table 3.2: Physiochemical properties of phenol and 4-chlorophenol	40
Table 3.3: Chemicals persistent to hydrolysis	41
Table 3.4: Chemicals less resistant to hydrolysis	42
Table 3.5: Oxidation reactions	42
Table 3.6: Organic fixation processes	43
Table 4.1: Oxide composition as determined by XRF analysis	58
Table 4.2: Surface area / Mean particle size data for starting reagents	58
Table 4.3: Ingredients of the geopolymeric matrices	59
Table 4.4: The differences between standard TCLP tests and adapted TCLP tests	59
Table 5.1: Compressive strength data for standard geopolymer matrices	74
Table 5.2: ICP data for SASOL fly ash	74
Table 5.3: ICP data for Eskom fly ash	75
Table 5.4: Si:Al ratios for Eskom and SASOL fly ash	76
Table 5.5: BET surface area results for fly ashes and geopolymers	76
Table 5.6: PIXE analysis for standard geopolymer matrices	77
Table 5.7: Geopolymer matrices for organic addition	77
Table 5.8: Compressive strength data for geopolymers containing organics	78
Table 5.9: ICP data (organics) for SASOL fly ash	78



Table 5.10: ICP data (organics) for Eskom fly ash	79
Table 5.11: Surface area measurements for geopolymers containing organics	80
Table 5.12: PIXE analysis for geopolymers containing organics	81
Table 6.1: 7 Groups of zeolites	114
Table 6.2: Chemical composition of clinoptilolite	114
Table 6.3: Chemical composition of gismondine	115
Table 7.1: Surface area results for synthesised zeolites	132
Table 7.2: Solubility of phenol and 4-chlorophenol	132
Table 7.3: Geopolymer matrices	132
Table 7.4: Compressive strength data for geopolymers containing zeolites	133
Table 7.5: Geopolymer (with encapsulated zeolite) surface area results	133
Table 7.6: Infrared absorption bands for geopolymer systems	134
Table 7.7: Infrared absorption bands for zeolites	134

# LIST OF SYMBOLS

## List of Abbreviations:

S/S	Solidification and Stabilisation
CFS	Chemical Fixation and Solidification System
PFA	Pulverised Fly Ash
PCB's	Polychlorinated Biphenyls
TCLP	Toxicity Characteristic Leaching Procedure
CEC	Ionic Exchange Capacity
ASR	Alkali-Silica Reaction
OPC	Ordinary Portland Cement
®	Samples were tested twice

## Geopolymer / Zeolite Abbreviations

Abbreviation	Meaning
36 Sasol / 19 Sasol	Geopolymers synthesised utilising Sasol fly ash and recipes 36 and 19 respectively.
PhOH / Cl-PhOH	Phenol and chlorophenol respectively.
36 Eskom / 19 Eskom	Geopolymers synthesised utilising Eskom fly ash and recipes 36 and 19 respectively.
36 Sasol (PhOH) / 36 Eskom (PhOH)	Geopolymers containing phenol.
36 Sasol Cl-PhOH / 36 Eskom (Cl-PhOH)	Geopolymers containing chlorophenol.
36 Sasol (5% fzeo)	Geopolymer 36 Sasol containing 5% of clinoptilolite (fine powder).
36 Sasol (5% czeo)	Geopolymer 36 Sasol containing 5% of clinoptilolite (pellet like form).
36 Sasol (5% NaP1)	Geopolymer 36 Sasol containing 5% of synthesised zeolite, zeolite NaP1.
36 Sasol (coated fzeo)	Geopolymer 36 Sasol containing clinoptilolite (fine powder) which is coated with a thin layer of geopolymer.
36 Sasol (coated czeo)	Geopolymer 36 Sasol containing clinoptilolite (pellet form) which is coated with a thin layer of geopolymer.

Abbreviations	Meanings
36 Sasol (coated zeo NaP1)	Geopolymer 36 Sasol containing zeolite NaP1 which is coated with a thin layer of geopolymer.
deal	Zeolites that were dealuminated.
36 Sasol [coated zeo NaP1(PhOH)]	Geopolymer containing coated zeolite NaP1 that has PhOH adsorbed onto its surface.
36 Sasol [coated zeo NaP1(Cl-PhOH)]	Geopolymer containing coated zeolite NaP1 that has Cl-PhOH adsorbed onto its surface.
36 Sasol [coated deal fzeo (PhOH)]	Geopolymer containing coated, dealuminated clinoptilolite (fine powder) that has PhOH adsorbed onto its surface.
36 Sasol [coated deal fzeo (Cl-PhOH)]	Geopolymer containing coated, dealuminated clinoptilolite (fine powder) that has Cl-PhOH adsorbed onto its surface.
36 Sasol [coated deal czeo (PhOH)]	Geopolymer containing coated, dealuminated clinoptilolite (pellet form) that has PhOH adsorbed onto its surface.
36 Sasol [coated deal czeo (Cl-PhOH)]	Geopolymer containing coated, dealuminated clinoptilolite (pellet form) that has Cl-PhOH adsorbed onto its surface.

### Cement Literature Symbols:

CSH	Calcium Silicate Hydrate
$C_3S$	$Ca_3SiO_5$
$C_2S$	$Ca_2SiO_4$
$C_3A$	$Ca_3Al_2O_6$
$C_4AF$	$Ca_4Al_2Fe_2O_{10}$

# Chapter 1

## INTRODUCTION

In earlier years the easiest means of waste disposal was dumping into waterways or onto land. The absence of proper legislation and enforcement thereof, resulted in uncontrolled pollution of the environment. Due to stricter environmental legislation and growing public concern the need for new technologies for hazardous waste containment has grown. The field of geopolymerisation has just begun to mature into an accepted environmental technology for the process of hazardous waste treatment. Yet, few people working in waste treatment have any knowledge of geopolymerisation technology other than that gained from a few publications, conferences and patents. The main reason for this dearth of information is due to a lack of fundamental knowledge, especially of the chemistry behind the different mechanisms that occur in geopolymerisation. There also exists some confusion regarding geopolymers and especially the terminology associated with them. Although Joseph Davidovits (1999) proposed a new terminology, there are still doubts regarding the novelty of these matrices.

Previous research by Davidovits (1990) and Van Jaarsveld (1996, 1997) provides detailed information on the use of geopolymerisation for the encapsulation of radioactive waste and toxic inorganic metals. Very little, if any, literature deals with the use of geopolymerisation technology for the encapsulation of organic waste. This thesis therefore is an attempt to better understand organic encapsulation by geopolymerisation. **The main aims of the thesis were to develop an understanding of the chemistry behind organic encapsulation in geopolymers and to develop a stable geopolymer matrix for the immobilisation of organics.** A stable geopolymer matrix is one that when exposed to severe leaching tests will leach minimal concentrations of organics.

Phenolics (phenol and 4-chlorophenol) were chosen as the organic waste to be encapsulated because as stated by the U.S. Environmental Agency they represent one of the more challenging groups of priority pollutants to be removed from wastewater streams. Encapsulation of these organics was achieved by utilising the technology associated with chemical fixation and solidification (CFS) systems. CFS systems are based on the principles of stabilisation and solidification. Stabilisation is a process where additives are mixed with the waste to minimise migration and toxicity of the waste. Solidification on the other hand involves encapsulation of the waste in a monolithic solid of high structural integrity (Conner, 1990). Geopolymer systems are also a combination of stabilisation and solidification.

The geopolymer matrices synthesised for experimental work were fly ash based. Fly ash produced from the combustion of coal poses a serious environmental problem due to the possible leaching of toxic metal contaminants. In some cases fly ash is used to immobilise toxic elements, even organic substances. Utilising the reactive properties of fly ash it was possible to synthesise a solid geopolymer structure from waste, for the encapsulation of organic waste.

The summary that follows provides a brief insight into the various chapters within the thesis.

**Chapter 2** contains a brief discussion on various other immobilisation systems available for organic waste treatment as well as other available adsorbents. **Chapter 3** contains information on the organics encapsulated and their chemical reactions in a chemical fixation and solidification system. A more in-depth look at the chemistry of geopolymer systems and applications of geopolymer technology is also discussed in Chapter 3. The zeolitic material was subjected to various modification procedures to increase their adsorption capacity. These modification procedures are detailed in Chapter 3. Addition of organics to an already complicated chemical system has led to a challenging problem of trying to analyse the system. Indeed several analytical tools (**Chapter 4**) were employed in order to identify and provide more conclusive information as far as structural analysis was concerned. In this study fly ash was mixed with organics (**Chapter 5**) to form a solid monolithic structure. The effects of organic addition on the chemical and physical properties of geopolymers are

discussed in Chapter 5. Due to the severe matrix breakdown that occurred to the system on addition of 5% organic an alternative method of encapsulation was needed. The adsorptive properties of zeolites suggested their use as adsorbents for organics (**Chapter 6**). Chapter 6 is also a discussion on the types of zeolites available and their physical/chemical properties. The geopolymer system was then used as an encapsulation medium for the organic containing zeolites (**Chapter 7**). Leaching tests were performed (Chapter 7) to test the efficiency of the system for organic encapsulation. For the leaching tests a modified Toxicity Characteristic Leaching Procedure (TCLP) was used, making use of an acetic acid buffer solution. Analysis of leaching data (Chapter 7) shows that organic immobilisation was efficient; with approximately < 2ppm organic being leached from the system.

In summary, this thesis presents an investigation into the use of geopolymers for organic waste stabilisation.

# Chapter 2

## LITERATURE SURVEY

### 2.1 INTRODUCTION

To gain a better understanding of any new technology or system, knowledge of other similar technologies is necessary. Chapter 2 therefore, provides a more in-depth discussion on other waste treatment technologies previously and currently used, adsorbents such as organoclays and activated carbon, which are utilised for organic adsorption and a discussion on the reagents used in geopolymer technology.

### 2.2 WASTE IMMOBILISATION TECHNOLOGIES

The complexity of a large number of hazardous wastes has necessitated the development of many different disposal techniques. In certain applications solidification and stabilisation (S/S) is already preferred over and above many already well known technologies. Indeed it is this S/S system that is used for the immobilisation of organics in this study. Other chemical fixation and solidification processes available for organic immobilisation include Portland cement based systems, lime-based systems, fly ash processes and certain nonchemical processes and systems.

## 2.2.1 Portland cement-based systems

Portland cement-based systems and variations of it were the first to be used in actual chemical fixation and solidification system work (in the nuclear field) in the early 1950s (Conner, 1990). It is now the most widely used ingredient in chemical fixation and solidification systems. Portland cement is basically a calcium silicate mixture that contains tricalcium ( $C_3S$ ) and dicalcium ( $C_2S$ ) with smaller amounts of tricalcium aluminate ( $C_3A$ ) and calcium aluminoferrite ( $C_4AF$ ). Portland cement processes are divided into two general types, Portland cement alone and Portland cement + additives. The other systems such as cement/soluble silicate and cement/fly ash that incorporate Portland cement are also discussed. The reasons why Portland cement processes are important are as follows (Conner, 1990):

- 1. Its composition is consistent from source to source, thus eliminating many variables in studying chemical fixation and solidification systems**
- 2. A substantial amount of information about the reactions of Portland cement (setting, hardening, and fixation of metals) is available.**
- 3. Good data on modelling of environmental effects from the leaching of cement-based waste forms are available.**
- 4. Studies at the Louisiana State University and elsewhere have been done on this process type.**
- 5. Portland cement processes are also similar to many of the reactions of pozzolanic processes, which make up much of the current commercial chemical fixation and solidification technologies.**

A typical weight proportion in Portland cement is 50%  $C_3S$ , 25%  $C_2S$ , 10%  $C_3A$ , 10%  $C_4AF$  and 5% other oxides (Conner, 1990). In the Portland cement process, water reacts chemically with the cement to form hydrated silicate and aluminate compounds (Figure 2.1). Cement powder and water are mixed to form hydrated  $C_3A$ .  $C_3A$  causes rapid setting of the cement. Gypsum is generally added to control the setting rate. The ettringite that forms coats the cement particles and retards the setting reactions.  $C_3S$  and  $C_2S$  are responsible for the strength development in Portland cement. The reaction products formed are  $Ca(OH)_2$  and calcium silicate hydrate (CSH) or tobermorite gel. Table 2.1 contains certain basic cement hydration reactions. The solids contained in



the waste act as an aggregate to form solid concrete like structure. The maximum amount of waste encapsulated within this solid structure will depend on the Portland cement used, any additives and the type and composition of the waste being encapsulated. Interactions between certain waste constituents (eg. organic compounds, silt, coal and lignite, some inorganic salts and metal compounds) and the cement may be deleterious to the setting and curing reactions of Portland cement. Other substances in waste that could negatively affect the reactions of Portland cement are contained in Table 2.2. Studies conducted by Cullinane et al. (1987) show that phenol additions result in a marked decrease in strength of the cement matrix (Table 2.3). In certain cases, the addition of lime and sodium silicate to Portland cement has been found to counteract the negative effects of the waste constituent and allow the cement to set properly (Conner, 1990). In other cases a cement/bentonite composition has been used commercially for chemical fixation and solidification treatment (Conner, 1990). The clay controls viscosity and reduces available water, as well as adsorbing organics and metals. There are numerous different types of Portland cement available. Eight of the different types of Portland cement that are available and their chemical and physical characteristics are contained in Table 2.4.

### **2.2.2 Portland cement/soluble silicate processes**

Soluble silicates are one of the oldest classes of industrial chemicals known (Conner, 1990). They have been used for a multitude of purposes ranging from special cements and coatings to moulded articles and catalysts. Indeed the history of silicate use in chemical fixation and solidification technology dates back to 1970 (Conner, 1990). According to Conner (1990) its roots go back further to similar technologies that were used for grouting, soil stabilisation, mine back filling, production of stabilised base courses for road construction and even the nuclear waste field. Insoluble silicates such as fly ash, kiln dusts and clays were used in many of these processes, however the use of soluble silicates were only detailed in the nuclear waste field and injection grouting of unstable soils.

In the Portland cement/soluble silicate system the soluble silicate is mixed with cement, slag, lime or any other source of multivalent metal ions that will promote gelation and precipitation of silicates to produce a solid matrix. The gel matrix produced is similar to that of geopolymerisation, where silicon atoms are tetrahedrally coordinated with alternating oxygen atoms along a linear backbone. The oxygen side groups when reacted with polyvalent metals ions (first set of reactions), form strong ionic bonds with adjacent chains to form a three-dimensional polymer matrix. According to Conner (1990) this type of structure displays properties of high stability, high melting point, and a rigid friable structure. Indeed, several similarities exist between this system and geopolymers (Chapter 4). For toxic inorganic metal encapsulation the soluble silicate reduces the leachability of the metal by encapsulation of the metal within a low-solubility silicate or metal silicate-gel matrix. This is the reason why soluble silicates are used in chemical fixation and solidification systems for the encapsulation of toxic metal ions.

A second set of reactions occurs between the soluble silicate and reactive components of Portland cement. The reaction can take place slowly under controlled conditions due to the limited solubility of the cross-linking calcium ion. The gel structure thus formed is more suitable to producing good solid properties and has the ability to hold very large quantities of water. Due to these properties the gel can encapsulate ions by various bonding mechanisms (Conner, 1990).

The third set of reactions occurs between Portland cement, the waste and water. These are a series of hydrolysis, hydration, and neutralisation reactions.

In this system the primary function of the soluble silicate is to reduce mobility of any encapsulated toxic metal contaminant. It does this by forming precipitates in the matrix, thus reducing the effective pore volume and hence slows down the mobility of any mobile species into the environment. It is this effect that could also be responsible for the reduced leachability of species such as organics and anions that would not be expected to react with soluble silicates (Conner, 1990).

### 2.2.3 Lime based processes

Lime was originally used for the neutralisation of acidic wastewater and to precipitate metals before discharge. Most central waste treatment facilities use lime as a fixating agent. Lime based processes generally cover the various chemical and physical forms of quick lime, hydrated lime, and hydraulic lime. Lime-based processes can be divided into the following groups:

1. Lime/fly ash processes
2. Lime/clay processes
3. Lime processes
4. Lime/kiln dust processes

Lime/fly ash processes involve combining lime and fly ash with water to produce a cementitious material. Initially the reaction product formed is a non-crystalline gel, but the gel eventually hardens to form calcium silicate hydrate. Many of the reactions are analogous to Portland cement (Conner, 1990). However, due to the differing composition of the fly ash, other differences in chemistry are observed. One of these differences occurs due to the unburned organics in fly ash. The organics cover the reactive surfaces preventing contact of the cementitious material, thus reducing the cementing action. Lime-based and lime/fly ash processes are able to accommodate large quantities of organics (Conner, 1990). Chestnut et al. (1985) reported on the solidification of oily wastes and other water-insoluble organic materials at organic levels above 20%.

One of the oldest processes that exemplify the reaction between lime and various silicas and silicates are the sand/lime mortars. The reaction of lime with clays which are silicates form calcium silicates with bonded properties. These cementation reactions are generally very slow in comparison to other solidification processes.

## 2.2.4 Portland cement/fly ash processes

For decades fly ash has been used in Portland cement. In fact one of the most extensive uses of fly ash is in fly ash concrete. Fly ash is known to impart certain desirable qualities to cement. It also gives a reduction in cost since fly ash replaces 25-35% of Portland cement. One of the earlier uses of fly ash in cement is recorded on work done on nuclear waste at Oak Ridge in 1970 (Conner, 1990).

In Portland cement fly ash serves a twofold function both as a bulking agent and as a pozzolan. Fly ash in Portland cement is also known to bind additional water, decrease pore pH and act as an adsorbent for metal ions. A more detailed discussion on the chemistry of fly ash is discussed in section 2.4. When fly ash is mixed with Portland cement the gypsum and calcium hydroxide act as activators for the pozzolanic reaction. The cement paste that forms is reported to have a higher compressive strength than ordinary Portland cement. At the same time the cement/fly ash system leaches out the lowest concentration of metal ions (Table 2.5). Côte (1986) attributes this to a moderation of pore water pH by the fly ash, as well as to other effects such as adsorption.

According to Conner (1990) a number of central treatment facilities use some version of cement/fly ash process for waste treatment.

## 2.2.5 Nonchemical processes and other systems

Excluding the systems listed above there are many other processes that claim to solidify and fixate hazardous wastes. These systems are listed as follows (Conner, 1990):

1. Miscellaneous inorganic processes.
2. Nuclear waste chemical fixation and solidification systems.
3. Organic-based processes.
4. Nonchemical solidification.
5. Systems combining dewatering and chemical fixation and solidification.
6. In situ processes and systems.

### 2.2.5.1 Inorganic processes

An example of an inorganic process is the use of an adsorbent to adsorb certain waste species such as metals or organics and then a solidification technique to encapsulate the waste in a solid monolith. Conner (1990) reported on the disposal of chlorinated hydrocarbons by first mixing them with a carbon adsorbent and then solidifying the mixture in Portland cement.

### 2.2.5.2 Organic processes

Organic based reactions fall into three categories, firstly the urea-formaldehyde system, secondly other polymerisation processes and thirdly thermoplastic systems. Urea-formaldehyde is not in use anymore due to its cost and also recent environmental concerns over formaldehyde. **Urea-formaldehyde resins** are aqueous emulsions of urea and formaldehyde combined to form linear polymeric chains. Addition of a catalyst to the system results in cross-linking polymerisation to form a solid. The waste is then trapped within the urea-formaldehyde system. Urea-formaldehyde systems have good tolerance for variations in the liquid waste, have the ability to solidify a fairly wide variety of wastes and have good physical properties after curing (Conner, 1990).

The use of other **organic polymers** has found wide applications in liquid waste treatment since they can be synthesised to form a variety of different compositions. The most commonly used polymers are polyester or vinyl ester resins. The monomer or prepolymer and the waste are mixed using high shearing mixing. A catalyst is then added to the water-in-resin emulsion. The catalyst polymerises the system to form a hard monolith. Their advantage over most other inorganic systems is that they have a higher degree of impermeability and tend to remain in monolithic solid due to their strength and elastic properties. These systems are therefore good in encapsulating and retaining toxic metals and organic compounds. Another desirable property of this system, is that the system very quickly gels to obtain the desired physical strength.

**Thermoplastic polymer systems** consist of 3-4% by weight of polybutadiene binder cemented with the waste and then encapsulation of the cemented waste in a quarter inch thick polyethylene jacket (Conner, 1990). The matrix formed has been reported to withstand considerable mechanical stress. The material exhibited excellent encapsulation efficiencies under leaching conditions with a broad range of aqueous solutions. It should be noted that when considering a thermoplastic polymer system interaction of the polymer with the waste components especially organics should be taken into consideration. Table 2.6 provides a list of several polymers that have a long time resistance to certain chemicals.

### 2.2.5.3 Nonchemical processes

Nonchemical solidification processes involve sorbents that do not chemically react with the waste or with additives. These include inexpensive materials such as clays and vermiculites. The use of clays as sorbents for hazardous waste is, however, limited due to the fact that there is no chemical reaction between the sorbent and the waste, hence the application of pressure can squeeze the waste from the sorbent. These systems can also be highly leachable, therefore rendering the system unsuitable for hazardous waste encapsulation. Sorbents are extensively used in spill control work. Examples of such spills are PCBs, or dioxin containing materials. The characteristics of certain sorbents for controlling spills are listed in Table 2.7. The following subsection contains more information on other available sorbents. It should be noted that sorbents themselves may not be good systems for hazardous waste containment, however, a combination of sorbents as an adsorption medium and cement based solid as an encapsulation medium provides very attractive possibilities for hazardous waste containment.

## 2.3 ADSORBENTS FOR PHENOLIC ADSORPTION

**Activated carbon** and **polymeric resins** are the most commonly used adsorbents for the adsorption of phenols and chlorophenols. Due to their large internal surface area coupled with high surface activity, activated carbons are among the most effective

adsorbents known for the removal of organic toxins. The surface area of activated carbon is typically in the range of 600-1500m<sup>2</sup>/g. The large number of surface functional groups has shown to significantly affect the adsorption of organic compounds. Activated carbon contains a complex network of pores, macropores (50-2000 nm), mesopores (5-50 nm) and micropores (0.8-5 nm). Activated carbon is however, a relatively expensive adsorbent and has high regeneration costs associated with its use.

**Polymeric resins/ion exchange resins** consist of functional groups attached chemically to an inert three-dimensional polymeric hydrocarbon matrix. Ion exchange resins consist of two groups namely, anion-exchange resins and cation-exchange resins. Anion exchange resins consist of quaternary ammonium groups or primary, secondary or tertiary amines as the active group. Cation exchange resins contain phenolic, carboxylic, phosphonic and sulphonic acid groups. The ion exchange resin contains a significant amount of water. The matrix swells when in contact with aqueous solutions.

Inorganic materials, especially **clay based materials**, have widely been investigated in the past few years in an effort to design efficient and recyclable adsorbents for the removal of organic pollutants from aqueous solutions. In order to adsorb organic molecules selectively from aqueous solutions, the adsorbent must be hydrophobic. Clays, due to their hydrophilic nature, are relatively poor adsorbents for removing hydrophobic water-soluble organic molecules from an aqueous stream. Thus, chemical modification of clay surfaces is necessary in order to change the nature of the surface from hydrophilic to hydrophobic. The inorganic exchangeable cations on the clay surface are replaced with organic cations containing long-chain alkyl groups. Through what has been called, hydrophobic binding, the clay-organic complex is exceptionally effective in adsorbing a variety of organic molecules which themselves are hydrophobic. Other properties such as unique polarity and pore size distribution add to their effectiveness as adsorbents.

Previous research has also detailed the use of zeolites as adsorbents for a variety of ions. A more detailed discussion on the chemical and physical properties of zeolites and their adsorptive properties is given in Chapter 6.

## 2.4 GEOPOLYMERS

Geopolymers are regarded as synthetic analogues of natural zeolites requiring similar hydrothermal synthesis conditions. A general geopolymeric matrix consists of fly ash, kaolin, sodium silicate, KOH/NaOH and water. Chapter 3 provides a more in depth look at the chemistry and applications of geopolymers. This section serves to provide a more detailed discussion on the chemistry and properties of the reagents used in geopolymerisation.

### 2.4.1 Fly ash

Fly ash, a by-product of the combustion of coal, is being produced in large quantities by most thermal power plants throughout the world. The generic name given to this type of fly ash is pulverised fly ash (PFA). 80% of the PFA is in a finely divided form, has the propensity to form airborne dusts and hence is called fly ash. Fly ash can generally be divided into two categories (Swamy, 1986):

**Low-lime PFA** possesses truly pozzolanic properties and need activators to react and form cementitious products.

**High-lime PFA** possesses both cementitious and pozzolanic properties.

For a more detailed description on these two categories of fly ash refer to Table 2.8.

Low-lime fly ashes are known to possess truly pozzolanic properties. *What is a pozzolan?* According to Kruger (1990) a **pozzolan** is a siliceous or aluminous compound which has minimal cementitious properties but in a finely divided form will react with  $\text{Ca}(\text{OH})_2$  in the presence of water and at ambient temperatures to form cementitious compounds.



### 2.4.1.1 Fly ash composition

Fly ashes are heterogeneous fine powders consisting of rounded or spherical glassy particles. Typical PFA consists of oxides of silicon, aluminium, calcium, magnesium and iron, and trace elements such as Co, Cr, V, Cu, Pb, Mo, Zn, Ni and Cd. The exact composition of fly ash varies depending on the difference in coal composition. In South Africa this difference is not significant since most power stations burn bituminous coals with high ash contents (20-45 %). Generally the active ingredient in fly ash is an amorphous glassy phase. Crystalline components present are quartz, mullite, ferrite, spinel and lime, with minor quantities of haematite and portlandite (Table 2.9). The glass content in high-lime PFA is of a more reactive nature than in low-lime PFA even though the glass content of high-lime PFA is lower than low-lime PFA. The other active components in high-lime PFA that are responsible for its self-cementing characteristics are free lime ( $\text{CaO}$ ), anhydrite ( $\text{CaSO}_4$ ), tricalcium aluminate ( $3\text{CaO}\cdot\text{Al}_2\text{O}_3$ ), and calcium sulpho-aluminate ( $4\text{Ca}_3\text{Al}_2\text{O}_3\cdot\text{SO}_4$ ). Fly ash composition is one of the most important contributing factors to pozzolanic activity especially the activity of the glass content.

### 2.4.1.2 Fly ash physical properties

#### (a) Morphology

Fly ash used in concrete consists mainly of spherical, glassy particles called cenospheres. PFA particles are essentially similar, however particles do vary from rounded to angular. Surface coatings called magnetite may also occur. The surface texture of the fly ash may vary from smooth and dense to highly porous. The source of the coal, combustion, method of PFA collection and pulverisation are all factors that contribute to the variations in fly ash.

### (b) Density

The loose bulk density of dry PFA is reported to be approximately  $800 \text{ kg/m}^3$  while specific gravity values range from 1.9-2.4. The specific gravity values are approximately two-thirds that of Portland cement.

### (c) Fineness

In the Portland cement industry the accepted method of fineness is measured as specific surface. Where PFA is concerned, this method is not very reliable as major difficulties arise due to the wide range in porosity and density of the fly ash particles. The specific surface area method is, however, simple and cheap and has been used to identify the overall quality of PFA for practical purposes.

## 2.4.1.3 The pozzolanic reaction

The pozzolanic reaction involves the reaction of lime with pozzolanic material such as silica, alumina and iron oxide to form cementitious products. Referring to the cement hydration reactions in subsection 2.2.1 it can be shown that the reaction products are similar for the pozzolanic reaction. Figure 2.2 provides a representation of the pozzolanic reaction. The concentration of the reactants determines the end products. These include calcium silicate hydrates (CSH), calcium aluminate hydrates ( $\text{C}_4\text{AH}_{10}$ ), calcium sulpho-aluminates (ettringite and gehlenite hydrate), and calcium aluminoferrite hydrates (CAFH). It should be noted that the pozzolanic reaction can be accelerated by temperature and the presence of alkalis. The final reaction products are therefore, determined by the composition of the glass phase, with high alumina glasses tending to form gehlenite hydrate, or if sufficient calcium is available hydrogarnets are formed. An essential difference between cementitious and pozzolanic materials is the formation of portlandite. In cementitious materials large amounts of portlandite are formed, while in pozzolanic matrices portlandite is utilised in the production of other reaction products.

Taking into consideration the properties of fly ash as discussed in the subsections above it has been shown that fly ash can successfully be used for a wide variety of applications from a cement replacement material which is resistant to sulphate attack to the production of zeolitic material for hazardous waste adsorption. It is for this reason that fly ash and its reactive properties are utilised in geopolymer technology.

## 2.4.2 Kaolin

Kaolin is clay in the form of hydrated aluminium silica (Figure 2.3). Clays are hydrous silicates or aluminosilicates and may broadly be defined as those minerals, which dominantly make up the colloidal fraction of soils, sediments, rocks, and waters (Theng, 1974). Kaolinite appears as more or less well-defined, hexagonal platelets, ranging in thickness from 0.05 to 2  $\mu\text{m}$ . The inability of kaolinite crystals to show interlayer expansion or swelling is indicative of strong interlayer bonding. The forces holding the layers together have been attributed to hydrogen bonding, however, Theng (1974) proposed that the interlayer attraction is largely electrostatic. The kaolinite layer is electrically neutral, in reality, however, most kaolinites carry a net negative charge. For interlayer sorption of species to occur the interactions arising from hydrogen bonding and van der Waals forces must be overcome. It is for this reason that adsorption of organic compounds onto kaolinite interlayers is difficult to achieve. The edges of kaolinite surfaces are therefore important as they contain unsatisfied valencies. The crystal edges influence the pH dependent charge and sorption of anions, electron transfer reactions involving organic compounds, and the initiation and/or inhibition of polymerisation of organic monomers.

Kaolin is an industrial mineral that is used primarily as filler. Researchers have combined kaolin with other raw materials and have developed over 600 different applications. One such application is geopolymerisation. In geopolymerisation, kaolin is mixed with fly ash to produce solid matrices with high early strength. The largest single application of kaolin is for the coating of paper to hide the pulp strands and to give it a gloss finish. Other uses of kaolin are: extenders in the paint industry, refractory of clays, plastics, ceramics, rubber and fibreglass.

### 2.4.3 Silica, silicate and aluminosilicate chemistry

Silicates are compounds containing polynuclear oxoanions of silicon that contain  $\text{SiO}_4$  tetrahedra which are linked in various ways to give chain, ring, sheet, cage, or framework structures (Cotton et al., 1986). Aluminosilicates are one of the most diverse and useful natural silicate minerals. Many aluminosilicates can be synthesised, and several are manufactured industrially for use as ion exchangers and molecular sieves. Among the most important framework aluminosilicates are the zeolites (Cotton et al., 1986). Silica exists in numerous variations, the most stable crystalline form being quartz ( $\text{SiO}_2$ ). The numerous variations are: tridymite, cristobalite, keatite, silica glass and biogenic silicas such as diatomaceous earth. Silicate chemistry is important in trying to understand geopolymer chemistry as silicon species are reported to be the basic building blocks of geopolymer structures.

#### 2.4.3.1 Silicate structures

Tetrahedral coordination is found in a great majority of silicates although some examples of octahedrally coordinated Si are known. Figure 2.4 is a representation of a simple drawing of a  $\text{SiO}_4$  unit. Each terminal oxygen atom contributes -1 to the charge of the  $\text{SiO}_4$  but each shared oxygen atom contributes 0. The  $\text{SiO}_2$  unit thus has no net charge because all oxygen atoms are shared. Silica and many silicates crystallise slowly and by cooling the melt at an appropriate rate amorphous solids known as glasses can be obtained. These glasses generally resemble liquids in certain aspects. Unlike liquids, however, their viscosities are very high. Silicate chemistry is further complicated when Al atoms replace Si atoms to form aluminosilicates. The aluminium occurs as Al(III) and its presence in the place of Si(IV) in an aluminosilicate renders the overall charge negative. Additional cations such as  $\text{H}^+$  or  $\text{Na}^+$  are therefore, required for each Al atom that replaces a Si atom.

### 2.4.3.2 Surface acidity

The most important reactions involving the Lewis acidity of inorganic compounds occur at solid surfaces. Lewis acid sites are used in the petrochemical industry for the isomerisation and alkylation of aromatic compounds. Lewis acid sites are also very important in the chemistry of soil and natural waters (Shriver et al., 1990).

#### (a) Alumina and aluminosilicates

The high oxidation number of Al (+3) in alumina ( $\text{Al}_2\text{O}_3$ ) makes it a surface acid. Hydrous aluminium oxide when heated above  $150^\circ\text{C}$  dehydrates and undergoes reactions such as those reported in Figure 2.5. As a result of these reactions  $\text{Al}^{3+}$  ions on the surface act as Lewis acids and  $\text{O}^{2-}$  ions act as Lewis bases. This acid-base pair is always produced together. In contrast aluminosilicates display strong Brønsted acidity. The condensation of  $\text{Si}(\text{OH})_4$  units with  $(\text{H}_2\text{O})\text{Al}(\text{OH})_3$  units may contribute to the formation of the surface (Figure 2.6). Where the proton is retained to balance the smaller positive charge of the  $\text{Al}^{3+}$  ion, a strong Brønsted acid is produced at this site. Organic dehydration reactions such as the conversion of alcohols to ethers and alkenes can occur on the surface acids (Figure 2.7).

#### (b) Silica surfaces

Brønsted acidity is dominant in silica surfaces since the  $-\text{OH}$  groups remain attached at the surface of  $\text{SiO}_2$  derivatives. The Brønsted acidity of silica surfaces is only moderate and can be compared to that of acetic acid, however aluminosilicates do display strong Brønsted acidity. According to Shriver et al. (1990) surface reactions carried out using Brønsted acid sites of silica gels are used to prepare thin coatings of a wide variety of organic groups (Figure 2.8). Silica gel surfaces can be modified to have affinities for specific classes of compounds.

According to Iler (1979) the main factors that affect the  $-\text{OH}$  surface groups of silica are:

1. SiOH groups beneath the surface that are uncondensed. Surface distortions generally occur due to these uncondensed groups.
2. SiOH groups that are located within the surface. These groups increase average packing density of SiOH groups on the surface.
3. Surfaces that are curved and have positive radii. This causes a decrease in hydrogen bonding; hence surface groups are further apart and less stable.
4. Points of negative radius. Surface groups are closer and increased hydrogen bonding is possible.
5. The presence of micropores and submicropores. These pores cause an increase in water retention thus reducing the reactivity of the available surface area.

Due to the large percentage by weight of SiO<sub>2</sub> present in fly ash the factors listed above can greatly influence the physical properties of geopolymers. It should, however, be noted that not all available –OH groups would react to form bonds.

#### 2.4.3.3 Silica polymerisation

To gain a better understanding of the geopolymerisation reaction, knowledge of the polymerisation of silica is essential. The presence of aluminium, however, greatly affects the reactivity and behaviour of soluble silicates. The polymerisation of silica can be summarised as follows (Iler, 1979):

- Polymerisation of H<sub>4</sub>SiO<sub>4</sub> monomers that are present in concentrations of more than 100-200ppm.
- The concentration of OH<sup>-</sup> ions in solution is proportional to the rate of the condensation polymerisation process (an ionic mechanism).
- The number of –Si-O-Si- bonds are maximised while the number of Si-OH bonds are minimised due to the polymerisation of the monomers. Closed three-dimensional and ring structures will form.
- The ring and closed three-dimensional structures serve as nuclei for particle growth.

- Repulsion of particles will occur above a  $\text{pH} = 7$ . The particles, however, continue to grow.
- The presence of ions such as  $\text{K}^+$  or  $\text{Na}^+$  will reduce charges between particles and gelling will occur.
- The gel phase finally hardens when the particles form a continuous structure. The presence of other adsorbed (eg. Al ions) species in the gel will affect the hardening of the gel phase

Figure 2.9 best represents the stages of silicon polymerisation.

## 2.5 SUMMARY

Chapter 2 provides a summary of the various methods that are available for the treatment of hazardous waste. When utilising solidification treatments, three major reactions are reported to be responsible for the solidification process. These are cementitious reactions, pozzolanic reactions and geopolymeric reactions. Geopolymer technology was, however, the method employed for the stabilisation of organic waste. Cementitious reactions and pozzolanic reactions are detailed in Chapter 2 while Chapter 3 contains information on the geopolymeric reactions. Chapter 2 also provides additional information on the chemistry of the reagents used in geopolymerisation. An in-depth look at geopolymer technology and the applications thereof are also contained in Chapter 3.

**Table 2.1: Basic hydration reactions (Conner, 1990)**

Reactants	Products	Heat evolved (cal/g)
$C_3A + 6H$	$C_3AH_6$	207
$C_3A + 3CS + 32H$	$C_6AS_3H_{32}$ (ettringite)	347
$2C_3S + 6H$	$C_3S_2H_3 + 3CH$ (tobermorite gel)	120
$2C_2S + 4H$	$C_3S_2H_3 + CH$ (tobermorite gel)	62
$C + H$	$CH$	279

**Table 2.2 Substances that negatively affect Portland cement reactions (Conner, 1990)**

Substance	Effect
Fine particles present in clay and silt	Weakens the bond between cement paste and the particulates.
Manganese salts	Strength reduction
Tin salts	Strength reduction
Zinc salts	Strength reduction
Copper salts	Strength reduction
Lead salts	Strength reduction
Sodium phosphate	Retarders
Sodium iodate	Retarders
Sodium borate	Retarders
Sodium sulphide	Retarders



**Table 2.3: Compressive strength as a percent of control specimen  
(Cullinane, 1987)**

<b>Interference chemical</b>	<b>Compressive strength (%) *</b>
Oil	-20
Grease	-12
Lead nitrate	-2
Copper nitrate	+91
Zinc nitrate	+3
Trichloroethylene	-28
Hexachlorobenzene	-5
Sodium hydroxide	+14
Sodium sulphate	-7
Phenol	-22

\* Results are reported as percent increase (+) or percent decreases (-) from the control experiment rounded to nearest whole percent.

**Table 2.4: Types of Portland cement (Conner, 1990)**

<b>Type of Portland cement</b>	<b>Description</b>
ASTM Type I	General purpose cement. Used most commonly in CFS work. Least expensive.
ASTM Type IA	Contains air-entraining agents for improved resistance to freeze-thaw and scaling.
ASTM Type II	Used where moderate sulphate attack is expected or where moderate heat of hydration is required.
ASTM Type IIA	Same as Type II but with air-entraining agents
ASTM Type III	Used when high early strength is required, and in cold weather.
ASTM Type IIIA	Same as Type III but with air-entraining agents
ASTM IV	Used in massive structures where temperature rise must be controlled. Low heat of hydration.

**Table 2.5: Leaching of cement/fly ash vs other processes (Côte, 1986)**

Process	Arsenic *	Cadmium*	Chromium*	Lead*
Cement/fly ash	3.97	0.02	0.19	0.11
Lime/fly ash	4.82	0.03	0.18	0.85
Cement/clay	3.42	0.04	0.11	0.68
Cement/silicate	15.16	0.14	0.19	0.42

\*Cumulative fraction leached (%)

**Table 2.6: Long-term resistance of organic polymers used in solidification (Conner, 1990)**

Chemical	Conventional Polyethylene	Linear Polyethylene	Polyvinyl chloride
Acetic acid (50%)	Excellent	Excellent	Moderate
Benzene	Poor	Moderate	Not resistant
Butadiene	Not resistant	Not resistant	Not resistant
Carbon tetrachloride	Poor	Moderate	Moderate
Chloroform	Poor	Moderate	Not resistant
Chromic acid	Excellent	Excellent	Excellent
Cresol	Poor	Poor	Poor
Dichlorobenzene	Poor	Poor	Not resistant
Diethyl ether	Not resistant	Not resistant	Not resistant
Gasoline	Poor	Moderate	Poor
Metallic salt soln.	Excellent	Excellent	Excellent
Sulphuric acid (conc.)	Moderate	Moderate	Not resistant
Trichloroethane	Not resistant	Not resistant	Not resistant

**Table 2.7: Characteristics of selected spill adsorbents (Conner, 1990)**

Product	Chemical type	Neutralises acids	Selectively absorbs organics	Typical final product characteristics
Granular clay	Inorganic	No	No	Particulate
Kaolin clay, powder	Inorganic	No	No	Cake
Lime kiln dust	Inorganic	Yes	No	Cake
Portland cement	Inorganic	No	No	Solid cake
Fly ash, Type C	Inorganic	No	No	Cake
Expanded sodium silicate	Inorganic	No	No	Particulate
Fumed silica	Inorganic	No	No	Gel

**Table 2.8: Fly ash characteristics (Swamy, 1986)**

<b>Fly ash</b>	<b>Description</b>
Low-lime PFA	Produced from bituminous and anthracite coals. Has a CaO content < 10%. Corresponds to class F fly ash.
High-lime PFA	Produced from sub-bituminous and lignite coals. Has a CaO content > 10%. Corresponds to class C fly ash.

**Table 2.9: Phase composition of fly ash (Kruger, 1990)**

<b>Phase</b>	<b>Composition (%)</b>
Amorphous	59
Mullite	19
Haematite	7
Magnetite	6
Quartz	5
Carbon	4

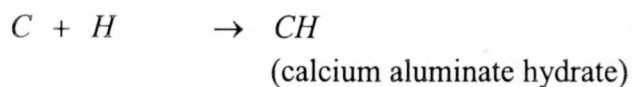
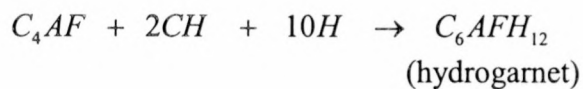
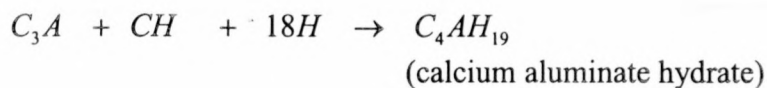
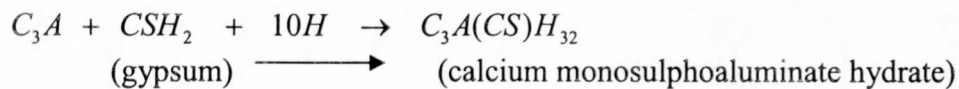
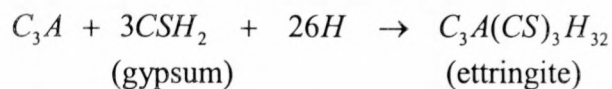
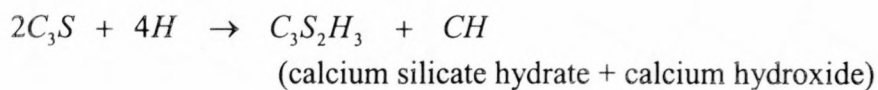
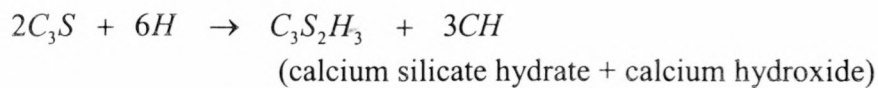
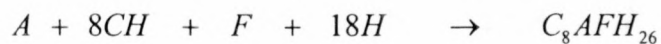
**Figure 2.1: Hydrated silicate and aluminate compounds (Kruger, 1990)****Figure 2.2: Pozzolanic reaction (Kruger, 1990)**

Figure 2.3: Structure of kaolin (Theng, 1974)

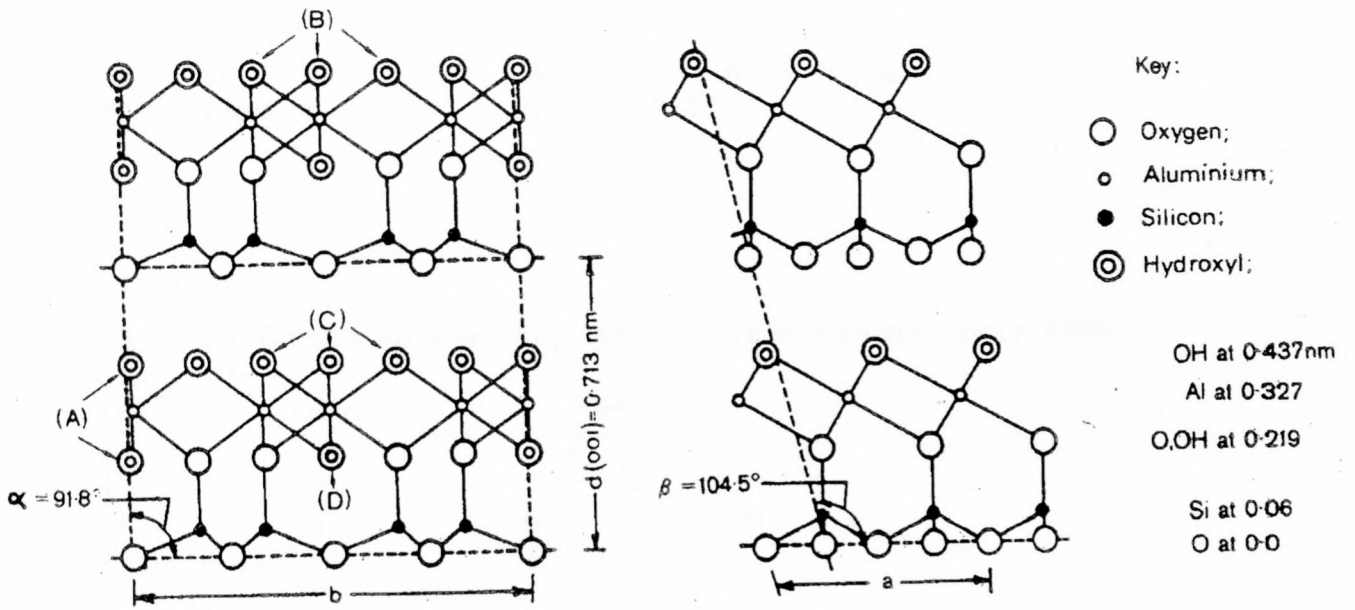
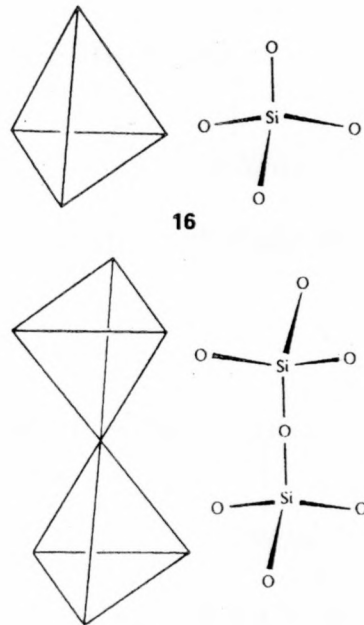
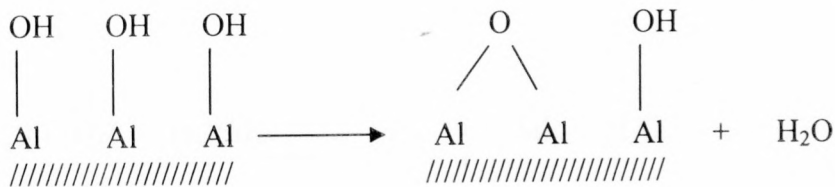


Figure 2.4: SiO<sub>4</sub> unit (Cotton, 1986)



**Figure 2.5: Dehydration reaction of aluminium oxide (Shriver, 1990)**



**Figure 2.6: Condensation reactions for structure formation (Shriver, 1990)**

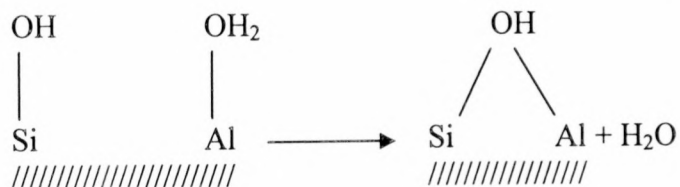


**Figure 2.7: Organic dehydration reactions (Shriver, 1990)**

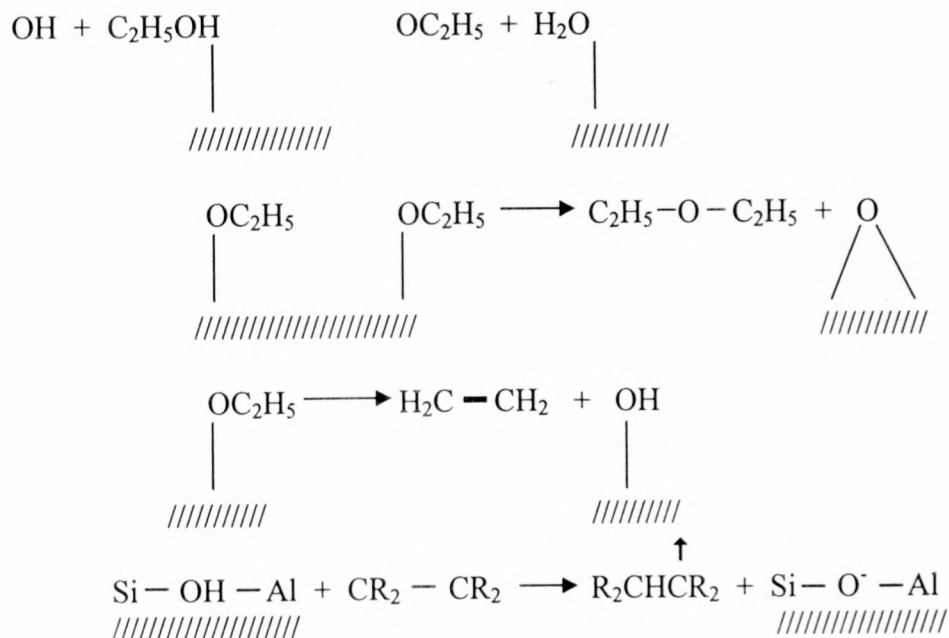


**Figure 2.8: Surface modification reactions (Shriver, 1990)**

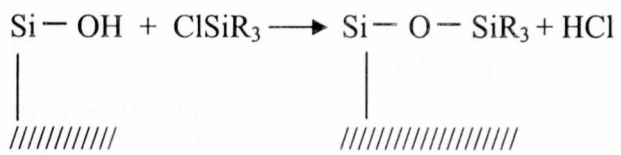
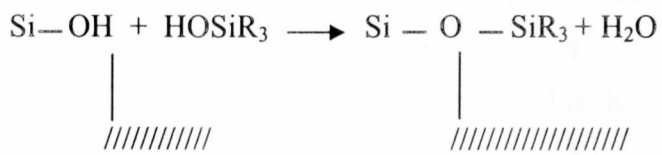
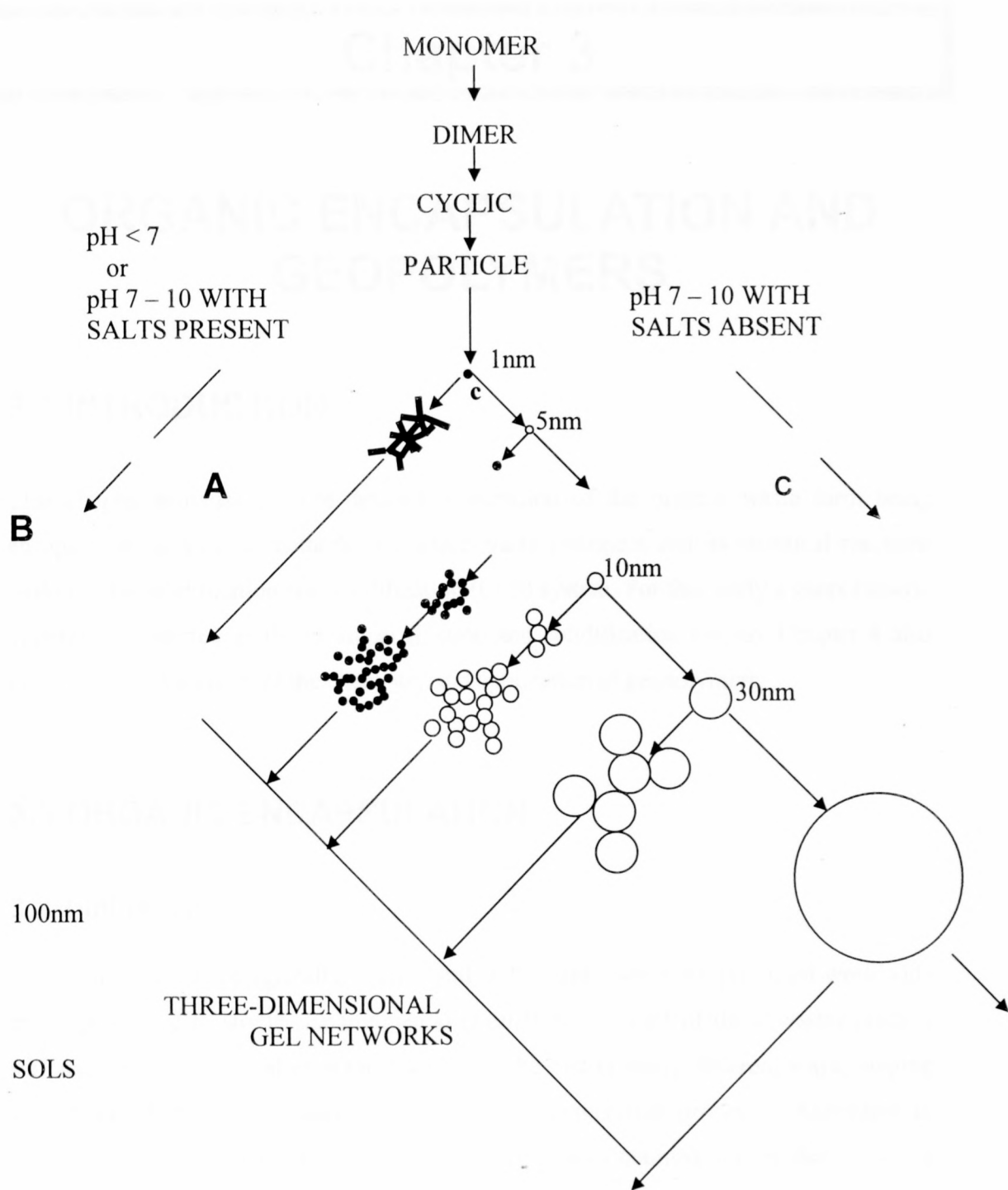


Figure 2.9: Stages of silicon polymerisation (Iler, 1979)





## Chapter 3

# ORGANIC ENCAPSULATION AND GEOPOLYMERS

### 3.1 INTRODUCTION

This chapter provides a more detailed explanation of the organic waste form being encapsulated as well as methods of organic waste treatment and its chemical reactions within a chemical fixation and solidification (CFS) system. For this study a geopolymeric system was selected as the chemical fixation and solidification system. Chapter 4 also gives a detailed account of the chemistry and application of geopolymers.

### 3.2 ORGANIC ENCAPSULATION

#### 3.2.1 Introduction

Enormous amounts of agricultural and synthetic organic waste are produced worldwide every year. Due to stricter environmental regulations disposal of these wastes poses a serious problem. Disposal of organic waste can be met in many different ways, ranging from crude dumping procedures to sophisticated incineration processes. According to Conner (1990) there are five distinct types of organic-containing wastes that might be encountered in chemical fixation and solidification treatment (Table 3.1). Group 5 (Table 3.1) organic-containing wastes are one of the more challenging/interesting waste groups when it comes to treatment by stabilisation and fixation. Research conducted for this study was based on a group 5 waste form.

### 3.2.2 Reasons for Organic Waste Encapsulation

Phenolic compounds can be toxic to soil microorganisms at the parts per million level (Kuwahara et al., 1970). Indeed several of the organic compounds classified by the U.S. Environmental Protection Agency as priority pollutants are phenols (Chapman et al., 1982). The fate of phenols in the environment and their removal from aqueous streams is complicated by their low solubility, ability to ionise, low vapour pressure, and tendency to undergo oxidation and oxidative polymerisation to humic and fulvic acid-type products (Wang et al., 1978; Flaig et al., 1975). The physiochemical properties of phenol and 4-chlorophenol are listed in Table 3.2. Phenols were selected because as noted above, they present one of the more challenging classes of pollutants to be removed from waste streams and ground waters.

### 3.2.3 Techniques for Organic Waste Treatment

Processes such as biodegradation, chemical oxidation, dechlorination and incineration generally destroy hazardous organic containing wastes. These processes are more often than not used as they completely destroy the hazardous organic waste and thereby eliminate any long-term effects that may be associated with its existence. The problems with these processes arise when toxic organics are present in small amounts. The use of destructive processes detailed above then becomes not only very expensive but sometimes also ineffective. It has, therefore, become necessary to develop stabilisation/solidification technologies for low-level organics. Most methods detailed use sorption techniques such as activated carbon and organoclays. The problem with these sorption techniques is that the organic remains within the activated carbon and organoclay and is partially reversible in a chemical fixation and solidification system. It is for this reason that the zeolite is coated with a layer of geopolymer before encapsulation within a geopolymeric matrix (Chapter 7).

### 3.2.4 Organic Reactions in a Chemical Fixation and Solidification System

The number of organic reactions that might occur in hazardous waste treatment is almost infinite (Conner, 1990). Aside from adsorption, volatilisation and biodegradation, the most likely reactions fall into four categories: hydrolysis, oxidation, reduction and salt formation (Conner, 1990).

#### (a) Hydrolysis

Hydrolysis generally results when another functional group substitutes the hydroxyl group at the reaction centre. Hydrolysis can be catalysed by both acidic and basic species,  $\text{OH}^-$ ,  $\text{H}^+$ , or  $\text{H}_3\text{O}^+$ . Typical hydrolysis reactions are shown in Figure 3.1. Dragun (1988) provides a summary of hydrolyzable chemical species that persist in water for more than a year at pH 7 and a temperature of 25°C (Table 3.3). Those less resistant to hydrolysis are listed in Table 3.4. Mabey and Mills have published work on the hydrolysis rates of organic chemicals in pure water systems. These data are useful for mainly comparative work but it suffers from certain limitations due to the fact that constituents and characteristics of a real waste system are not accounted for. In a real system adsorption on surfaces (eg. clay and activated carbon) may accelerate reactions, also metal ions present within the system (eg. copper and calcium) may act as catalysts for certain chemical reactions. These reactions are known to affect not only hydrolysis but also sorption, biological degradation and even volatilisation.

#### (b) Oxidation

Oxidation is one of the most common reactions that occur in a chemical fixation and solidification system. Table 3.5. lists a series of oxidation reactions. Oxidation of organics occurs via two pathways (Conner, 1990). The first pathway involves an electrophilic agent attacking an organic molecule and removing an electron pair. This is referred to as a heterolytic reaction. The second pathway involves the removal of only

one electron, thus forming a free radical, a homolytic reaction. Figure 3.2 is a summary of certain free radical reactions (Dragun, 1988). According to the summary (Dragun, 1988) free radical reactions involve three steps: initiation or formation of a free radical; propagation, which forms other free radicals; and termination, which destroys the free radicals. Previous research has shown that crystalline aluminosilicates at elevated temperatures and pressures catalyse organic oxidation reactions. Recently it has been shown that this catalysis can occur at ambient temperatures and pressures. With regard to oxidation reactions, Dragun and Helling (1985) have shown that certain generalities can be stated. These are:

- 1. Many substituted aromatics undergo free radical oxidation, for example benzene, benzidine, ethyl benzene, naphthalene, phenol and others among the organic priority pollutants.**
- 2. Chlorinated aromatics and polynuclear organics are unlikely to be oxidised.**

### **(c) Reduction**

When considering reduction in metals, a metal is said to be reduced if its valence state is lowered. For organics the definition is, however, different i.e. reduction is defined as an increase in hydrogen content or a decrease in its oxygen content. An example of organic reduction is shown in Figure 3.3. An organic species is also reduced if it experiences a net gain of electrons. Reduction of organic wastes is one of the least studied reaction areas, and is subsequently least understood. The system redox potential provides an indication of whether reduction is possible. Reduction is known to occur if the oxygen supply is deficient and if the system potential is less than that of the organic species.

#### **(d) Salt Formation**

Many organic compounds react easily with metals to form less soluble salts. According to Conner (1990) this may be the cause of the changes in morphologies and electron diffraction patterns observed by Chou et al. (1988) in cement matrices. The studies by Chou et al. (1988) show that these changes were observed with ethylene glycol and p-bromophenol. Conner (1990) states that it is likely that a number of organic acids of environmental concern could be effectively immobilised in the calcium rich environment of commercial chemical fixation and solidification systems. For example, the solubility of oxalic acid is 95,000 mg/l, compared with 6 mg/l for the calcium salt (Conner, 1990). Phenolics can be chemically changed in a chemical fixation and solidification system by precipitation as a calcium salt.

### **3.2.5 Commercial Processes**

Conner (1990) lists a few examples of organic “fixation” processes. These are contained in Table 3.6. Several researchers have conducted research into a number of chemical fixation and solidification systems that claim to immobilise organic pollutants. According to Conner (1990) several of these studies make mention of low level leaching without any indication of the initial levels of organic within the waste, or the effects of dilution and volatilisation of the constituents. Of interest is the work conducted on organoclays. Clays are altered by reacting them with quaternary ammonium compounds thus altering the surface of the clay from hydrophilic to hydrophobic. These alterations increase the adsorption capacity of the clay for organics. Other products of interest include activated carbon and ion exchange resins. Geopolymers provide an interesting and challenging solution as a chemical fixation and solidification system for organic waste treatment. It is this relatively new technology that will be discussed in the follow subsection.

## 3.3 GEOPOLYMERISATION

### 3.3.1 Introduction

The phenomenal durability of ancient mortars prompted research into the nature of these ancient compounds. Joseph Davidovits, a French chemist, pioneered the technology of geopolymerisation beginning in the 1970s and continuing throughout the 1980s and the 1990s. In the past ten years geopolymerisation has emerged as a possible solution to toxic waste treatment. By utilising waste materials (fly ash) and their reactive properties it is now possible to create geopolymer systems that are not only mechanically durable enough to be used as construction materials, but are also potential immobilisation systems for toxic waste. The remarkable achievements (Davidovits et al., 1994a, 1994b, 1988; Davidovits et al., 1990, 1999a, 1999b) made through geopolymerisation include mineral polymers (geopolymers), flexible ceramics, ceramic composites and concrete composites, which after 4 hours have higher strength and durability than the best currently used concrete. Geopolymerisation allows products to exhibit properties of rock-forming elements, namely chemical stability, hardness and longevity. A more detailed explanation of the chemistry, properties and applications of geopolymers are contained in the subsections that follow.

### 3.3.2 Chemistry

Geopolymers are inorganic polysialate species formed by the liberation of aluminium and silica species from starting materials. The starting materials are normally silica and aluminium rich waste materials such as fly ash. Geopolymers based on alumino-silicates are designated as poly (sialate), which is an abbreviation for poly (silico-oxo-aluminate) or  $(-\text{Si}-\text{O}-\text{Al}-\text{O}-)_n$ , with  $n$  being the degree of polymerisation (Davidovits, 1999a). The chemical structure shown in Figure 3.4 represents a poly (sialate-siloxo) geopolymer. The geopolymer forms as a result of the geosynthesis of poly (silicic) acid  $(\text{SiO}_2)_n$  and

potassium alumino-silicate, in an alkali medium (KOH, NaOH). In the structure the cross-linking element is the sialate (Si-O-Al-O-). The network consists of tetrahedral units of SiO<sub>4</sub> and AlO<sub>4</sub> linked alternatively by sharing all oxygen atoms. Aluminium in AlO<sub>4</sub> is IV-coordinated and carries a negative charge. Charge balancing cations such as Na<sup>+</sup>, K<sup>+</sup>, Ca<sup>2+</sup>, and Mg<sup>2+</sup> are needed for electrical neutrality.

A typical geopolymeric matrix consists of fly ash, kaolin, NaOH/KOH and sodium silicate. According to Davidovits et al. (1988) for geopolymerisation to occur the overall molar ratio Al<sub>2</sub>O<sub>3</sub>:SiO<sub>2</sub> must be between 1:5.5 and 1:6.5. Research by Van Jaarsveld et al. (1995) has shown that the ratio is not very critical when dealing with waste materials. The ratio for the most part is only an indication of the approximate composition of the waste. The geopolymer reaction has been shown (Van Jaarsveld et al., 1996) to proceed along three main steps:

1. **Dissolution:** The complexing action of the hydroxide species forms mobile polysialate species
2. The mobile precursors undergo **partially orientation**. The alkali polysilicates are also known to undergo **partial internal restructuring**.
3. **Reprecipitation** where the geopolymer system hardens into a solid monolithic inorganic polymeric structure.

Figure 3.5 (Davidovits, 1994a) is an example of a polycondensation reaction to form poly(sialate) and poly (sialate-siloxo). By utilising geopolymers and their cementitious properties it is now possible to create systems that can be used for a multitude of different purposes. It is these properties and applications thereof that are being discussed in the following subsection.

### 3.3.3 Applications

Geopolymers are cementitious products with the following properties:

**High early mechanical strength:** The compressive strength of a poly (sialate) geopolymer after 1 hour of drying at 65°C was 48.1 MPa. Type I concrete only reaches a maximum compressive strength of 45 MPa. Certain geopolymer matrices can achieve compressive strength values of 75 MPa (Van Jaarsveld et al., 1988).

**Excellent fire resistance:** The poly(sialate) geopolymer has good high temperature related properties being stable up to 1300°C whereas concrete begins to degrade at 300°C.

**Thermal insulation:** A geopolymer matrix carbon fibre composite and a glass- or carbon-reinforced polyester was irradiated at levels of 50 kW/m<sup>2</sup> (typical of the heat flux in a well-developed fire). The reinforced polyester ignited readily and released appreciable heat and smoke, while the carbon-fibre reinforced geopolymer composite did not ignite, burn or release any smoke (Lyon et al., 1999).

**Low density:** The density of a cured geopolymer carbon fibre composite was measured at 1.85 g/cm<sup>3</sup> (Lyon et al., 1999)

**Acid resistance:** Only 7% of a geopolymer matrix is destroyed in a 5% H<sub>2</sub>SO<sub>4</sub> solution in comparison to a 95% matrix breakdown for Portland cement (Van Jaarsveld et al., 1997).

**Low permeability:** The hydraulic permeability of the geopolymeric cement manufactured by Davidovits (1994b) was measured at 1.0<sup>-9</sup> at 28 days and 1.0<sup>-11</sup> at 364 days. Permeability values for Portland cement are 10<sup>-10</sup>.

**Fast setting:** According to Van Jaarsveld et al. (1998) a geopolymer cured at 1 day reaches a compressive strength of 75 MPa. Type I concrete can only reach a maximum compressive strength of 45 MPa after a 90-day curing period.

**Less CO<sub>2</sub> emission than Portland cement:** Geopolymeric cement produces five times less CO<sub>2</sub> during manufacture than Portland cement (Davidovits, 1999b).



According to Davidovits geopolymer composites have three main properties that make them superior to ceramics, plastics and organic composite materials.

**First:** Geopolymers are very easy to make, as they handle easily and do not require high heat.

**Second:** Geopolymeric composites have a higher heat tolerance than organic composites.

**Third:** The mechanical properties of geopolymer composites are as good as those of organic composites. In addition, geopolymers resist all organic solvents (only affected by strong hydrochloric acid).

Utilising the geopolymer properties listed above it is now possible to create matrices that have the following applications:

- Geopolymer binders can be mixed with rock aggregates (fly ash) to produce geopolymer cement or mixed with carbon fibres to produce non-flammable composites. These binders have numerous environmental applications, such as the encapsulation of hazardous, radioactive wastes and toxic metals. They are also used as cappings in waste dumps and landfill sites, as water barriers where water deflection is needed as sealants and other structures necessary for toxic waste containment sites.
- Geopolymer cements could also replace any current building component being used such as bricks and ceramic tiles. The mouldability of geopolymeric pastes is very good, hence their use in simple structures such as fences, paving materials and low cost pipes.
- Geopolymeric concretes generally have very high compressive strengths and early setting properties; this makes them ideal for structural surfaces like floors and storage areas. The strength of geopolymeric concrete is such that a heavy Boeing can land on a runway freshly patched with geopolymer concrete only 4 hours after it has been laid (Davidovits, 1999b).

- Utilising the fire resistant properties of geopolymers, a (GEOPOLYMER) matrix carbon fibre composite was manufactured (Lyon et al., 1999) which was tested for use in aeroplane cabins to render the panels fireproof.
- Geopolymers are now finding widespread applications in all fields of industry namely, aerospace industries, plastic industries, waste management, art and decoration, automotive and many more.

### **3.4 SUMMARY**

As Van Jaarsveld et al. (1997) stated: “In order to optimise the advantages offered by geopolymers derived from waste materials, it is imperative to identify as well as quantify critical parameters that affect the eventual structural stability of the finished product”. A more comprehensive solid state analytical technique or method is needed to provide conclusive results as far as structural analysis is concerned. Methods and techniques currently available are both expensive and time consuming, providing limited and inconclusive results. Chapter 5 is a discussion on the method of encapsulation of organics within geopolymers and the analytical techniques utilised to study the effects of organic addition on geopolymerisation. The last few years have seen spectacular technological progress in the development of geopolymer applications and procedures, thus transforming ideas in inorganic and mineral chemistry. It is apparent from the discussion above that geopolymerisation could find applications in many varying industrial fields.

**Table 3.1: Organic-containing wastes (Conner, 1990)**

Group	Waste Form
1	Oil and solvent based waste forms eg. refinery waste.
2	Aqueous waste containing large quantities of water soluble/insoluble emulsified organics that are hazardous according to regulations.
3	Aqueous waste containing large quantities of water soluble/insoluble emulsified organics that are not hazardous.
4	Aqueous wastes containing small amounts of non hazardous organics < 1% and usually in the 10-1000 mg/l range -that are of interest in CFS systems
5	Aqueous wastes containing small amounts of hazardous organics < 1% and usually in the 10-1000 mg/l range.

**Table 3.2: Physiochemical properties of phenol and 4-chlorophenol**

Compound	pKa	$\lambda_{\max}$ (nm)	$\epsilon_{\max}$
Phenol	9.89	270	1449.6
4-Chlorophenol	9.18	278	1465.6

**Table 3.3: Chemical resistant to hydrolysis (Dragun, 1988)**

Category	General Structure	Persistent Chemicals
Esters	$R_1C(O)OR_2$	All Al esters of Al, Ar, or allylic acids.
Amides	$R_1C(O)NR_2R_3$	All amides where $R_1$ , $R_2$ are Al or Ar; only amides with halogenated alkyl $R_3$ hydrolyse rapidly.
Nitriles	$RCN$	All aliphatic or aromatic nitriles.
Acyl chlorides	$RC(O)Cl$	No acyl chlorides
Carbamates	$R_1OC(O)NR_2R_3$	All carbamates having only Al or Ar on N and O.
Alkyl halides	$RX$	All AlF and polychloro- or poly-bromo-methanes
Phosphorous acid esters	$R_1P(O)R_2R_3$	All esters where $R_1$ is Al or Ar and $R_2$ and $R_3$ are AlO and ArO.
Epoxides, lactones, sultones		Only hindered, bicyclic epoxides; no simple lactones or sultones.

**Table 3.4: Chemicals less resistant to hydrolysis (Dragun, 1988)**

Alkyl and benzyl halides
Polymethanes
Substituted epoxides
Aliphatic acid esters
Chlorinated acetamides
Certain carbamates
Phosphoric acid halides
Phosphoric acid and thiophosphoric acid esters
Acylating and alkylating agents

**Table 3.5: Oxidation reactions (Conner, 1990)**

Reactants	Products
Phenol + 14 H <sub>2</sub> O <sub>2</sub> + Fe <sup>+2</sup>	6 CO <sub>2</sub> + 17 H <sub>2</sub> O
R - CH <sub>3</sub>	R - COOH
R - CH <sub>2</sub> OH	R - COOH
RCHOH - CHOHR'	R - COOH + R' - COOH
R - CHO	R - COOH
R <sub>2</sub> CH <sub>2</sub>	R <sub>2</sub> CO
R <sub>2</sub> CH(OH)	R <sub>2</sub> CO
R <sub>3</sub> CH	R <sub>3</sub> C(OH)
R <sub>3</sub> CH + HCR' <sub>3</sub>	R <sub>3</sub> - C - C - R' <sub>3</sub>
R <sub>2</sub> N - H + H - NR' <sub>2</sub>	R <sub>2</sub> N - NR' <sub>2</sub>
RCH = CHR'	RCHOH - CHOHR'
2R - SH	R - S - S - R
R - S - S - R'	R'SO <sub>3</sub> H + RSO <sub>3</sub> H

**Table 3.6: Organic fixation processes (Conner, 1990)**

<b>Waste description</b>	<b>CFS System</b>	<b>Leaching Test</b>
Synthetic waste	Cement/soluble silicate	TCLP
Synthetic waste	Cement/soluble silicate + FeCl <sub>2</sub>	TCLP
Synthetic waste	Cement/soluble silicate + Na <sub>2</sub> S	TCLP
Leaded gasoline	Proprietary sorbent	TCLP
Unleaded gasoline	Proprietary sorbent	TCLP
Diesel fuel	Proprietary sorbent	TCLP
Kepone-contaminated sediment	None	Water
Kepone-contaminated sediment	Cement/soluble silicate	Water
Kepone-contaminated sediment	Organic	Water
Kepone-contaminated sediment	Sulfur-based	Water
Waste caulking compound latex	Cement	EPT
Lagoon sludge	Kiln dust	EPT

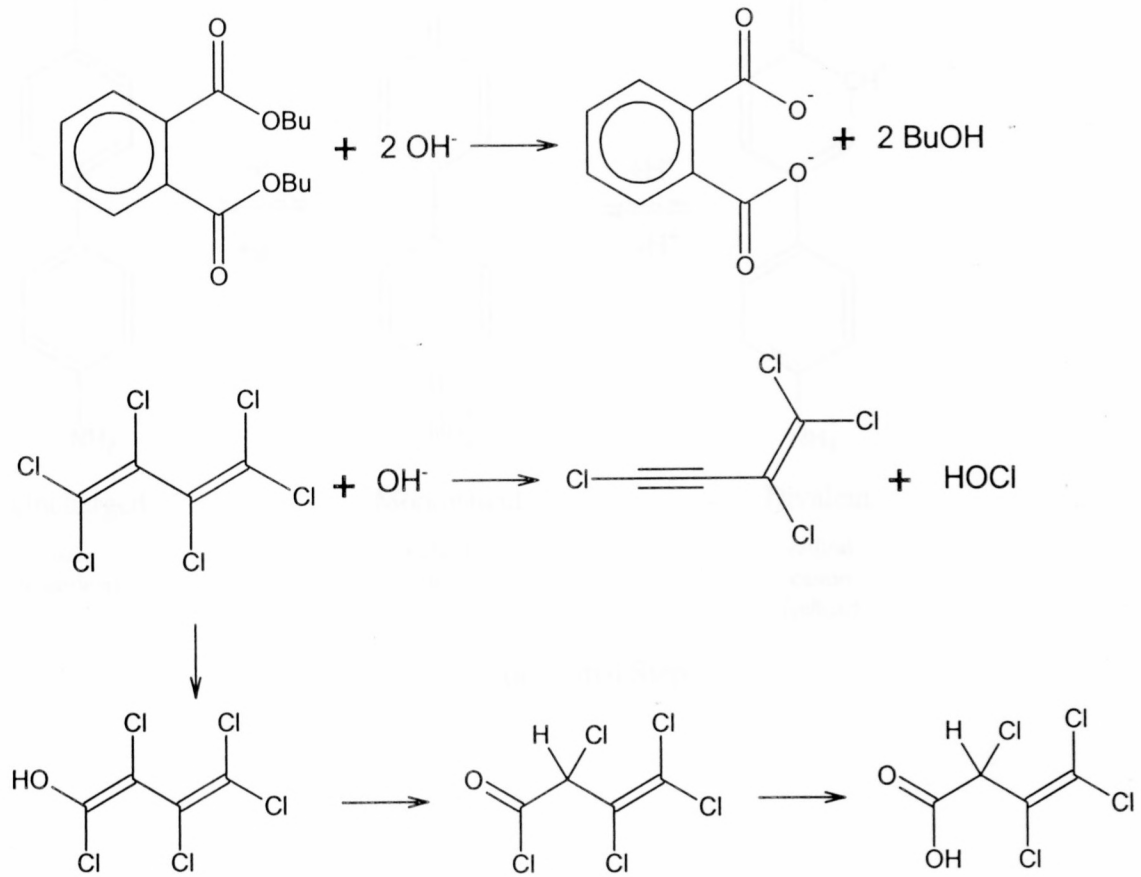
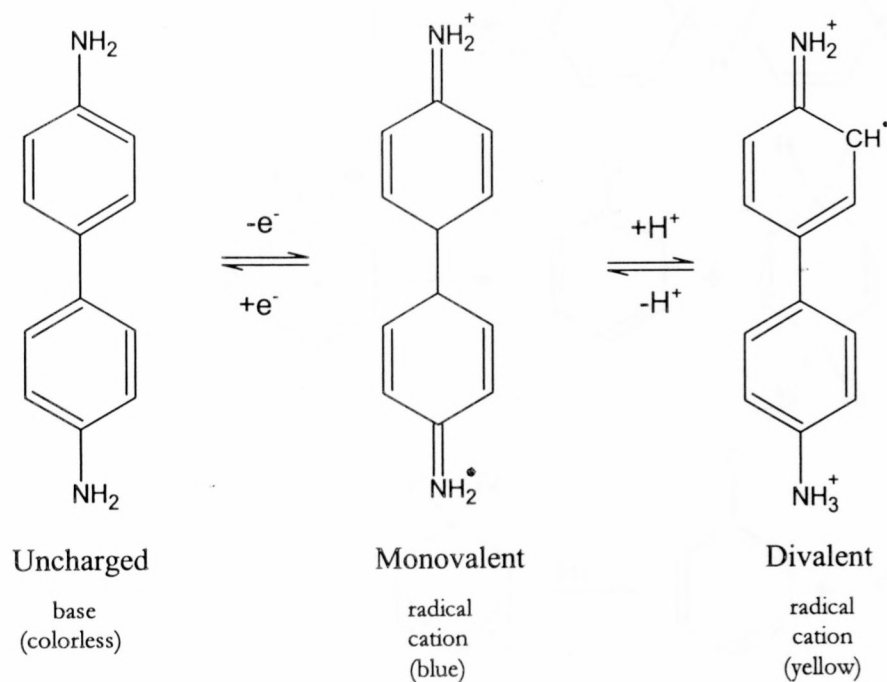
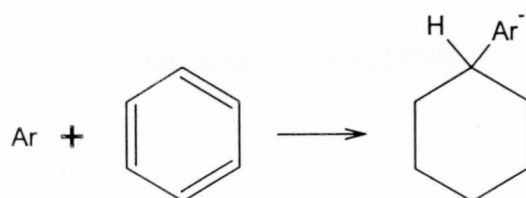
**Figure 3.1: Hydrolysis reactions (Dragun, 1988)**

Figure3.2: Free radical reactions (Dragun, 1988)

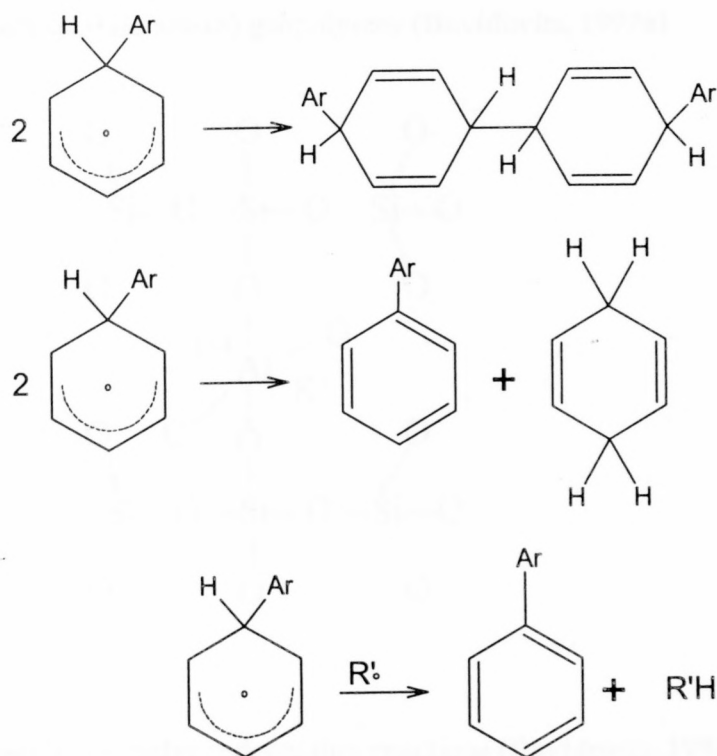


(a) Initial Step



(b) Propagation step





(c) Termination step

**Figure 3.3: Organic reduction reactions (Conner, 1990)**

Increase in hydrogen content



Decrease in oxygen content



**Figure 3.4: A poly (sialate-siloxo) geopolymer (Davidovits, 1999a)**

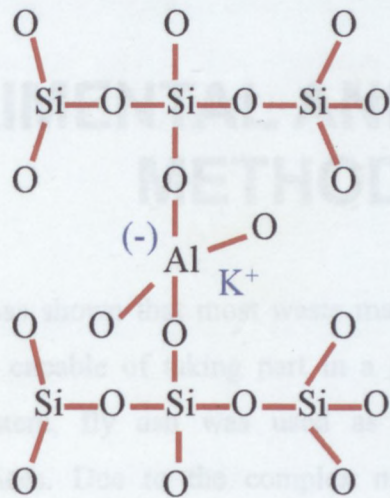
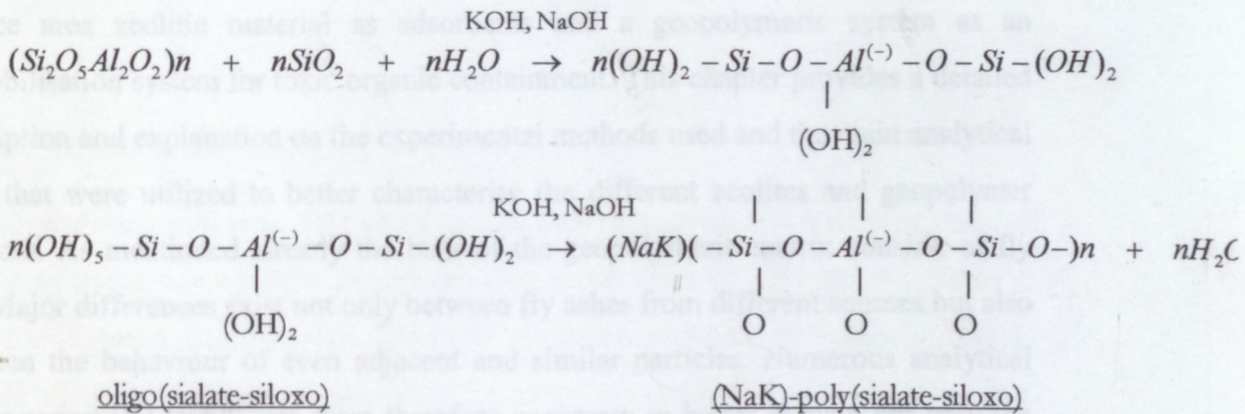
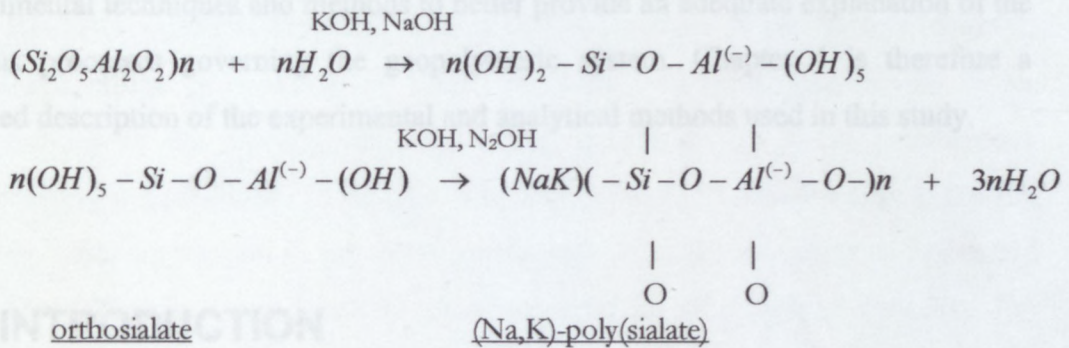


**Figure 3.5: Geopolymer polycondensation reactions (Davidovits, 1994a)**



# Chapter 4

## EXPERIMENTAL AND RESEARCH METHODS

Previous research has shown that most waste materials containing sources of silica and aluminium are capable of taking part in a geopolymerisation reaction (Forss, 1983). In this system, fly ash was used as the reactant in creating various geopolymeric matrices. Due to the complex nature of fly ash, analysis of the geopolymeric matrices is complicated. Further complications arise as a result of numerous interactions between the contaminant (waste organic material) and the bulk of the geopolymer phase. In this study we have therefore resorted to a combination of experimental techniques and methods to better provide an adequate explanation of the various processes governing the geopolymeric system. Chapter 4 is therefore a detailed description of the experimental and analytical methods used in this study.

### 4.1 INTRODUCTION

The main objectives of this study were to explore the possibility of utilising high surface area zeolitic material as adsorbents and a geopolymeric system as an immobilisation system for toxic organic containment. This chapter provides a detailed description and explanation on the experimental methods used and the main analytical tools that were utilized to better characterise the different zeolites and geopolymer matrices. As mentioned already the bulk of the geopolymeric matrix consists of fly ash. Major differences exist not only between fly ashes from different sources but also between the behaviour of even adjacent and similar particles. Numerous analytical and experimental techniques were therefore necessary to better explain not only the geopolymeric system, but also zeolite synthesis and characterisation. The main analytical tools described in this chapter include X-ray diffraction (XRD), X-ray

fluorescence spectroscopy (XRF), infrared spectroscopy (IR), scanning electron microscopy (SEM), inductively coupled plasma spectroscopy (ICP), compressive strength tests, specific area tests, particle size distribution analysis, proton induced x-ray emission (PIXE), adsorption analysis, zeta potential analysis, and atomic adsorption spectroscopy (AA). The experimental techniques for zeolite and geopolymer synthesis used in this study will also be discussed in this chapter.

## **4.2 EXPERIMENTAL METHODS**

### **4.2.1 Experimental Materials**

The fly ashes used for all experimental work were obtained from two different sources, SASOL (Sasolburg, South Africa) and Eskom (Ash Resources, South Africa). The fly ashes were of coal origin. Kaolinite (Grade G3) was obtained from G & W Base and Industrial Minerals. A more detailed analysis of the starting materials (physical/chemical properties) is listed in Table 4.1 and Table 4.2. Oxide compositions of the starting materials were determined by X-ray fluorescence spectroscopy and are listed in Table 4.1. The chemicals, KOH, sodium silicate and the phenolic compounds used in the experiments were of analytical grade and obtained from Merck, South Africa. Distilled water was used for all sample preparation. The natural zeolite, clinoptilolite was obtained from Pratley, South Africa.

### **4.2.2 Preparation of Geopolymer Matrices**

Fly ash and kaolinite were mixed for 1 minute by hand, after which a solution of potassium hydroxide mixed with sodium silicate was added, followed by a further 2 minutes of mixing. Samples were cast in 50 x 100mm cylinders, vibrated for 1 minute and set at 30°C for 7 days. Figure 4.1 is a photograph of a cured geopolymer matrix. The mass percent of the various components (flyash, kaolinite etc.) of the geopolymer matrices was varied to produce geopolymer matrices that exhibited good compressive

strength results. The result thereof was that recipe 19 and 36 produced matrices that gave good compressive strength data. Recipes 19 and 36 were therefore utilised to produce standard geopolymer matrices. The composition of the standard geopolymeric matrices that will be investigated in this study is given in Table 4.3. For zeolite and organic encapsulation the mass percent of kaolin, sodium silicate and potassium hydroxide was held constant throughout the matrices while only varying the mass percent of zeolitic material and organics being added to the matrix. Compositions of the matrices containing organic contaminants and zeolitic material will be described in more detail in Chapter 5 and Chapter 7, respectively.

### **4.2.3 Zeolite Synthesis**

The zeolite samples were prepared using a modification of the procedure of Woolard et al. (2000). 40g of Eskom fly ash were refluxed with a 3M sodium hydroxide solution at 100°C for 72 hours. The slurries were then filtered, repeatedly washed with distilled water to remove excess sodium hydroxide and then vacuum dried at 60°C for 24 hours. This method converts the ash into zeolite minerals and solubilises the toxic trace elements, which are in the base medium. Zeolite Na-P1 was identified in the ash treated with 3M sodium hydroxide. It should be noted that the 3M sodium hydroxide solution used for the treatment of fly ash can be reused up to 4 times without there being any significant difference in the ion exchange capacity value (CEC) of the zeolite.

#### **4.2.3.1 Acid Treatment of Zeolite NaP1**

The acid treatment of zeolite NaP1 is an adaption of the experimental procedure of Woolard et al. (2000). 20g of zeolite NaP1 were refluxed with a 3M hydrochloric acid solution for 6.5 hours. The slurry was then washed with distilled water, filtered and vacuum dried at 60°C for 24 hours. Acid treatment of zeolite NaP1 is done primarily to remove cementitious materials such as calcium carbonate, which promotes agglomeration of particles.

#### **4.2.3.2 Dealumination of Zeolite NaP1 and Clinoptilolite**

Aluminium was removed from the framework of zeolite NaP1 and clinoptilolite by following the procedure of Shu et al. (1997). The dealuminated zeolites were converted to a more hydrophobic structure with a higher adsorption capacity for organic molecules. Aluminium was removed from the framework as follows: 20g of zeolite were mixed with 800ml 1M ammonium chloride solution and aged at 90°C for 2 hours. The sample was filtered, washed with deionised water and air-dried. The air-dried sample was calcined at 600°C for 2 hours. After calcining, the sample was refluxed in a 2M hydrochloric acid solution for 2 hours. The sample was then washed repeatedly with deionised water until chloride free, and then air-dried.

#### **4.2.3.3 Ion Exchange Capacity (CEC)**

The ion exchange values (CEC) of zeolite NaP1 were determined using the procedure of Hesse (1972) and Woolard et al. (2000). 1g of the zeolite sample was stirred with a 1M sodium acetate (30ml) solution for 5 minutes. The sample was centrifuged and the procedure repeated twice more on the same sample. The solid was then stirred three times with 95% ethanol (30ml). The solid was thereafter mixed with a 1M ammonium acetate (30ml) solution and shaken 3 times. The CEC of the sample was determined by analyzing the ammonium acetate solution for sodium content. The concentration of sodium in solution provides an indication of the exchangeable ions on the surface of the zeolite, since the ammonium ion replaces sodium.

#### **4.2.3 Dissolution Experiments**

Dissolution tests were performed to determine the relative solubilities of silica and aluminium from the different fly ashes as this is thought to be analogous to the first stage of geopolymerisation. The experiment consisted of mixing 1 to 9 grams of fly ash with different molar concentrations of alkaline and phenolic solutions over a 16 hour time period. The samples were then centrifuged and 20ml of the liquid solution was mixed with 10ml of a 36% hydrochloric acid solution and 10ml of a 500ppm scandium internal standard solution.

## 4.2.4 Leaching Tests

Leaching experiments are normally conducted when evaluating the efficiency of an immobilisation system as an encapsulation method for organic waste. When evaluating a material for leachability, the concentration of the hazardous constituent in the leachate is compared to that in the original immobilisation system. Leaching experiments were performed using a modified TCLP (U.S. Federal Register, 1990) adapted by Van Jaarsveld (2000). A summary of the difference between the standard TCLP tests and the adapted test of Van Jaarsveld, is provided in Table 4.4. The modified TCLP method was used because an acid rain test has a varying pH, resulting in an alkaline environment, which slows down leaching. This does not necessarily represent the long-term effects of acid rain on the immobilisation system. The adapted test was also utilised due to the very low ion concentrations, which were leached with the TCLP test. These low ion concentrations made analysis difficult.

Samples that underwent leaching tests were crushed and sieved into two particle sizes, 3350 and 250 $\mu\text{m}$ . The samples were stirred in a leaching vessel utilising an acetic acid buffer solution at  $\text{pH} = 3.3$ . The purpose of the acetic acid is to simulate the organic acids generated in a landfill site during the decomposition of organic matter in the refuse. The solid /liquid ratio was kept at 1:25 and the test was performed at room temperature. Samples were taken at 1, 5, 10, 20 and 30 minutes. Samples were also taken at 1, 2, 6, 8, 24 and 48 hours. Sampling was done using a syringe and the sampling volume was 10 $\text{cm}^3$ .

The main objective of the leaching experiments was to predict the long-term behaviour of the immobilisation system by using a short-term laboratory scale test.

## 4.3 METHODS OF ANALYSIS

### 4.3.1 X-ray Diffraction (XRD)

The detection of crystalline phases within the geopolymer and zeolite samples was determined by X-ray diffraction (XRD). Identification of the various crystalline

phases was determined by comparing zeolite/geopolymer diffraction patterns to JCPDS (Joint Committee on Powder Diffraction Standards) data. Samples were finely crushed by mortar and pestle and analysed using Cu-K $\alpha$  radiation. A step size of 0.02°2 $\theta$  and a counting rate of 10 seconds per step were employed. This is a very slow scanning speed with the purpose of obtaining the maximum diffraction resolution. The samples were scanned over a range of 5 to 80°2 $\theta$ . This configuration gives a detection limit of approximately 4 mass per cent of the crystalline phases present in the sample.

### **4.3.2 X-Ray Fluorescence Spectroscopy (XRF)**

The mineral oxide compositions of the starting materials were determined by X-ray fluorescence spectroscopy (XRF) analysis. Samples were dried at 60°C to expel excess moisture. The samples were then ignited overnight to determine loss on ignition (LOI) values. A glass fusion disc was used to analyse major elements accurately. The glass disks were analysed on a PW 1404 Philips sequential wavelength dispersive X-ray fluorescence spectrometer. Data were first corrected for drift then put through the UCT programme "trace" to correct for line overlaps and spectral background.

### **4.3.3 Infrared Spectroscopy (IR)**

Infrared spectra for the geopolymer matrices and the zeolite samples were recorded on a Fourier Transform Infrared Spectrometer, Perkin Elmer Paragon 1000 PC (FTIR) with a Photo-acoustic Cell Spectrometer (PAS) accessory. The IR spectrometer measures the transmittance (or absorbance) of a sample as a function of wavelength (or frequency). When the wavelength of the spectrometer radiation has the same vibrational frequency as the molecules in the sample, energy is removed from the optical laser beam, and this appears as an absorption band in the recorded spectrum. The FTIR/PAS instrument makes it possible to identify polymers (provided they are transparent or in solution film), by matching the test spectra with known spectra. The



PAS is an important accessory to the FTIR, as it enables the analyst to scan samples with no sample preparation required, irrespective of whether the sample is a solid or liquid.

#### **4.3.4 Scanning Electron Microscopy (SEM)**

Scanning Electron Microscopy (SEM) analysis was conducted on certain geopolymer and zeolite samples. The samples were crushed and the particles sputter coated with pure gold before the analysis. SEM tests were utilised to reveal any significant morphological changes that were brought about by the modification procedures. SEM tests were also used in conjunction with XRD tests for the detection of crystalline phases after the modification procedures.

#### **4.3.5 Inductively Coupled Plasma Spectroscopy (ICP AES)**

Inductively coupled plasma spectroscopy (ICP) tests were performed on the liquid samples of different fly ashes and leaching experiments. ICP tests were utilised to obtain maximum amounts of silicon and aluminium (from the different fly ashes) that are available for polysialate formation. ICP tests were also performed to gain an indication of the amount of silicon and aluminium leached from the geopolymeric matrices.

The ICP test consisted of filtering 20ml of the liquid solution, and adding to it 36% of a hydrochloric acid solution. 10ml of a scandium solution was added as an internal standard to both the blanks and the samples used throughout the analysis.

#### **4.3.6 Compressive Strength Tests**

Compressive strength analysis was performed according to Australian Standard 10129 (1986). All samples were vibrated for 1 minute, cast in cylinders, 50 mm in diameter and 100 mm in length and cured for 7 days at 30°C. The samples were then tested

after 7 days using a Contets 3114 compressive strength analysis apparatus. Compressive strength analysis was used to measure the physical strength of the geopolymeric matrix as well as to get an indirect measurement of the strength of the bonds (Al-O-Si) within the geopolymer. Compressive strength results were also utilised as an indication of the efficiency of organic incorporation within the geopolymeric matrix.

#### **4.3.7 Surface Area Analysis**

Specific area tests were determined for all zeolite samples and certain geopolymeric matrices. All samples were analysed using an Accelerated Surface Area and Porosimetry System (ASAP 2010). The samples were first vacuum dried at 100°C for 3 hours before degassing at 95°C for 24 hours. Specific surface area test results provided information on the porosity of the geopolymeric matrix before and after the modification procedures, while specific surface area measurements on the zeolite samples provided an illustration of the variation in specific surface area after the modification treatments.

#### **4.3.8 Particle Size Distribution Tests**

Particle size measurements of the fly ash were measured using a Malvern Mastersizer, S Longbed version 2.15. The particles were suspended in distilled water and measurements were taken by means of a laser.

#### **4.3.9. Proton Induced X-ray Emission (PIXE)**

Proton induced X-ray emission (PIXE) spectroscopy is a new technique for elemental analysis. The analysis is based upon the excitation of the inner most electrons of the atom by moderately energetic protons. These protons have sufficient energy to penetrate the outer electron orbitals of the target atom and knock out the K and L shell electrons. The outer cascading electrons fill up these vacancies and x-rays are given

off. The electron configurations of all atoms are different; hence the x-rays emitted are unique fingerprints of the target atoms. The x-rays are sorted by energy and counting them tells us which and how much of an atom is present. PIXE set-ups generally utilise more than one x-ray detector; one detector is used to measure the x-rays generated and the other to count the protons used to generate these x-rays. These are the two measurements generally required to do quantitative analysis. PIXE analysis was utilised as a tool to gain quantitative data on the elements present in geopolymer matrices after the geopolymerisation process, that is to check how elemental concentrations are affected by geopolymerisation.

#### **4.3.10 Organic Adsorption Measurements**

The concentration of organics in solution was determined using a Dionex A1450 Basic Chromatography Module with UV detector. A 70/30 mixture of water and acetonitrile was used as the mobile phase for phenol analysis while a 60/40 mixture of water and acetonitrile was used as the mobile phase for chlorophenol analysis. Adsorption analysis was carried out on a Phenomenex Luna C<sub>18</sub> (2) column with a flow rate of 1ml per minute. 5g of zeolite NaP1 and clinoptilolite was rolled in a 500ppm phenol/chlorophenol solution for 48 hours. Adsorption was determined by the difference between initial and final concentration of organics in solution. In quantifying the adsorption measurements of the zeolites, the adsorption efficiency of the different zeolitic material could be determined.

#### **4.3.11 Zeta Potential Data**

Zeta potential of the synthesised zeolites was analysed on a Zetasizer over a pH range of 2-12. Approximately 0.1g of sample is ground to a fine powder and suspended in 50ml of 0.05M KCl solution. Aliquots of this are adjusted to cover the full pH range from 2-12 using HCl and KOH. The zeta is then read on the Zetasizer giving an average of 3 readings. These values are plotted against the specific pH. Zeta potential data provide information on the surface charge of the zeolite. This information is necessary to find the pH range where maximum organic adsorption is possible.

### **4.3.12 Atomic Absorption Spectroscopy (AA)**

The ionic exchange capacity (CEC) of zeolite NaP1 was determined using Atomic Absorption Spectroscopy (AA). For CEC determinations the fly ash solutions were analysed for sodium content. The concentration of sodium in solution gives an indication of the ions on the surface of the zeolite readily available for surface reactions.

## **4.4 SUMMARY**

Chapter 4 provides a description of the numerous experimental procedures used in this study as well as the different analytical tools required to provide a more adequate explanation of the synthesis, encapsulation methods and leaching mechanism of the geopolymeric matrices. The results of these experiments are discussed in Chapters 5, 6 and 7.

**Table 4.1: Oxide composition as determined by XRF analysis**

<b>% Oxide Composition</b>	<b>Eskom fly ash</b>	<b>SASOL fly ash</b>	<b>Kaolin G3</b>
SiO <sub>2</sub>	53.8	55.0	66.5
Al <sub>2</sub> O <sub>3</sub>	33.0	28.4	22.0
Fe <sub>2</sub> O <sub>3</sub>	3.4	3.5	0.4
CaO	4.4	7.2	0.1
MgO	1.1	1.7	0.3
K <sub>2</sub> O	0.7	0.5	2.9
Na <sub>2</sub> O	0.4	0.4	0.5
TiO <sub>2</sub>	1.7	1.7	0.7
P <sub>2</sub> O <sub>5</sub>	0.5	0.3	0.2
BaO	0.1	0.2	
MnO	0.05	0.04	
(LOI)	0.8		5.4
Total	99.9	98.8	99.0

**Table 4.2: Surface area / Mean particle size data for starting reagents**

<b>Mineral</b>	<b>BET Surface Area (m<sup>2</sup>/g)</b>	<b>Mean Particle Size (d<sub>90</sub>, μm)</b>
Kaolin	11.1462	11.09
Eskom fly ash	1.0850	26.56
SASOL fly ash	5.3959	136.89

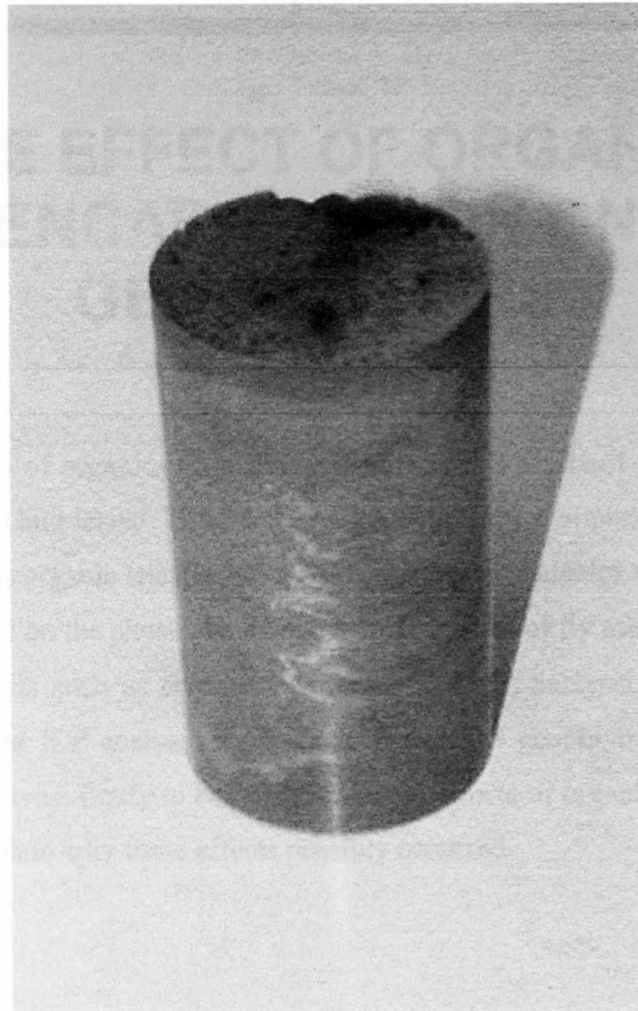
**Table 4.3: Ingredients of the geopolymeric matrices**

<b>Ingredient</b>	<b>Composition (mass%) [Recipe 19]</b>	<b>Composition (mass%) [Recipe 36]</b>
Fly ash	59.2	60.0
Kaolinite	6.6	6.7
KOH	6.6	8.0
Sodium Silicate soln	14.5	14.7
Water	13.2	10.7

**Table 4.4: The differences between standard TCLP tests and adapted TCLP tests  
(Van Jaarsveld, 2000)**

<b>Criteria</b>	<b>TCLP Test</b>	<b>Adapted TCLP tests</b>
Liquid:solid ratio	20:1	25:1
Extraction medium	Acetic acid (unbuffered)	Acetic acid (buffered)
Extraction time	18 hours	24-72 hours
pH control	3.0, No	3.2 ± 0.5
Agitation method	Tumbler	Overhead stirrer
Temperature Control	19-25°C	30°C
Sampling	Once	18-12 times
Particle size	<4000µm	212-2360µm

**Figure 4.1: Photograph of a cured geopolymer matrix.**



## Chapter 5

# THE EFFECT OF ORGANIC ENCAPSULATION ON GEOPOLYMERS

To study the effects of organics on geopolymer matrices a standard geopolymer matrix was first formulated and tested. The matrix with a fairly high compressive strength value was then utilised for organic encapsulation. This chapter investigates the effect of phenol and 4-chlorophenol on the physical and chemical properties of fly ash based geopolymer binders. Various tests such as compressive strength, PIXE analysis, X-ray diffraction, infrared analysis and ICP analysis were conducted on the geopolymer matrices. These tests had two objectives, firstly to better describe the effects of organics on geopolymers and secondly to explain why these effects possibly occurred.

### 5.1 BACKGROUND

The geopolymer matrices synthesised for experimental work conducted in this study were fly ash based. The use of fly ash and clays as a starting material for geopolymer synthesis has been reported by numerous authors, including Van Jaarsveld et al. (1998), Davidovits (1991) and Rahier et al. (1997). Van Jaarsveld et al. (1998) reported on the use of fly ash based geopolymers for the encapsulation of toxic metal contaminants. The differences in mineralogy and solubility of fly ashes significantly affect the setting time and final strength of geopolymer matrices (Van Jaarsveld, 2000). These differences were also observed when a standard geopolymer matrix was formulated.



## 5.2 GEOPOLYMER MATRICES

Two different types of recipes (19 and 36) and two different types of fly ashes (SASOL and Eskom) were utilised to synthesise various geopolymer matrices that would be the standard matrices for organic and zeolitic encapsulation. Recipes 19 and 36 were used because the geopolymers that formed exhibited better compressive strength results than the other synthesised recipes. The mass percent of reagents needed for each recipe is detailed in Table 4.3. XRF (Table 4.1), surface area and mean particle size tests (Table 4.2) were conducted on the starting reagents as an indication of the physical properties of these materials. ICP tests, compressive strength tests, infrared analysis, X-ray diffraction, SEM analysis, specific surface area results and PIXE analysis were then conducted on the standard geopolymer matrices.

### 5.2.1 Compressive Strength

Compressive strength analysis was utilised to measure the strength of the geopolymeric matrices and thereby indirectly provide an indication of the strength of the Al-O-Si bond. Matrices were also synthesised using NaOH as a starting reagent (Table 5.1).

Comparing the compressive strengths of the matrices synthesised from SASOL fly ash to those from Eskom, it is evident that matrices manufactured from SASOL fly ash exhibit higher compressive strength values. These differing values could be attributed to the difference in mineralogy between SASOL fly ash and Eskom fly ash. A significant difference is the higher CaO content in SASOL fly ash (Table 4.1). Generally the Ca cations provide extra strength by forming various calcium aluminosilicate hydrates. XRD analysis, however, shows no such formation, therefore a possible explanation for the difference in these strength values may be contained in the ICP data.

A difference in compressive strength also exists between matrices 19 and 36, with matrices synthesised from recipe 36 exhibiting higher compressive strengths. Recipe 36

has a higher mass percent of KOH and lower mass percent of water. This difference in mass percent increases the KOH concentration thereby increasing Al and Si dissolution rates (Refer to ICP data, Table 5.2 and Table 5.3). It should be noted that due to the higher compressive strength values attained for recipe 36, it was this recipe that was then utilised for further testing.

In the case of 36 Sasol (NaOH) and 36 Sasol the same amount (g) of NaOH and KOH was added respectively This resulted in 36 Sasol (KOH used as the basic medium) having a higher compressive strength. The larger  $K^+$  favours the formation of larger silicate oligomers with which  $Al(OH)_4^-$  prefers to bind. Therefore, in KOH solutions more geopolymer precursors exist, which results in better setting and stronger compressive strength of the geopolymer than in the case of NaOH. Research reported by Van Jaarsveld (2000) provides a more detailed explanation on the effect of alkali metal cations on geopolymerisation.

## 5.2.2 ICP Analysis

In order to quantify the relative amounts of Al and Si released from Eskom and SASOL fly ashes, dissolution experiments were conducted. Table 5.2 and Table 5.3 contain a summary of these results. The ICP results reported are total Si and Al.

When NaOH and KOH concentrations increased from 3.3M-6.6M the concentrations of Al and Si in solution increased. Analysis of these results clearly indicates that the dissolution of Al and Si is dependent on the type of alkali cation present in the hydroxide solution. NaOH solutions increase the dissolution rates of Si and Al. However, the concentrations of Si are higher than that of Al, which could be due to the higher Si content, in the form of  $SiO_2$  in the minerals. Generally Si has a higher dissolution rate than Al. The higher the Si:Al (Si:Al  $\gg$ 3:1), the higher the compressive strength values, the stronger the geopolymer, the better the mechanical properties. The higher compressive strength values occur because of the 2D cross-link polymeric character of

the geopolymer (20:1<Si:Al<35:1). Table 5.4 summarises the Si:Al ratio for the various fly ashes. For a geopolymer to be an effective radioactive and toxic waste encapsulation matrix a Si:Al 2:1 is required. ICP data illustrate that KOH and NaOH solutions are effective in the dissolution of Si and Al to achieve the desired Si:Al. KOH was, however, chosen due to oligomer formation.

The dissolution of Al and Si from Eskom fly ash is significantly lower than that of SASOL (Table 5.2 and Table 5.3). This indicates that the glassy phase of Eskom fly ash is not as reactive as that of SASOL fly ash. It is this reason that could possibly explain the difference in compressive strength between Eskom and Sasol geopolymer matrices.

### **5.2.3 Specific Surface Area Analysis**

Specific surface area measurements were carried out on Eskom and SASOL fly ashes and geopolymer matrices. Results (Table 5.5) clearly show that the surface area data for SASOL fly ash and geopolymer matrix are significantly higher than that of Eskom. Taking into consideration the fact that geopolymers synthesised from SASOL fly ash have a higher compressive strength, one would expect the stronger 36 Sasol geopolymer sample to have less porosity. Surface area measurements, however, show the contrary. This therefore, means that another possible occurrence or reaction offsets any negative effects on the structure that may result due to the increased surface area.

Specific surface area results (Table 5.5) also show higher surface area values for the geopolymer matrices (36 Eskom and 36 Sasol) than the fly ashes (Eskom and SASOL). A possible explanation for the increased surface areas of the geopolymer matrices is that during geopolymerisation the hollow spheres (fly ash) open up thereby increasing surface area. This phenomenon is clearly demonstrated in the SEM images of Eskom fly ash (Figure 5.9) and SASOL fly ash (Figure 5.10) and the geopolymer matrices, 36 Eskom (Figure 5.11) and 36 Sasol (Figure 5.12).

## 5.2.4 X-ray Diffraction Analysis

The X-ray diffraction patterns for Eskom (Figure 5.1) and SASOL (Figure 5.2) fly ash are very similar. The degree of crystallinity present is due to the quartz and mullite phases present in the fly ash. The hump that occurs between 20 and 40 degrees  $2\theta$  is as a result of the large amorphous content present in the fly ash. Analysis of the diffractograms show a more pronounced hump for Eskom fly ash than SASOL fly ash, indicating a greater amorphous content.

36 Eskom (Figure 5.3) and 36 Sasol (Figure 5.4) geopolymer matrices also exhibit crystalline and amorphous phases similar to those of the fly ash they were synthesised from. However, the increased amorphous content present in Eskom fly ash is not present in 36 Eskom geopolymer matrix. Indeed quartz and mullite present in fly ash is also present in the geopolymer matrix, confirming that only partial dissolution of the fly ash occurred.

## 5.2.5 Infrared Analysis

The main peaks to consider when analysing infrared spectra are the Si-O and Al-O stretching and bending modes. These bonds are generally assigned as T-O bonds where T is either Si or Al. According to Rahier et al. (1997) and Flanigan et al. (1971) the peaks around  $460\text{-}470\text{ cm}^{-1}$  are assigned to the in-plane bending mode of T-O bonds while the peaks between  $950\text{-}1050\text{ cm}^{-1}$  are attributed to asymmetric stretching of T-O bonds. The peaks between  $950\text{-}1050\text{ cm}^{-1}$  are present in the fly ash infrared spectra (Figure 5.5 and 5.6) but do not show up in the geopolymer spectra. The 36 Eskom (Figure 5.7) and 36 Sasol (Figure 5.8) geopolymer matrices do, however, show a prominent peak at  $1049\text{ cm}^{-1}$ . The vibrations that occur between  $1050\text{-}1200\text{ cm}^{-1}$  have been assigned to asymmetric stretching of linkages between tetrahedra. The peaks at  $460$ ,  $1010$  and  $1033\text{ cm}^{-1}$  are indicative of the degree of polymerisation that has taken place. These bands are associated with vibrations originating from within the Al and Si tetrahedra. Van Jaarsveld

(2000) reported on energy changes that occur in this region as a result of different alkali metals. The spectra for 36 Sasol and 36 Eskom, however, show no such peaks. The region around  $1090\text{ cm}^{-1}$  is sensitive to vibrations of linkages between tetrahedra as well as topology and arrangement of the secondary building blocks of the structure. The geopolymer matrices show no evidence of any peaks in this region. Peaks at  $913\text{ cm}^{-1}$  are generally assigned to  $\text{-OH}$ -bending bands where  $\text{-OH}$ -groups are bonded to Al. The spectra of the synthesised geopolymer matrices show no peaks in this region as well. The  $700\text{-}800\text{ cm}^{-1}$  region is associated with bonds containing tetrahedrally co-ordinated Al and specifically Si-O-Al. The IR spectra of the geopolymer matrices show numerous peaks in this area. This means that dissolution has taken place, as this is the only way that tetrahedrally co-ordinated Al could become part of the structure. Peaks in the  $559\text{ cm}^{-1}$  region originate from double structures that are formed by Si and Al. Also of interest is the sharp peak at  $593\text{ cm}^{-1}$ . For 36 Eskom this is a relatively sharp peak with high intensity, for 36 Sasol, however, this peak has shifted to  $594\text{ cm}^{-1}$  and has a much lower intensity. The other peaks appearing in the IR spectra have not been assigned to particular vibration modes.

### 5.2.6 Scanning Electron Microscopy

Scanning electron microscopy (SEM) studies were a useful tool in determining the morphology of the fly ash and geopolymer particles. For the geopolymer matrices SEM analysis was utilised to assess whether or not any unreacted fly ash was present in the matrices as well as to gauge the extent of reaction of starting materials. SEM images of Eskom fly ash (Figure 5.9) and SASOL fly ash (Figure 5.10) show spherical like particles of varying sizes. After geopolymerisation these spherical fly ash particles are interdispersed within an amorphous gel phase. 36 Eskom (Figure 5.11) indicates a greater number of unreacted fly ash particles in comparison to 36 Sasol (Figure 5.12). ICP data confirms that Eskom fly ash has a lower Si and Al dissolution rate than SASOL fly ash. Indeed the 36 Sasol geopolymer matrix has a much better adhesion to unreacted fly ash particles (greater amorphous gel phase region) than 36 Eskom. This better adhesion is reflected in the higher compressive strength of these matrices.

### 5.2.7 PIXE Analysis

As a method of monitoring the effect of geopolymerisation on the dissolution rates of Al and Si, PIXE analysis was utilised. Analysis of the gel phase of a series of geopolymer samples yielded interesting results with regard to the percentage of Al, Si and other trace metal species present. Referring to Table 5.6, it can be seen that a significant difference exists between the concentration of metals present in the amorphous phase of both geopolymer matrices (36 Eskom and 36 Sasol). Of interest is the higher percentage of Ca present in 36 Sasol in comparison to 36 Eskom. Generally Ca present in fly ash forms various CSH species which can be detected using X-ray diffraction, however, no such phases were present in the X-ray diffraction patterns of either these geopolymer matrices. The trace elements Cl, Mg and S which are present in 36 Eskom are not present in 36 Sasol, highlighting the significant differences that exist between geopolymer matrices due to differing mineralogies of the various fly ashes. If one has to analyse the XRF data (Table 3.1) of the various fly ashes and compare the oxide compositions of the fly ashes to the PIXE analysis, it is interesting to note that the gel phase contains between 60-75% of the Ca that was present as CaO in the fly ash. For Mn and Mg two different scenarios exist. Mn is neither present in the gel phase of 36 Eskom or 36 Sasol, this could be attributed to its very low concentration levels in the different fly ashes. Mg, however, is present in the gel phase of 36 Eskom at a higher concentration level than the oxide composition, clearly indicating that Mg dissolution rate is significant during geopolymerisation. 36 Sasol on the other hand contains no traces of Mg in its gel phase. Also of interest are the higher concentration levels of S in 36 Eskom. No traces of S were however, observed for 36 Sasol.

Comparing Si and Al concentration values obtained from PIXE analysis to those obtained from ICP analysis, a similar trend is observed, i.e. the concentration of Si is higher than that of Al. Of interest, however, is that the PIXE analysis for 36 Eskom shows a greater concentration of Al in the gel phase than for 36 Sasol. Analysis of the ICP data, however, shows that the concentration of Al dissolved from SASOL fly ash is much higher than Eskom.

## 5.3 THE EFFECT OF ORGANICS ON GEOPOLYMERISATION

To study the various effects that organics could possibly have on geopolymerisation/geopolymers, analytical tools similar to those used for the analysis of the various geopolymer matrices were utilised. The data obtained for the various geopolymer matrices (Section 5.2) were compared with the data obtained for the matrices containing organics. This was done to illustrate better the differences that exist due to the presence of organics. Organic addition was carried out by adding 1% and 5% by weight phenol and 4-chlorophenol to the geopolymer mixtures (Table 5.7) respectively. The geopolymer matrices were then oven cured for 7 days at 30°C before being analysed.

### 5.3.1 Compressive Strength

Compressive strength data illustrate an interesting trend with regard to the percentage of organic added versus the compressive strength. Also note that there exists a variability in compressive strength results from batch to batch, i.e 36 Sasol (Table 5.1) compressive strength value will be different to 36 Sasol containing organics (Table 5.8). Analysis of the data shows that a 1% addition of phenol to 36 Sasol significantly increases the compressive strength of the geopolymer matrix (Table 5.8), however, a 1% addition of 4-chlorophenol decreases the compressive strength slightly. For 36 Eskom on the other hand a 1% addition of organic causes a slight decrease in compressive strength. A 5% organic addition severely destroys the matrices of both 36 Sasol and 36 Eskom. Indeed a 5% organic addition to the geopolymer system destroys the matrices to such an extent that after 7 days of curing the geopolymer matrices break on removing them from their moulds. Physical inspection of the matrices shows a soft, crumbly texture, which has a distinctive phenolic odour. It is also significant to note that the compressive strength of the matrices is also dependent on the type of organic and the matrix. For 36 Sasol, phenol addition produces a higher compressive strength than 4-chlorophenol addition, whilst for Eskom fly ash the opposite occurs. Possible reasons for this trend are contained in the analyses that follow.

### 5.3.2 ICP Analysis

In order to quantify the relative amounts of Al and Si leached from the fly ashes by the organics, dissolution tests were conducted on SASOL and Eskom fly ash. Tables 5.9 and 5.10 summarise these results. The concentration values were extremely low in comparison to the values obtained for KOH and NaOH. This is not surprising since natural minerals have a lower solubility in acidic mediums than alkaline mediums. Phenols are fairly acidic compounds with  $K_a$  values of  $10^{-10}$ .

For SASOL fly ash phenol solutions leached a greater concentration of Al than 4-chlorophenol, however, analysis of Si released from SASOL fly ash shows the opposite, that is 4-chlorophenol leaches more Si than phenol.

Considering the general trend for Eskom fly ash, the data illustrate a greater concentration of Al being leached from the fly ash by 4-chlorophenol than by phenol. The Si data are, however, too erratic to attribute any trend to these values.

### 5.3.3 Specific Surface Area Analysis

A 1% phenol addition to 36 Sasol not only serves to strengthen the structure but also seems to increase the matrices specific surface area. As described earlier this indeed is a relatively unexpected phenomenon. Analysis of the results contained in Table 5.11 shows that the sample exhibiting a greater compressive strength value also exhibits a larger specific surface area measurement. For 36 Sasol the geopolymer containing phenol has a higher compressive strength than that of chlorophenol and this is mirrored by its equally high surface area measurement. For 36 Eskom, however, the reverse is true; geopolymer samples containing 4-chlorophenol have a higher compressive strength value, and it is this matrix that exhibits the greater surface area measurement. A 5% organic addition to the matrix serves not only to severely destroy the matrix, but it also greatly reduces the



value of the specific surface area. Data shows a reduction in specific surface area measurements from between 50-73 m<sup>2</sup>/g to 6-11 m<sup>2</sup>/g.

### 5.3.4 X-ray Diffraction Analysis

As stated before and repeatedly in other sections of this thesis, geopolymers are essentially amorphous and semi-amorphous and therefore not suitable for detailed study by X-ray diffraction. Why then the utilisation of this technique? The answer to this question lies in our quest to try and find a plausible explanation for why compressive strength increased with a 1% phenol addition. A possible explanation for this could have been the formation of crystalline phases due to the organics acting as nucleation sites within the matrices. Analysis of XRD spectra (Figures 5.13-5.16), however, shows no appearance of any new crystalline phases. Although the product is amorphous to X-rays, this does not guarantee the absence of very small disordered crystals and therefore some crystallinity could well be present. It is for this reason that the crystalline outgrowths on the surface of the fly ash (contained in the SEM images) could not be detected by XRD analysis. The only point of relative interest is the intensity of the hump between 20° and 40° 2θ.

### 5.3.5 Infrared Analysis

Peaks between 950-1050 cm<sup>-1</sup> are attributed to asymmetric stretching of T-O bonds. 36 Eskom (Figure 5.7) and 36 Sasol (Figure 5.8) geopolymer matrices do show a prominent peak at 1049 cm<sup>-1</sup>. Analysis of the spectra for 36 Sasol (PhOH) (Figure 5.17) and 36 Sasol (Cl-PhOH) (Figure 5.18) shows that the intensity of the peak at 1049 cm<sup>-1</sup> has been reduced significantly. From this it can be inferred that organic addition has an effect on geopolymer structure. The spectra of 36 Eskom (PhOH) (Figure 5.19) and 36 Eskom (Cl-PhOH) show no such changes. For 36 Sasol, phenol addition (Figure 5.17) has shifted the peak at 594 to 593 cm<sup>-1</sup>, chlorophenol addition (Figure 5.18), however, has increased the

intensity of the peak at  $594\text{ cm}^{-1}$ . For 36 Eskom the opposite has occurred; the peak at  $594\text{ cm}^{-1}$  has shifted to  $598\text{ cm}^{-1}$ . The intensity of the peak for 36 Eskom (Cl-PhOH) matrix (Figure 5.20) is greater than that for 36 Eskom (PhOH) (Figure 5.19) matrix. Organic addition has produced no extra peaks nor has it resulted in the complete disappearance of any existing peaks.

### 5.3.6 Scanning Electron Microscopy

SEM studies were useful in determining the effect of organic addition on the morphology of the geopolymer matrices. SEM analysis was utilised to assess whether or not organic addition had any effect on the gel phase of the geopolymer matrices. SEM images of the various geopolymer matrices are contained in Figures 5.21-5.26. For a 1% phenol addition, 36 Sasol (PhOH) (Figure 5.21), analysis of the images clearly shows the appearance of crystalline outgrowths on the surface of the fly ash particles. The increased physical strength of the matrix could hence be attributed to the increased crystallisation contacts between the crystalline and amorphous regions. The rest of the matrices that contain a 1% organic addition have SEM images similar to that depicted in Figure 5.22. The SEM images show a substantial gel phase between the fly ash particles. No other crystalline phases as that seen in 36 Sasol (PhOH) could, however, be seen. Analysis of the matrices containing 5% organic addition (Figures 5.23-5.26) shows a completely different scenario. Indeed the images show very little to no gel phase between the fly ash particles. The spherical fly ash particles can clearly be seen indicating very little dissolution taking place. This lack of amorphous gel phase could be the reason contributing to the non-existent compressive strength of these matrices.

### 5.3.7 PIXE Analysis

PIXE analysis was utilised as a quantitative method of analysis to study the effects of organics on the concentration of ions in the gel phase. As expected, an increase in

concentration of the organic from 1% to 5% reduces the concentrations of Al and Ca in the gel phase. The reduction in Al concentration in the gel phase could possibly mean that the concentration of polymeric species in the matrices has been reduced, thus lowering the resultant bulk physical strength of the matrices. Analysis of the data shows no such reduction in Si concentration for matrices containing organics. Indeed for Sasol geopolymers, phenol and chlorophenol addition has increased the concentration of Si in the gel phase. The concentration of Ca in the gel phase of matrices containing organics is significantly lower than for the standard geopolymer matrices. This reduced Ca content is more prominent for matrices containing a 5% organic addition.

As expected, PIXE data for the matrices containing chlorophenol shows an increased chloride ion concentration. For Sasol geopolymers containing organics, the gel phase of the matrices exhibit high S and Mg concentrations; therefore implying that organic addition has also catalysed the dissolution of S and Mg.

### **5.3. 8 Immobilisation Efficiencies**

The geopolymer samples containing the encapsulated organics produced a white powdery layer on the surface of the geopolymer. Analysis of the powder confirmed that the powder was phenol in the case of matrices containing phenol and chlorophenol in the case of matrices containing chlorophenol. This illustrates that the geopolymers have very poor immobilisation efficiencies for the organics. Indeed, the severe destruction of the matrices containing a 5% organic addition confirms that geopolymer systems are poor encapsulation media for organics.

## 5.4 SUMMARY

Previous research (Xu et al., 2000) shows that the % CaO, the molar ratio of Si:Al in the original mineral, the use of KOH, the extent of dissolution of Si and the molar Si:Al ratio in solution contribute to higher compressive strength values whilst the % K<sub>2</sub>O and the use of NaOH are associated with low compressive strength values. Similar trends were observed in this study. It is also evident that organic affect numerous stages in geopolymerisation. For a 1% organic addition these effects are, however, not as destructive to the matrix as a 5% organic addition. Due to the poor immobilisation efficiencies of the geopolymer, an alternative method was thus needed for organic encapsulation, hence the use of zeolites (Chapter6).

**Table 5.1: Compressive strength data for standard geopolymer matrices**

Sample	Age (days)	Mass (kg)	Force (kN)	Strength (MPa)
36 Sasol	7	0.40	61.18	28.80
36 Sasol®	7	0.38	55.23	26.00
19 Sasol	7	0.40	51.90	24.40
19 Sasol®	7	0.38	50.96	24.00
36 Sasol (NaOH)	7	0.43	23.84	11.20
19 Sasol (NaOH)	7	0.42	47.95	22.60
36 Eskom	7	0.42	22.60	10.60
36 Eskom®	7	0.40	30.78	14.50
19 Eskom	7	0.40	13.00	6.10

**Table 5.2: ICP data for SASOL fly ash**

Concentration (ppm) of Al in solution

Mass (g) of fly ash	3.3M KOH	6.6M KOH	3.3M NaOH	6.6M NaOH
1	65.220	190.390	80.800	153.000
3	142.800	330.690	269.00	256.100
5	254.330	456.670	369.000	567.100
7	308.030	636.410	556.400	650.000
9	366.450	467.630	546.500	784.100

Concentration (ppm) of Si in solution

Mass (g) of fly ash	3.3M KOH	6.6M KOH	3.3M NaOH	6.6M NaOH
1	146.140	339.500	220.600	326.900
3	372.320	639.870	565.400	533.000
5	463.310	953.460	675.500	1092.600
7	451.320	1379.800	819.500	1188.300
9	390.920	1016.200	791.000	1425.100

**Table 5.3: ICP data for Eskom fly ash**

Concentration (ppm) of Al in solution

Mass (g) of fly ash	3.3M KOH	6.6M KOH	3.3M NaOH	6.6M NaOH
1	50.162	59.848	89.030	72.338
3	150.609	109.951	166.815	112.577
5	213.567	181.393	215.078	185.045
7	244.272	259.356	247.174	250.717
9	243.584	272.790	233.284	260.814

Concentration (ppm) of Si in solution

Mass (g) fly ash	3.3M KOH	6.6M KOH	3.3M NaOH	6.6M NaOH
1	48.465	87.864	47.800	116.372
3	102.001	160.496	104.122	174.019
5	124.912	233.129	162.112	257.645
7	125.091	318.671	257.079	331.270
9	131.749	331.617	212.861	337.771

**Table 5.4: Si:Al ratios for Eskom and SASOL fly ash**

Ratio of Si:Al in solution (SASOL fly ash)

Mass (g) of fly ash	3.3M KOH	6.6M KOH	3.3M NaOH	6.6M NaOH
1	2.2:1	1.8:1	2.7:1	2.1:1
3	2.6:1	1.9:1	2.1:1	2.1:1
5	1.8:1	2.1:1	1.8:1	1.9:1
7	1.5:1	2.2:1	1.5:1	1.8:1
9	1.1:1	2.2:1	1.4:1	1.8:1

Ratio of Si:Al in solution (Eskom fly ash)

Mass (g) of fly ash	3.3M KOH	6.6M KOH	3.3M NaOH	6.6M NaOH
1	1.0:1	0.68:1	1.9:1	0.62:1
3	1.5:1	0.69:1	1.6:1	0.65:1
5	1.7:1	0.78:1	1.3:1	0.72:1
7	1.9:1	0.81:1	0.96:1	0.76:1
9	1.8:1	0.82:1	1.1:1	0.77:1

**Table 5.5 BET surface area results**

Sample	BET Surface Area (m <sup>2</sup> /g)
Eskom fly ash	1.0850
SASOL fly ash	5.3959
36 Eskom	34.7260
36 Sasol	52.7369

**Table 5.6: PIXE analysis for standard geopolymer matrices**

		<b>Trace Element Summary: Concentrations given in W% or ppm</b>										
Sample	Analysed on	Al	Si	Cl	Mg	K	Ca	Ti	Mn	Fe	S	Cr
		%	%	ppm	%	%		%		%	ppm	ppm
GEO36 ESKOM	Gel	16.20	24.00	< 95.	2.81	5.31	2.76	0.39	n/a	3.95	0.29	164.0
GEO36 ESKOM	Gel	19.00	21.90	346.00	2.58	5.92	1.48	0.40	n/a	0.86	225.0	89.60
GEO36 ESKOM	Particle	8.43	37.10	272.00	1.29	7.36	2.01	0.81	n/a	0.98	106.0	130.0
GEO36 ESKOM	Gel	11.20	25.40	666.00	1.66	8.48	1.31	0.57	n/a	1.13	157.0	114.0
GEO36 SASOL	Gel	7.38	38.50	n/a	n/a	3.76	4.12	0.54	n/a	0.98	n/a	n/a
GEO36 SASOL	Gel	14.10	25.10	n/a	n/a	7.71	5.16	0.43	n/a	0.80	n/a	869.0
GEO36 SASOL	Gel*	88.10	n/a	n/a	20.80	4.98	9.47	390.0	n/a	n/a	n/a	n/a

\*Possibly a particle

**Table: 5.7: Geopolymer matrices for organic addition**

<b>Ingredient</b>	<b>Composition (mass%) [Recipe 36]</b>
Fly ash	60.0
Kaolinite	6.7
KOH	8.0
Sodium Silicate soln	14.7
Water	10.7
Phenol	1 and 5
4-Chlorophenol	1 and 5



**Table 5.8: Compressive strength data for geopolymers containing organics**

Sample	Age (days)	Mass (kg)	Force (kN)	Strength (MPa)
36 Sasol	7	0.40	74.57	35.11
36 Sasol (1% PhOH)	7	0.40	85.22	40.13
36 Sasol (1% Cl-PhOH)	7	0.38	72.06	33.93
36 Eskom	7	0.38	59.85	28.18
36 Eskom (1% PhOH)	7	0.40	48.44	22.81
36 Eskom (1% Cl-PhOH)	7	0.38	56.07	26.40

**Table 5.9: ICP data (organics) for SASOL fly ash**

Concentration (ppm) of Al in solution

Mass (g) of fly ash	2M Phenol	4M Phenol	2M Cl-Phenol	4M Cl-Phenol
1	2.701	1.036	0.704	0.280
3	1.492	4.247	0.492	0.395
5	1.271	0.000	0.454	0.402
7	1.500	1.065	0.432	0.407
9	0.685	1.569	0.391	0.168

Concentration (ppm) of Si in solution

Mass (g) of fly ash	2M Phenol	4M Phenol	2M Cl-Phenol	4M Cl-Phenol
1	23.474	22.751	23.561	21.277
3	19.760	26.574	22.792	32.592
5	19.438	4.940	24.420	22.397
7	10.573	24.010	25.604	24.088
9	16.543	11.625	27.329	26.384

**Table 5.10: ICP data (organics) for Eskom fly ash**

Concentration (ppm) of Al in solution

<b>Mass (g) fly ash</b>	<b>2M Phenol</b>	<b>4M Phenol</b>	<b>2M Cl- Phenol</b>	<b>4M Cl- Phenol</b>
1	0.087	0.199	0.674	0.371
3	0.218	0.136	0.458	0.446
5	0.291	0.432	0.440	0.389
7	0.642	1.035	0.375	0.289
9	0.158	6.026	0.416	0.389

Concentration (ppm) of Si in solution

<b>Mass (g) of fly ash</b>	<b>2M Phenol</b>	<b>4M Phenol</b>	<b>2M Cl- Phenol</b>	<b>4M Cl- Phenol</b>
1	17.117	17.155	17.749	12.973
3	20.590	23.636	20.843	23.632
5	22.181	23.878	29.776	27.354
7	22.684	25.006	25.085	25.642
9	23.415	48.208	30.744	30.895

**Table 5.11: Surface area measurements of geopolymers containing organics**

<b>Sample</b>	<b>BET Surface Area (m<sup>2</sup>/g)</b>
36 Sasol (1% PhOH)	72.3226
36 Sasol (1% Cl-PhOH)	49.2019
36 Sasol (5% PhOH)	10.1056
36 Sasol (5% Cl-PhOH)	7.4262
36 Eskom (1% PhOH)	17.5107
36 Eskom (1% Cl-PhOH)	32.9093
36 Eskom (5% PhOH)	6.4605
36 Eskom (5% Cl-PhOH)	8.3691

Table 5.12: PIXE analysis for geopolymers containing organics

Trace Element Summary: Concentrations given in W% or ppm

Sample Name	Analysed on	Al	Si	Cl	Mg	K	Ca	Ti	Mn	Fe	S	Cr	V	N
Standard		10.90 %	13.40 %	185.00	17.10 %	n/a	<20	76.00	n/a	2.61 %	182.00	1.11 %	115.00	0.17 %
Standard		5.01 %	12.70 %	799.00	17.20 %	n/a	2420	51.00	n/a	2.60 %	0.12 %	1.58 %	99.80	0.19 %
ESKOMFHCH(1%)	Gcbal	11.90 %	21.90 %	n/a	1.91 %	6.28 %	1.66 %	0.59 %	n/a	1.22 %	n/a	n/a	n/a	n/a
ESKOMFHCH(1%)	Gcl	9.68 %	26.10 %	n/a	0.98 %	10.20 %	2.25 %	0.47 %	n/a	0.97 %	n/a	n/a	n/a	n/a
ESKOMFHCH(1%)	Gcl	12.50 %	26.90 %	n/a	2.07 %	4.74 %	1.65 %	0.34 %	n/a	0.48 %	n/a	n/a	n/a	n/a
ESKOMFHCH(1%)	Gcl	9.56 %	21.50 %	n/a	1.86 %	8.24 %	1.17 %	0.48 %	n/a	0.97 %	n/a	n/a	n/a	n/a
ESKOMFHCH(1%)	Gcl	10.10 %	25.90 %	n/a	1.63 %	9.53 %	1.92 %	0.58 %	n/a	0.83 %	n/a	n/a	n/a	n/a
ESKOMCI FHCH(1%)	Gcl	10.20 %	23.30 %	856.00	0.66 %	6.45 %	1.47 %	0.63 %	n/a	1.75 %	n/a	n/a	n/a	n/a
ESKOMCI FHCH(1%)	Gcl	11.70 %	42.00 %	232.00	0.45 %	2.60 %	1.07 %	0.39 %	n/a	0.74 %	n/a	n/a	n/a	n/a
ESKOMCI FHCH(1%)	Gcl	17.20 %	24.60 %	n/a		6.91 %	1.56 %	1.31 %	n/a	1.42 %	181.00	n/a	n/a	n/a
ESKOMCI FHCH(3%)	Gcbal	3.64 %	11.00 %	0.11 %	0.25 %	12.10 %	0.87 %	0.32 %	n/a	0.94 %	2.41 %	145.00	n/a	n/a
ESKOMCI FHCH(3%)	Gcl	2.00 %	7.43 %	0.11 %	<631	7.65 %	1.20 %	0.35 %	n/a	0.77 %	<93	169.00	n/a	n/a
ESKOMCI FHCH(3%)	Gcl	3.43 %	11.20 %	0.90 %	0.27 %	10.20 %	0.71 %	0.13 %	n/a	0.33 %	133.00	47.30	n/a	n/a
ESKOMCI FHCH(3%)	Gcl	5.30 %	17.90 %	0.16 %	0.65 %	8.73 %	0.80 %	0.36 %	n/a	0.48 %	<9.95 %	140.00	n/a	n/a
ESKOMFHCH(3%)	Gcl	13.00 %	23.50 %	n/a	1.32 %	15.60 %	1.88 %	0.37 %	n/a	0.85 %	684.00	330.00	n/a	n/a
ESKOMFHCH(3%)	Gcl*	0.42 %	1.05 %	22.90	337.00	0.79 %	0.62 %	849.00	n/a	0.27 %	32.60	32.10	n/a	n/a
ESKOMFHCH(3%)	Gcl	9.15 %	29.00 %	311.00	0.89 %	12.70 %	1.02 %	0.42 %	n/a	0.64 %	621.00	245.00	n/a	n/a
Standard		11.40 %	13.80 %	82.50	17.60 %	n/a	n/a	64.90	n/a	2.60 %	246.00	1.10 %	100.00	0.17 %
Standard		10.40 %	14.70 %	187.00	18.00 %	n/a	n/a	37.90	n/a	2.61 %	250.00	1.60 %	125.00	0.15 %
SASCLCI FHCH(1%)	Gcl	6.72 %	24.30 %	0.15 %	0.34 %	9.12 %	1.44 %	0.43 %	n/a	0.62 %	436.00	n/a	n/a	n/a
SASCLCI FHCH(1%)	Gcl	5.58 %	35.20 %	309.00	n/a	7.11 %	1.50 %	0.37 %	n/a	0.71 %	613.00	n/a	n/a	n/a
SASCLCI FHCH(1%)	Gcl	11.30 %	22.70 %	867.00	0.63 %	8.49 %	1.54 %	1.83 %	n/a	0.62 %	377.00	n/a	n/a	n/a
SASCLCI FHCH(1%)	Gcl*	1.52 %	5.94 %	0.16 %	0.38 %	2.74 %	1.12 %	877.00	n/a	0.12 %	0.32 %	n/a	n/a	n/a
SASCLFHCH(1%)	Gcl	13.90 %	31.10 %	n/a	n/a	7.01 %	3.05 %	0.64 %	n/a	16.50 %	676.00	n/a	n/a	n/a
SASCLFHCH(1%)	Gcl	10.60 %	42.50 %	n/a	n/a	9.64 %	2.58 %	0.98 %	n/a	1.05 %	565.00	n/a	n/a	n/a
SASCLFHCH(1%)	Gcl	8.05 %	44.90 %	n/a	n/a	8.66 %	4.84 %	0.57 %	n/a	0.81 %	619.00	n/a	n/a	n/a
SASCLFHCH(3%)	Gcl	3.96 %	11.80 %	452.00	0.33 %	6.99 %	1.78 %	0.40 %	n/a	0.61 %	0.26 %	151.00	n/a	n/a
SASCLFHCH(3%)	Gcl	1.89 %	6.40 %	129.00	0.14 %	6.14 %	1.12 %	0.43 %	n/a	0.62 %	0.26 %	138.00	n/a	n/a
SASCLFHCH(3%)	Gcl	8.53 %	30.30 %	471.00	0.54 %	13.50 %	2.45 %	0.45 %	n/a	0.87 %	0.82 %	277.00	n/a	n/a
SASCLCI FHCH(3%)	Gcl	7.34 %	57.80 %	n/a	0.42 %	18.40 %	1.49 %	0.17 %	n/a	0.35 %	7.33 %	n/a	n/a	n/a
SASCLCI FHCH(3%)	Gcl	7.23 %	24.40 %	0.46 %	0.64 %	10.80 %	2.06 %	0.38 %	n/a	1.11 %	822.00	n/a	n/a	n/a
SASCLCI FHCH(3%)	Gcbal	8.12 %	24.50 %	0.46 %	0.75 %	9.85 %	2.51 %	0.49 %	n/a	0.97 %	0.22 %	n/a	n/a	n/a
SASCLCI FHCH(3%)	Gcbal	4.80 %	73.50 %	0.37 %	n/a	6.18 %	1.32 %	0.33 %	n/a	0.91 %	723.00	n/a	n/a	n/a
SASCLCI FHCH(3%)	Gcbal	9.63 %	26.70 %	0.53 %	0.76 %	14.30 %	1.84 %	0.42 %	n/a	0.52 %	155.00	n/a	n/a	n/a
Average Conc.		10.80 %	25.00 %	0.14 %	3.28 %	8.25 %	1.92 %	0.44 %	n/a	1.45 %	0.38 %	0.29 %	110.00	0.17 %
		<b>Al</b>	<b>Si</b>	<b>Cl</b>	<b>Mg</b>	<b>K</b>	<b>Ca</b>	<b>Ti</b>	<b>Mn</b>	<b>Fe</b>	<b>S</b>	<b>Cr</b>	<b>V</b>	<b>N</b>

Figure 5.1: XRD graph of Eskom fly ash

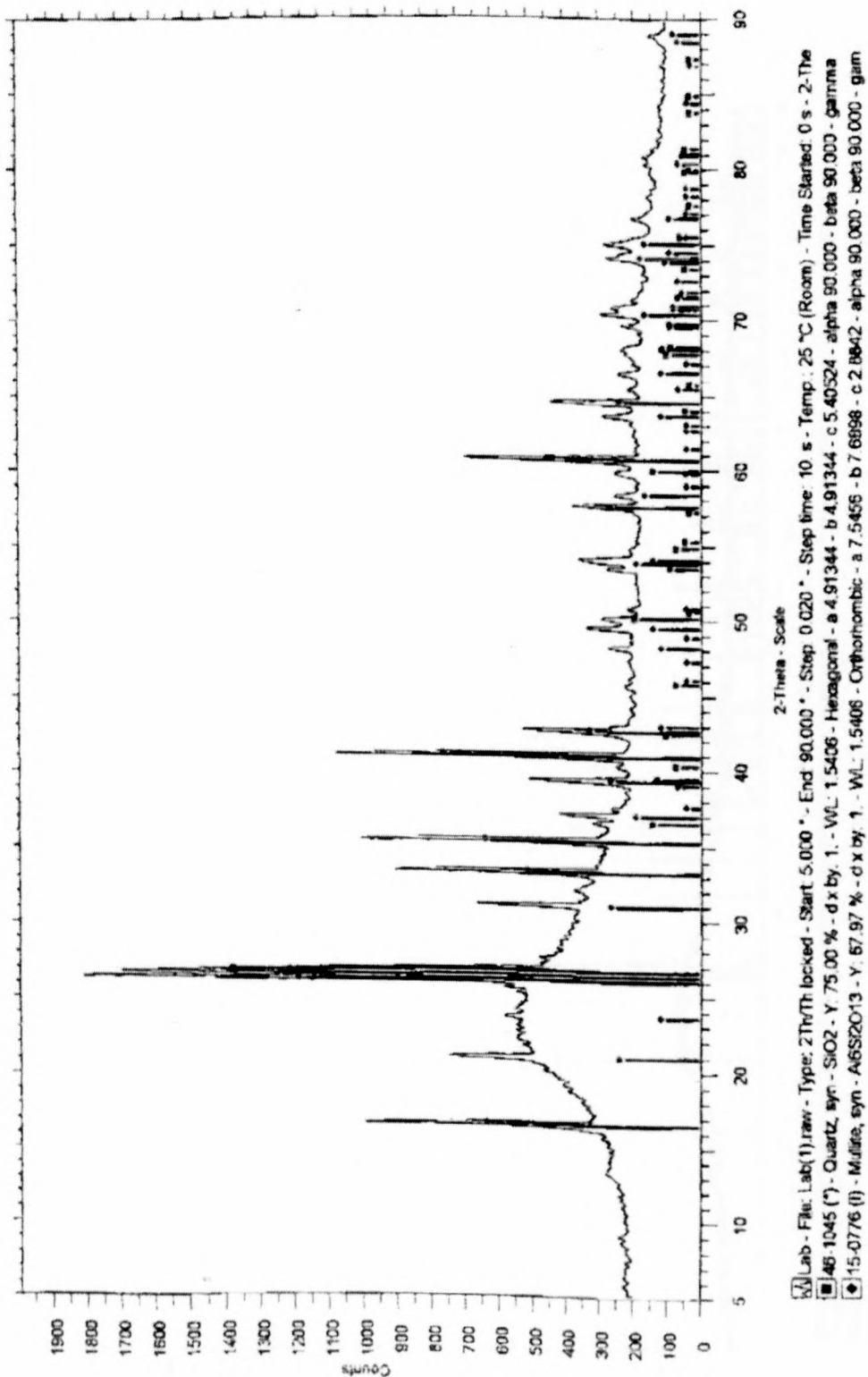


Figure 5.2: XRD graph of SASOL fly ash

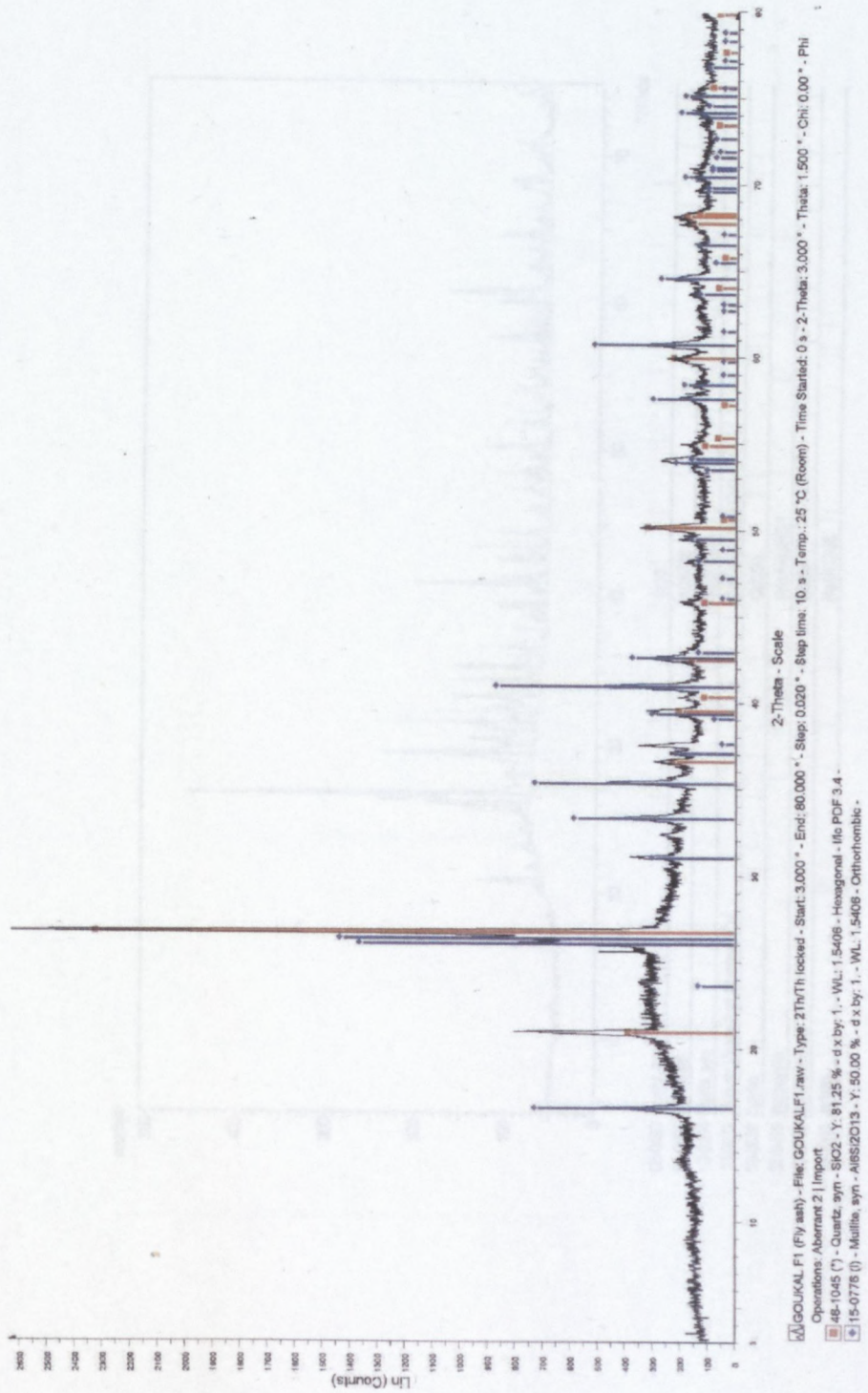


Figure 5.3: XRD graph of 36 Eskom

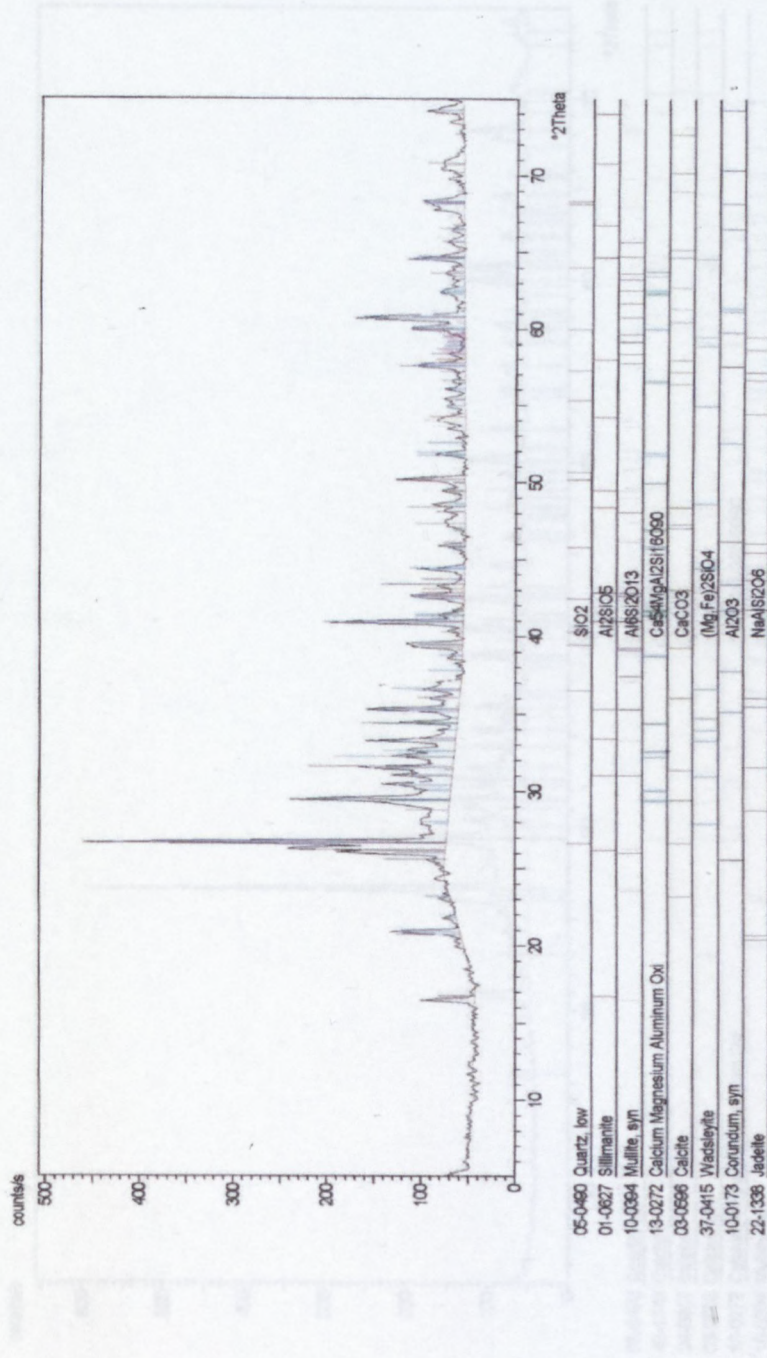


Figure 5.4: XRD graph of 36 Sasol

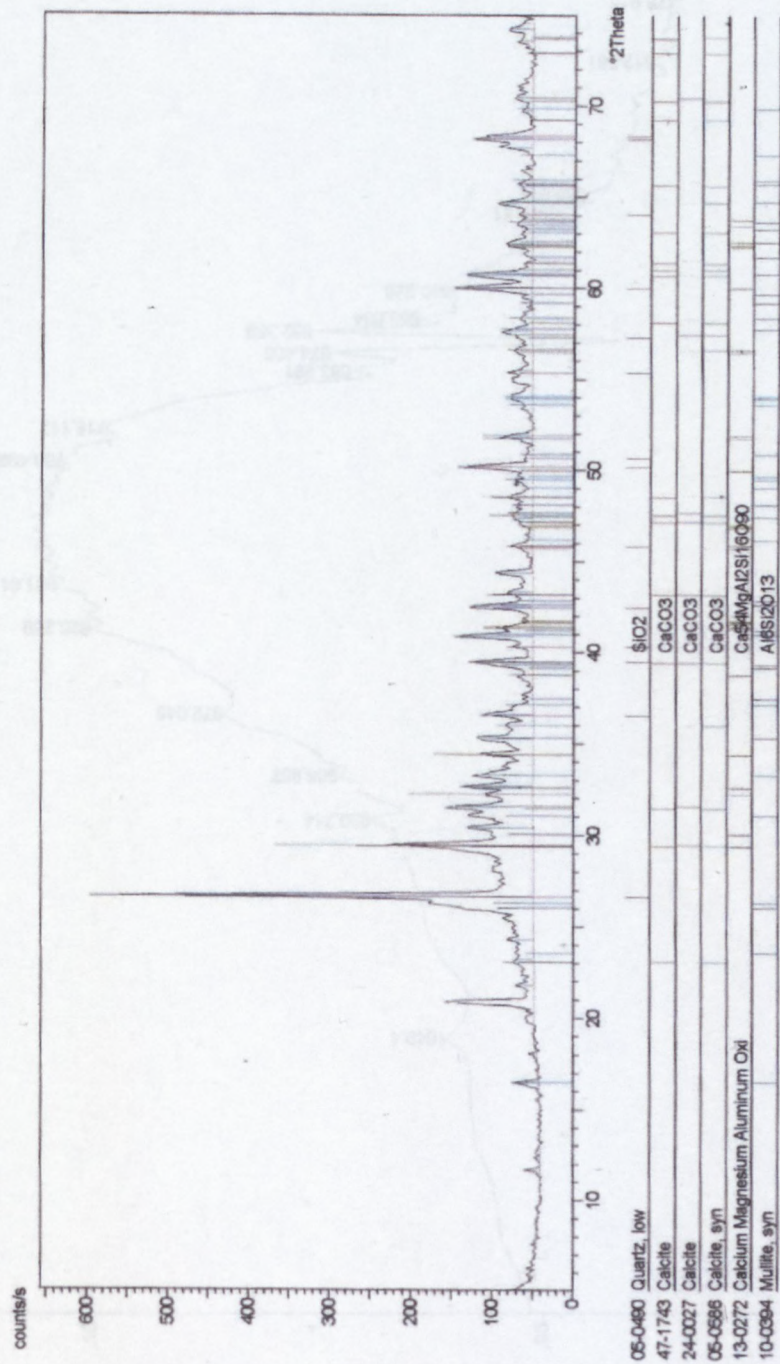




Figure 5.5: IR graph of Eskom fly ash

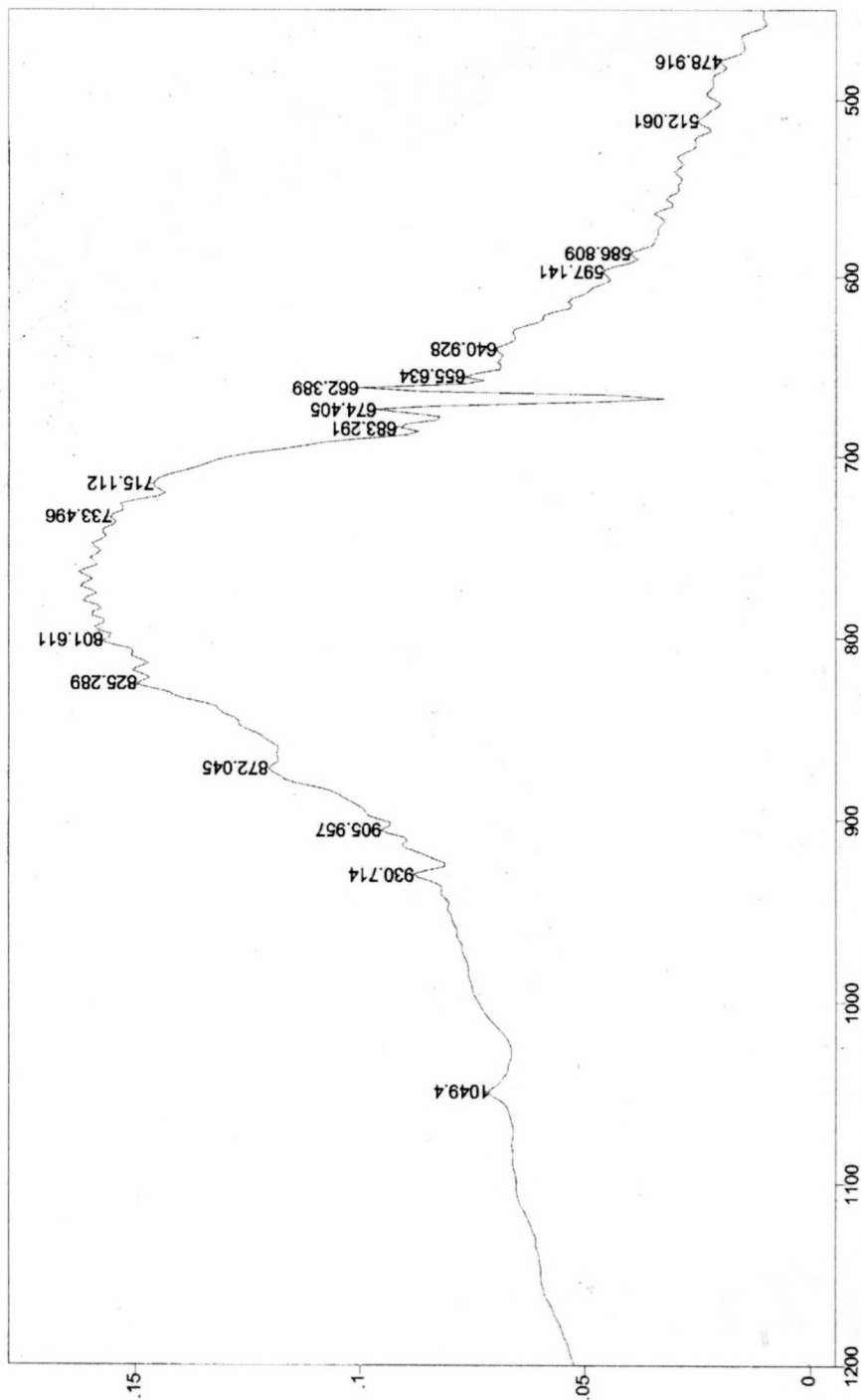


Figure 5.6: IR graph of SASOL fly ash

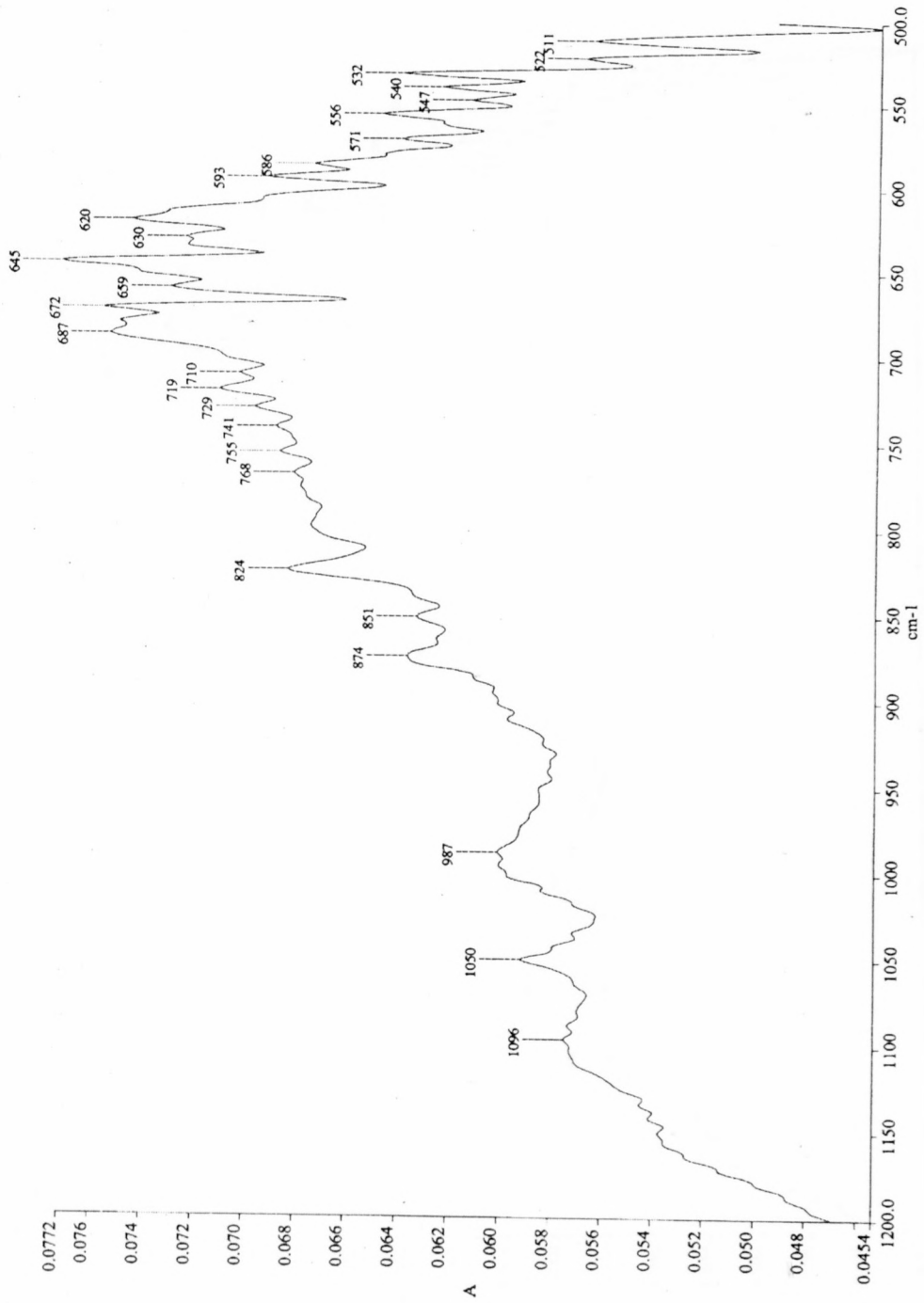


Figure 5.7: IR graph of 36 Eskom

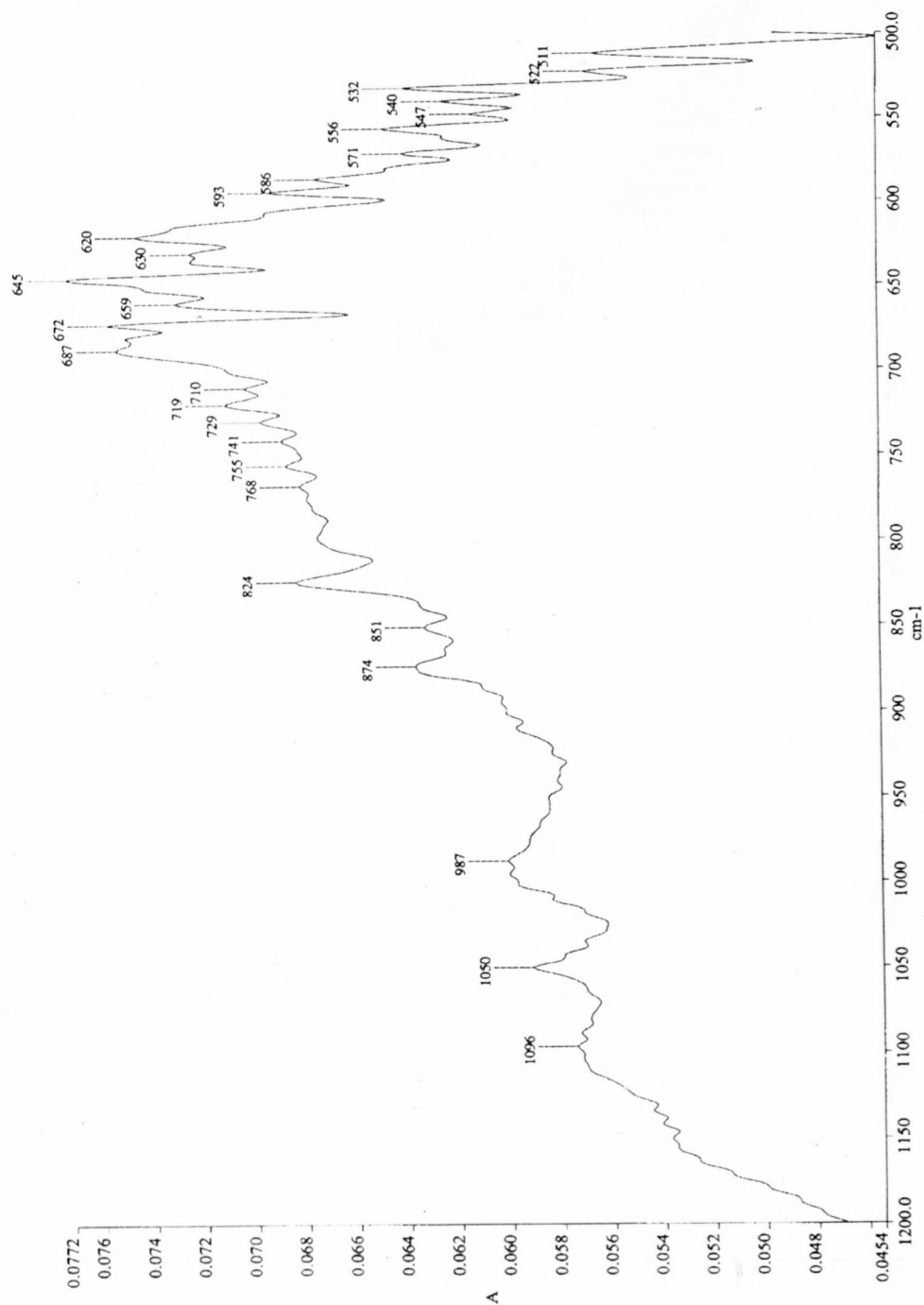


Figure 5.8: IR graph of 36 Sasol

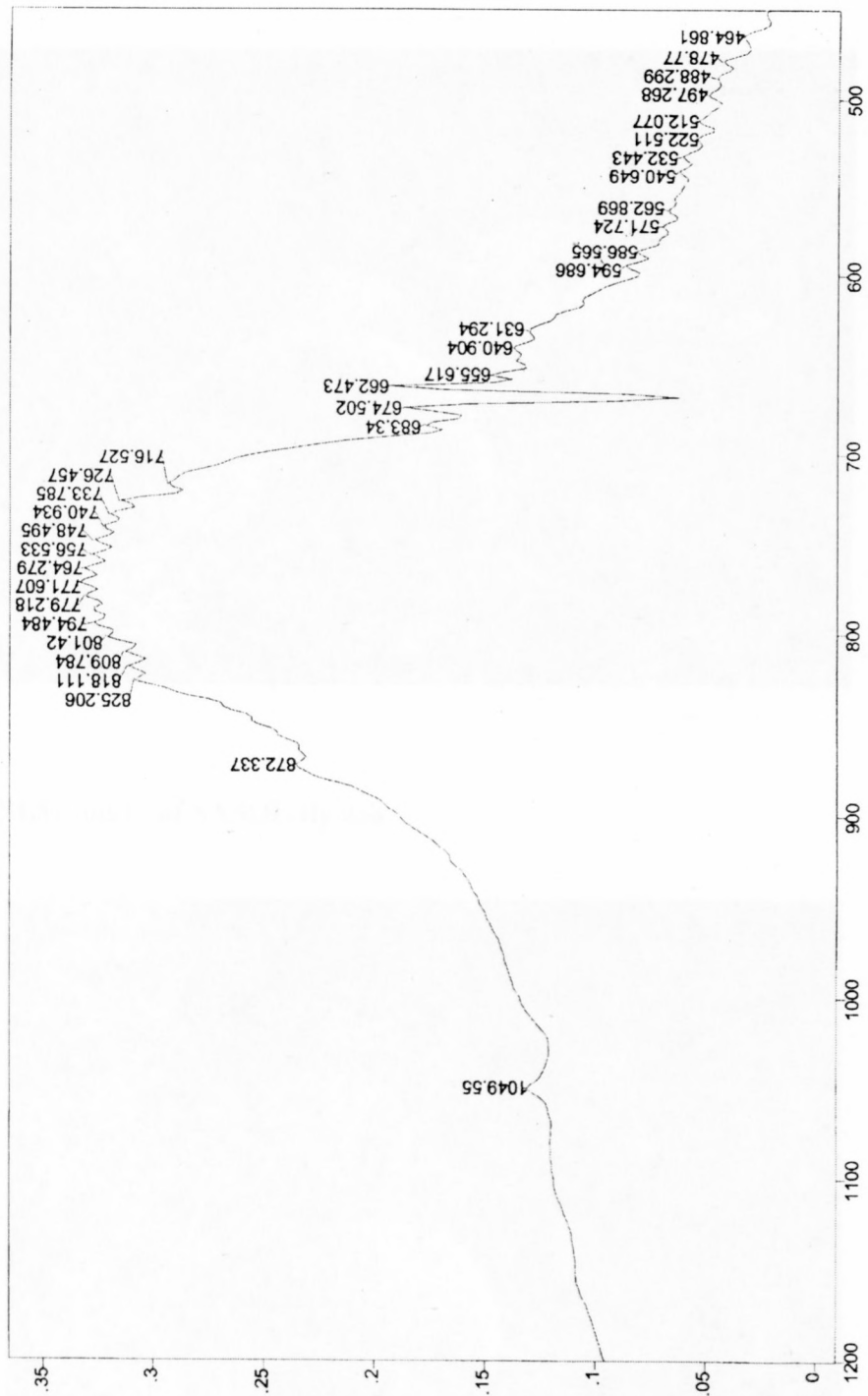


Figure 5.9: SEM image of Eskom fly ash

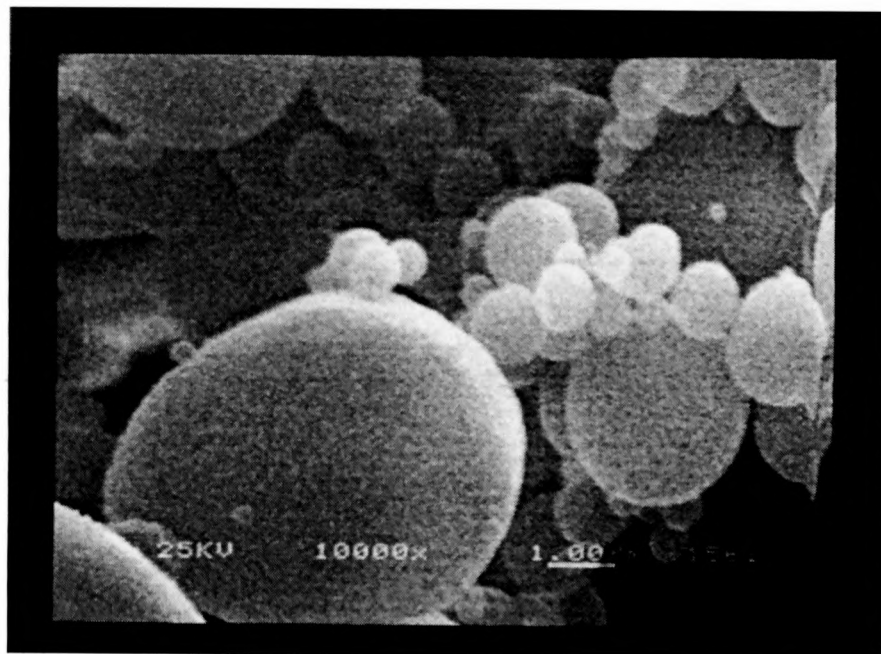


Figure 5.10: SEM image of SASOL fly ash

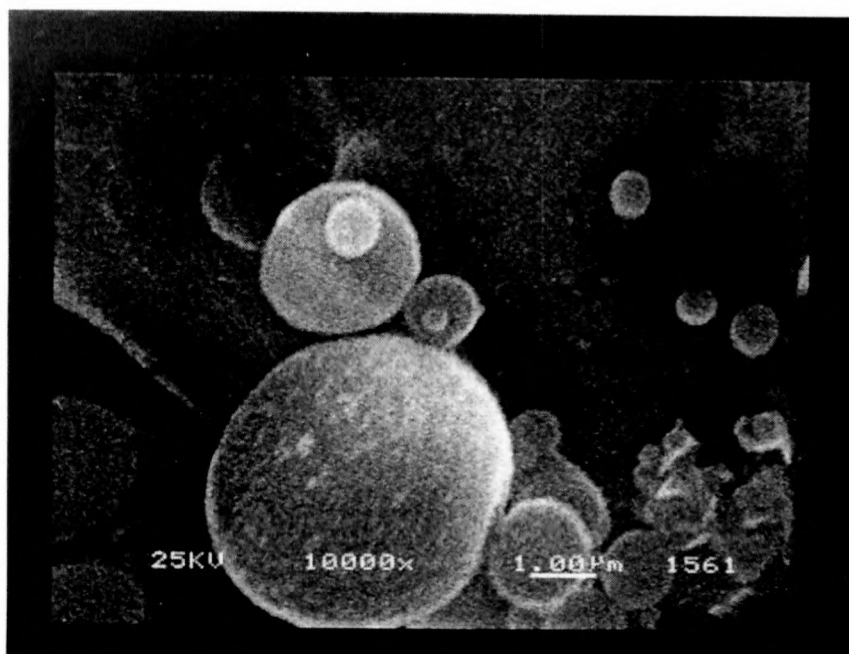


Figure 5.11:SEM image of 36 Eskom

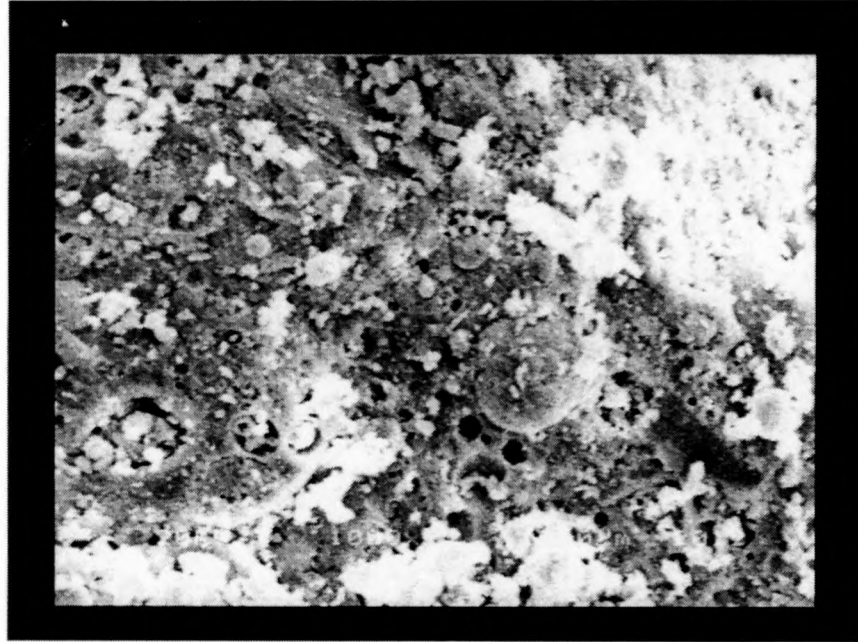


Figure 5.12: SEM image of 36 Sasol

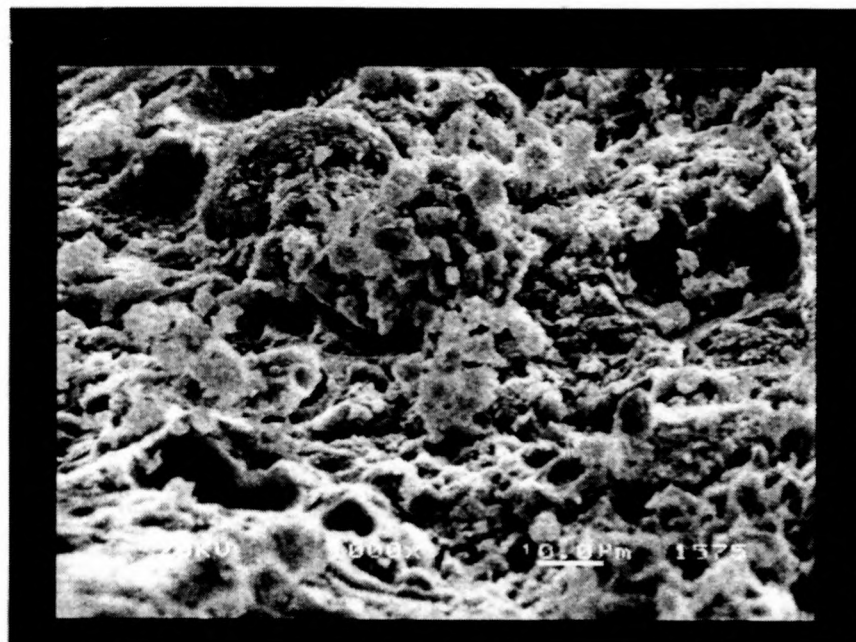


Figure 5.13: XRD graph of 36 Sasol (PhOH)

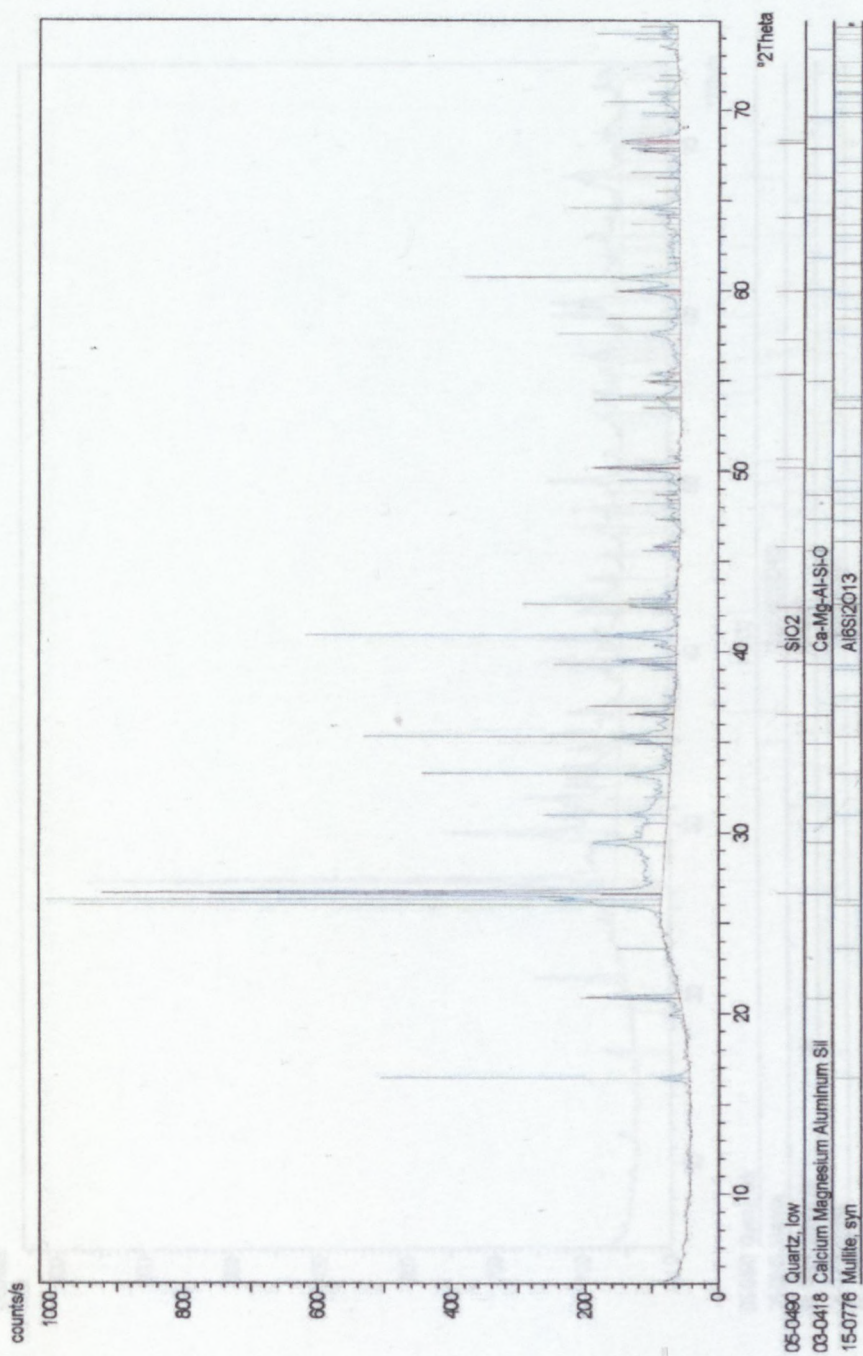


Figure 5.14: XRD graph of 36 Sasol (Cl-PhOH)

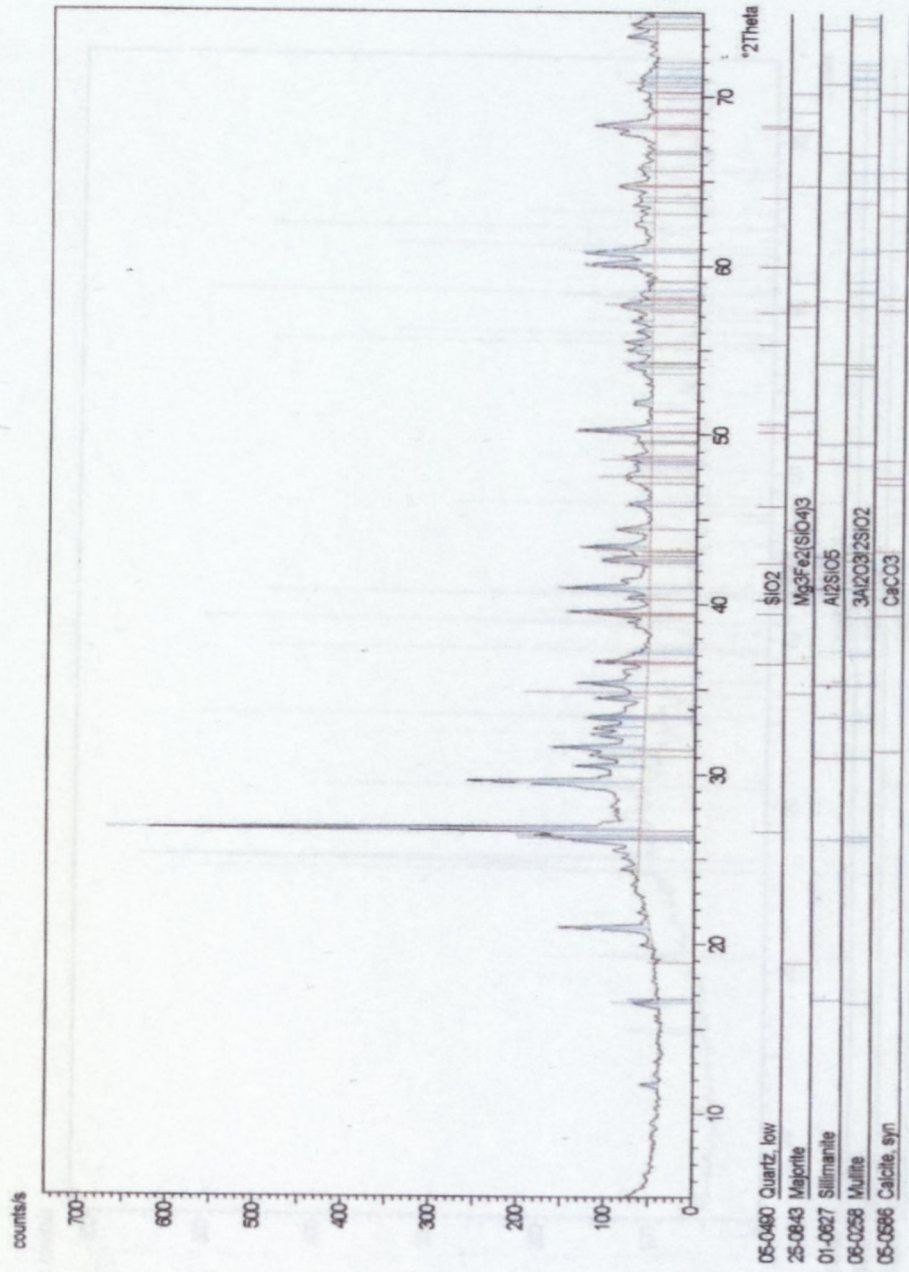




Figure 5.15: XRD graph of 36 Eskom (PhOH)

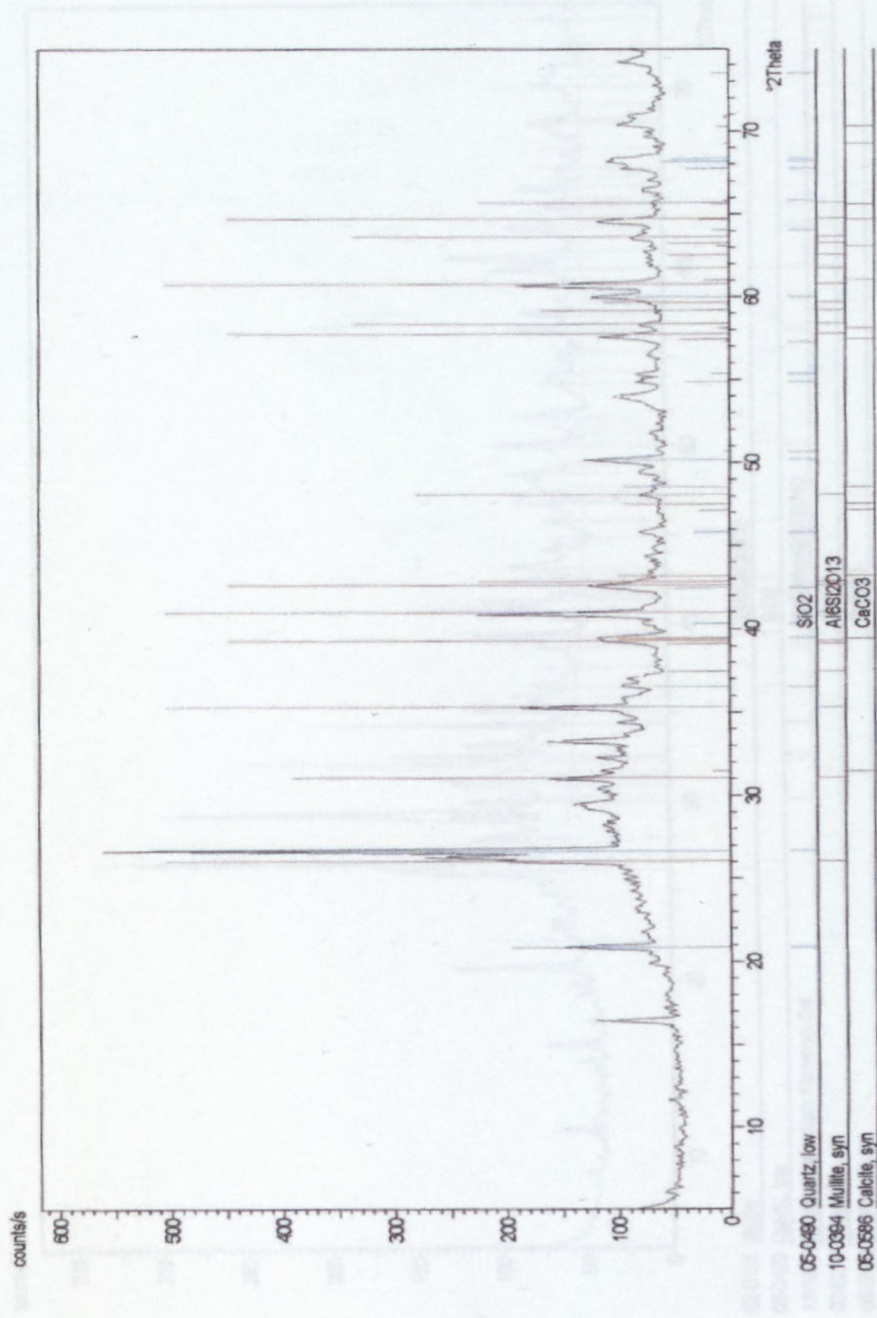


Figure 5.16: XRD graph of 36 Eskom (Cl-PhOH)

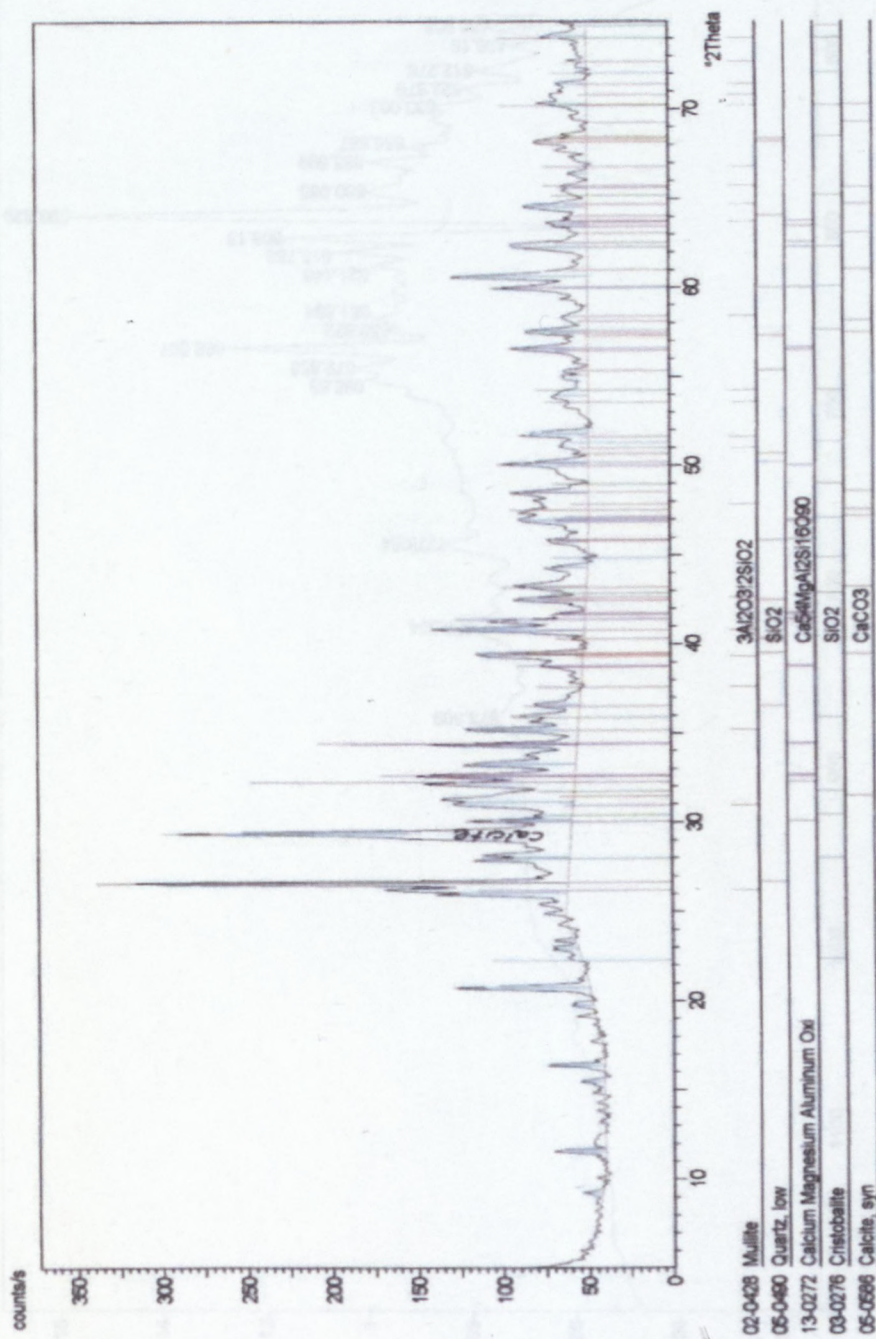


Figure 5.17: IR graph of 36 Sasol (PhOH)

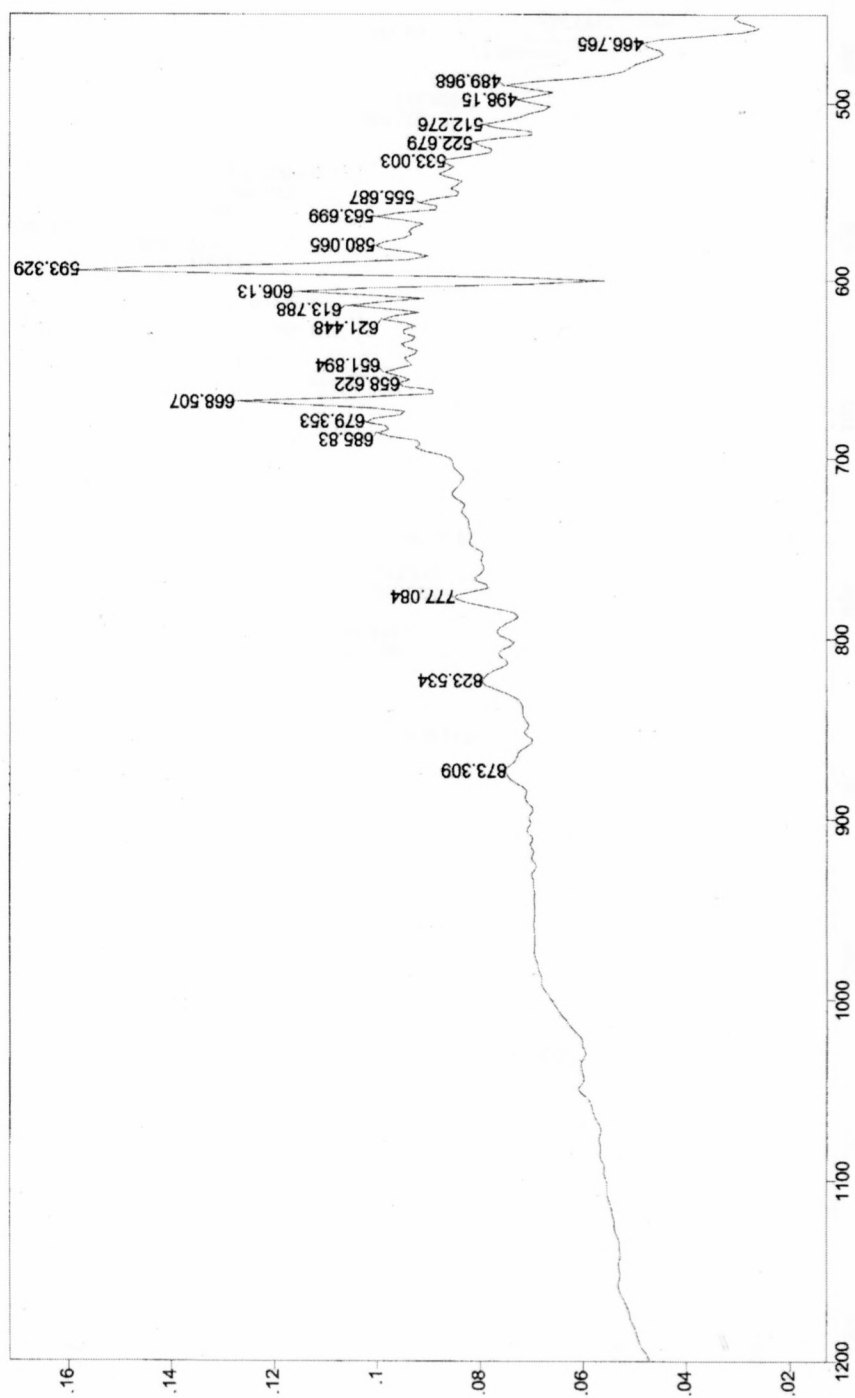


Figure 5.18: IR graph of 36 Sasol (CI-PhOH)

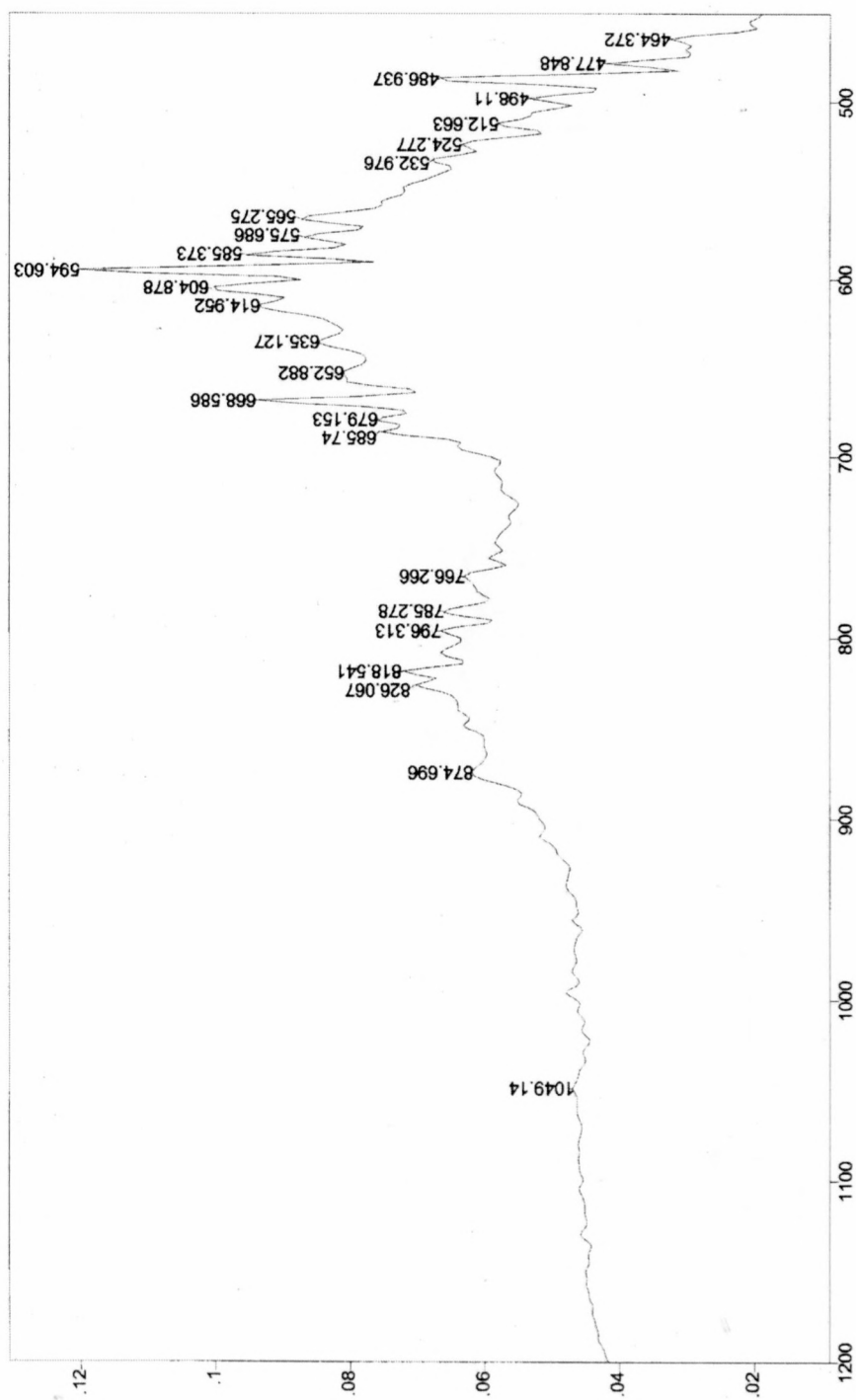


Figure 5.19: IR graph of 36 Eskom (PhOH)

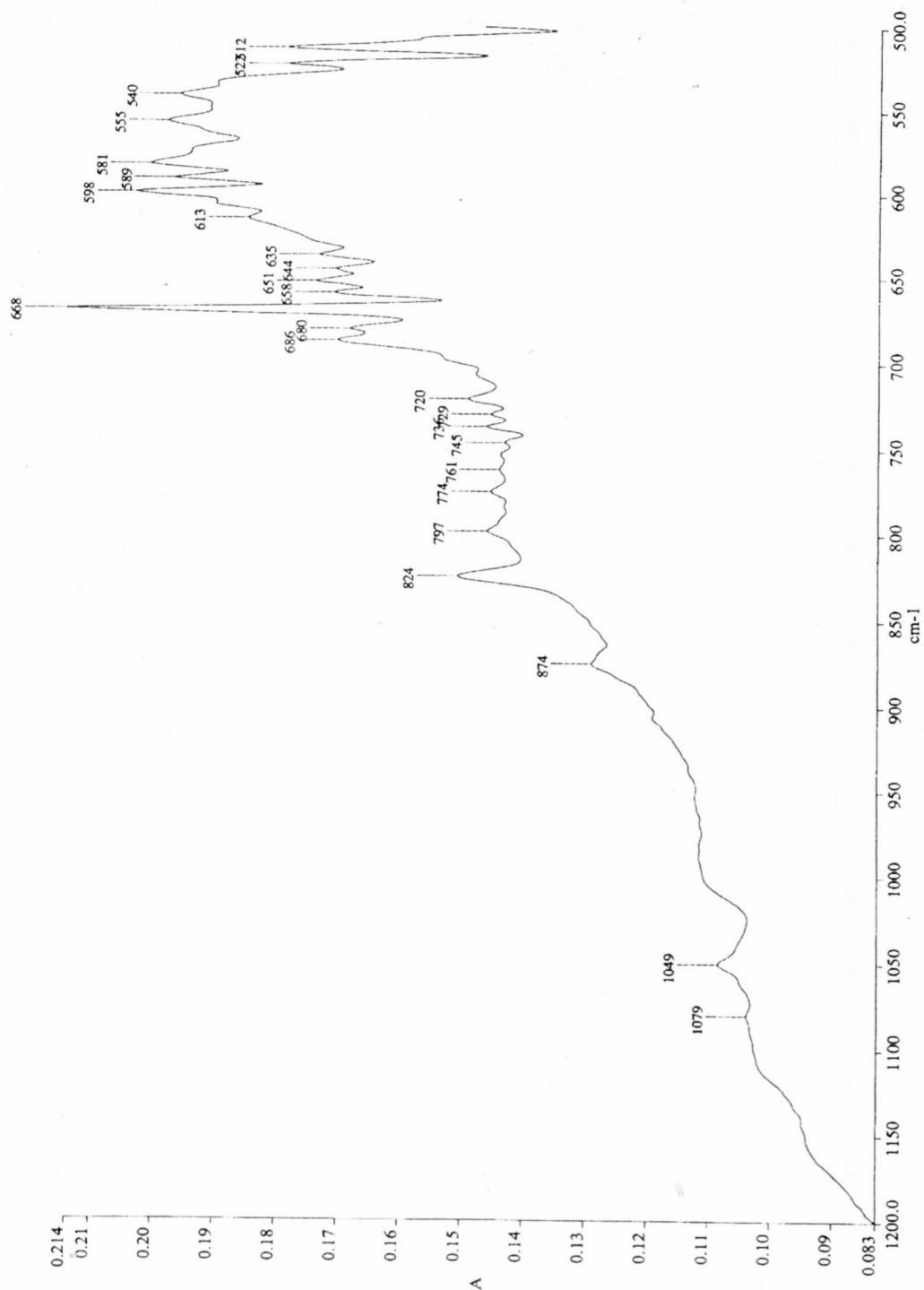


Figure 5.20: IR graph of 36 Eskom (Cl-PhOH)

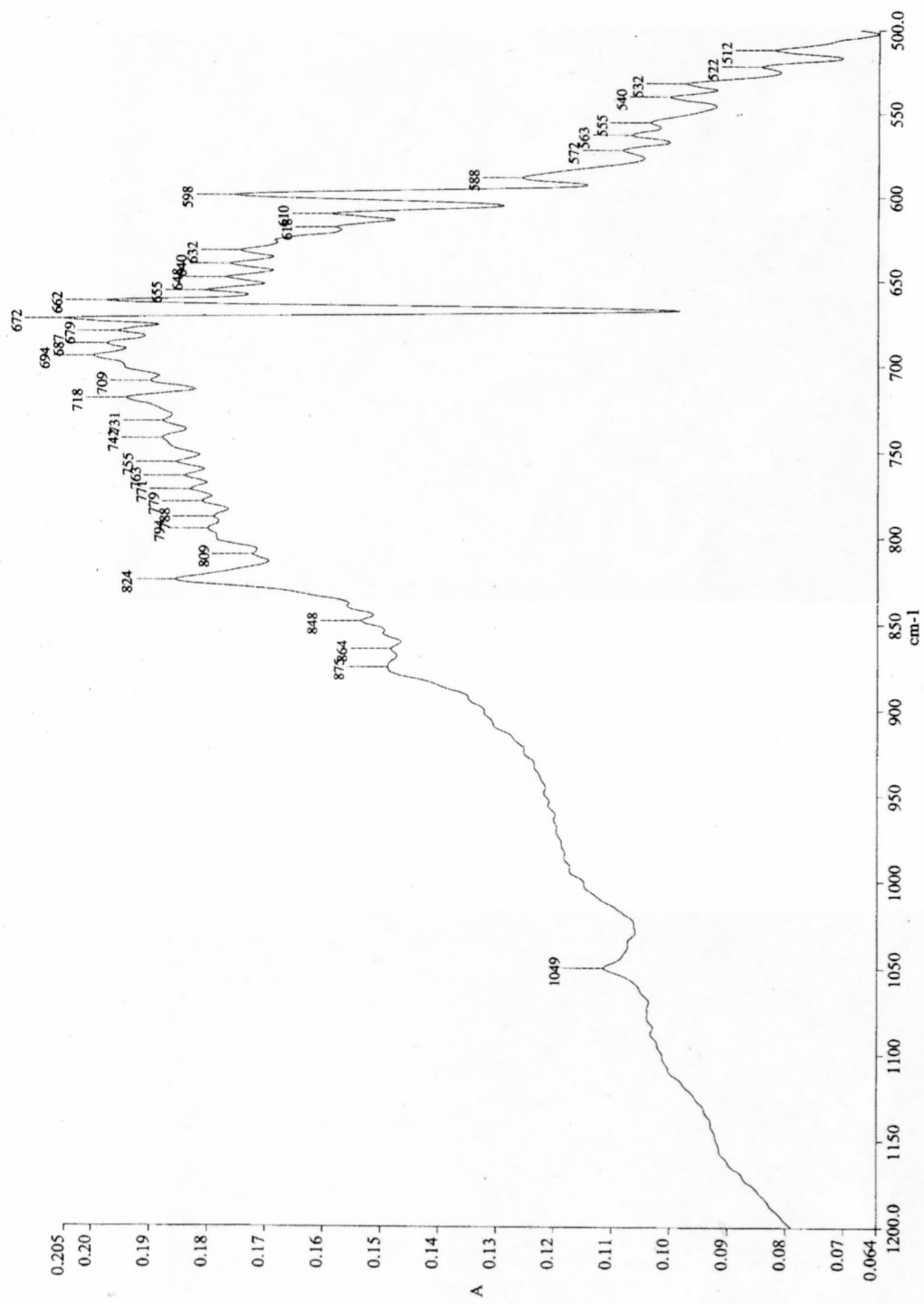


Figure 5.21: SEM image of 36 Sasol (1% PhOH)

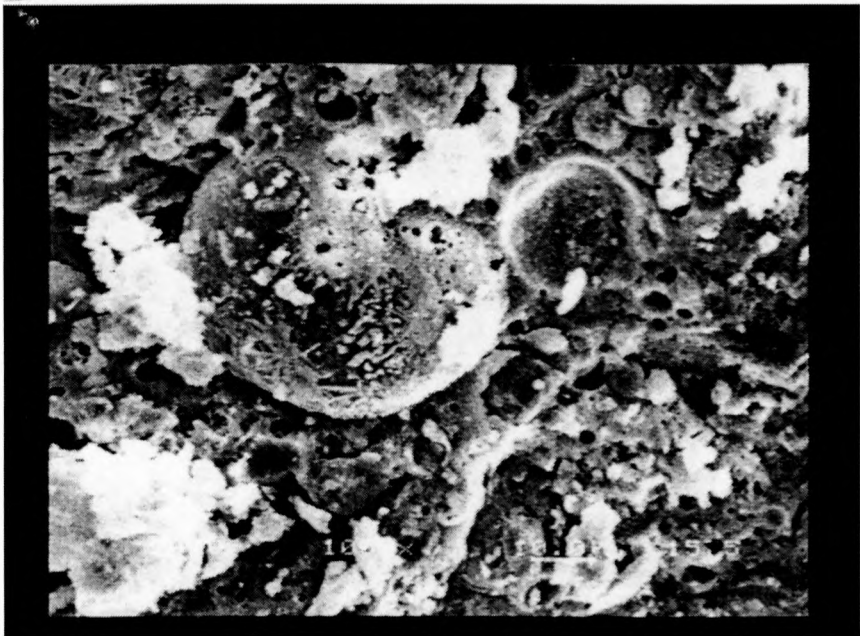
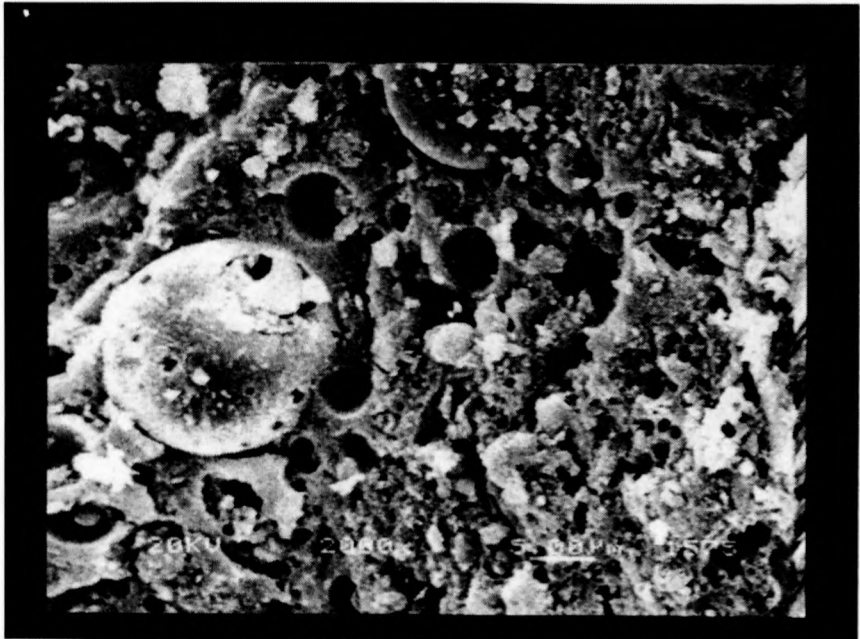
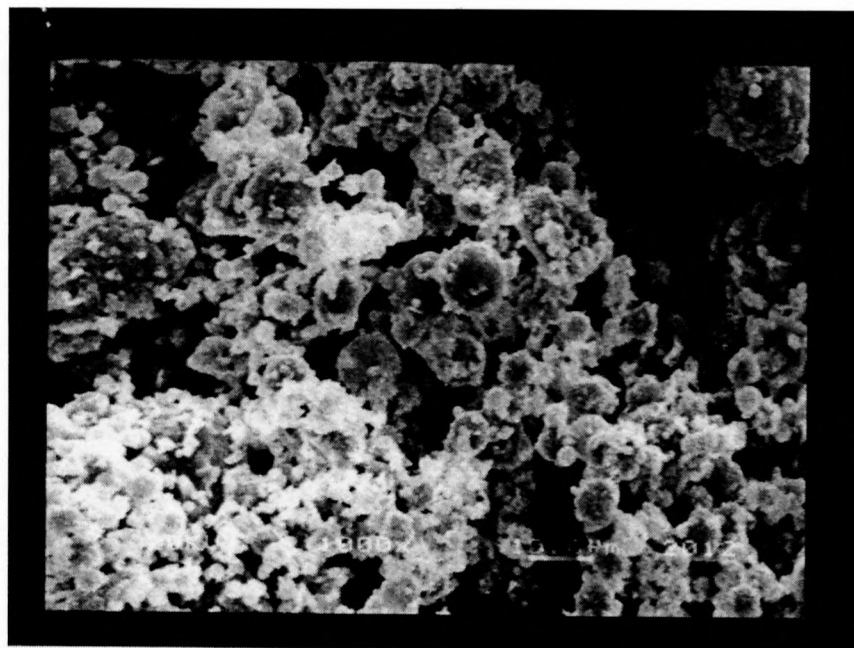


Figure 5.22: SEM image of 36 Eskom (1% PhOH)



**Figure 5.23: SEM image of 36 Sasol (5% PhOH)**



**Figure 5.24: SEM image of 36 Sasol (5% Cl-PhOH)**

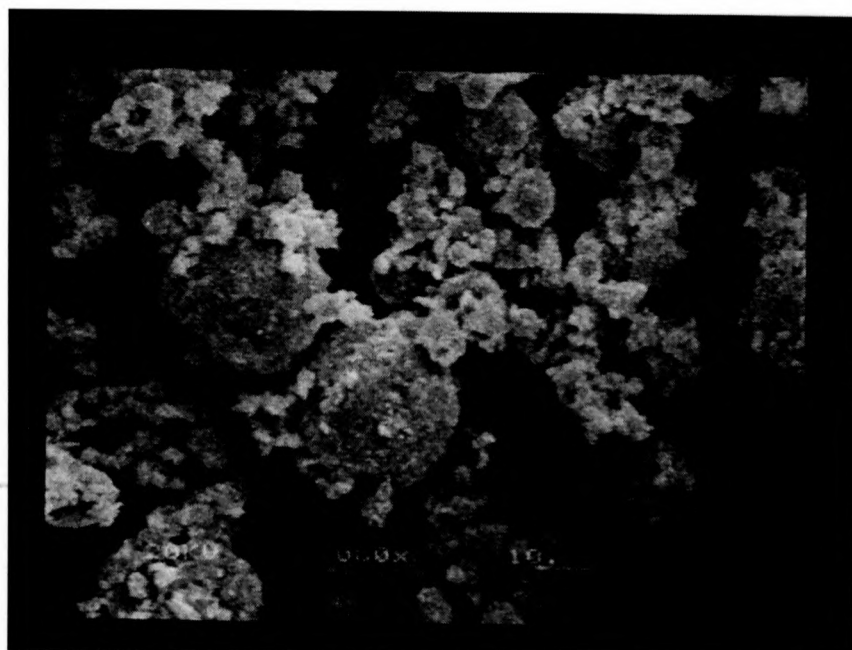




**Figure 5.25: SEM image of 36 Eskom (5% PhOH)**

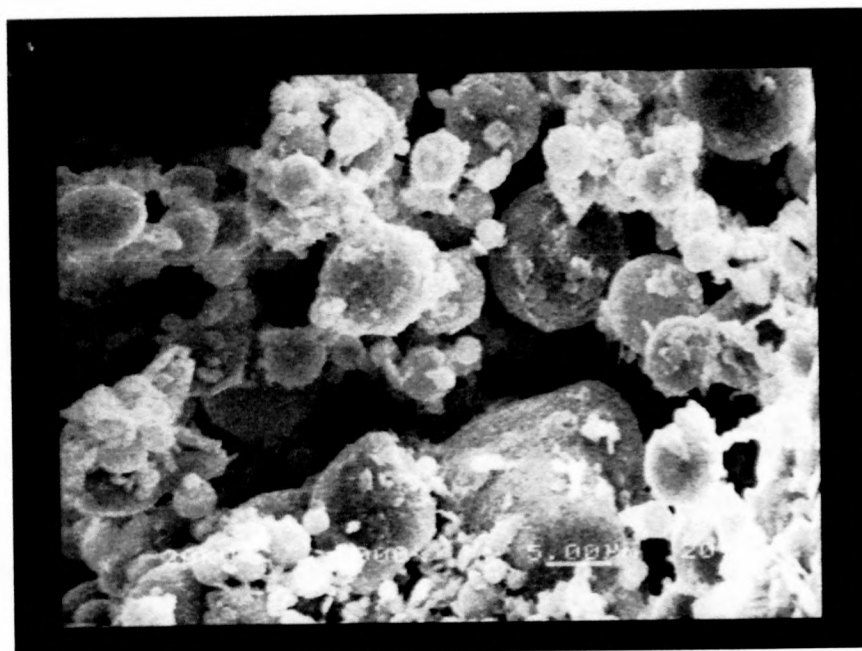
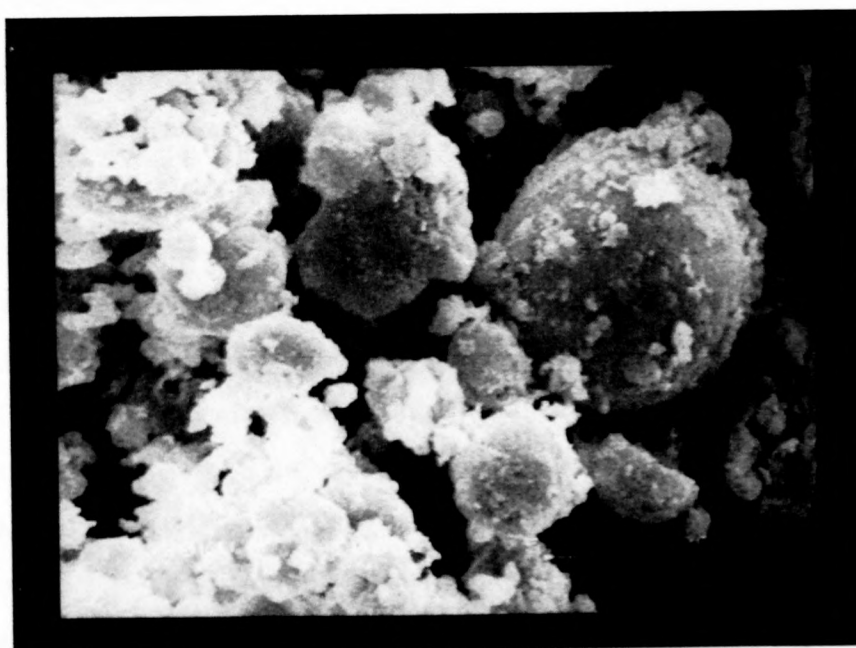


**Figure 5.26: SEM image of 36 Eskom (5% Cl-PhOH)**



# Chapter 6

## ZEOLITES

The lack of available landfill sites and growing environmental concern have resulted in a move to reduce industrial and organic waste. Zeolites are gaining widespread recognition in industrial and commercial applications for the removal of radioactive waste from contaminated water, clean up of oil rig leakages, adsorption of heavy metals and adsorbent linings in landfills. For this study zeolites were utilised for their adsorption capacity in the removal of organics from aqueous solutions. Chapter 6 provides a description on zeolite types, synthesis and properties.

### 6.1 BACKGROUND

#### 6.1.1 Previous Studies

As a result of growing environmental concerns and regulations regarding organic waste from industrial streams, new research efforts have emerged on adsorption processes and adsorbent materials for separating organics from wastewater streams. One such approach involves methods of converting various coal ashes into zeolites. Zeolites are another important class of aluminosilicates, which have gained increasing recognition as commercial adsorbents for heavy metals. However, studies of adsorption of organic molecules onto zeolites from wastewater streams are rare. Earlier work on the adsorption of organics by aluminosilicates includes the adsorption of alcohols (Milestone and Bibbey, 1981), and the adsorption of phenols, cresols and benzyl alcohols (Narita and Okabe, 1985) in silicalites. In another study (Franklin and Williams, 1988) reported on the selective adsorption of sugars and sugar alcohols by zeolite X and zeolite Y. Shu et al. (1997) investigated the adsorptive properties of microporous aluminosilicate materials for the removal of organics from aqueous

streams. The three adsorbents investigated were surfactant-modified zirconium pillared clays, silicalites and zeolite Beta.

The disposal of fly ash generated from the combustion of coal poses a serious environmental problem, due to the shortage of landfill sites. Stringent environmental regulations and lack of available landfill sites catalysed research into new ways of utilising fly ash. This culminated in the synthesis of zeolites from fly ash. Traditionally zeolites have been synthesised using laboratory reagents (Breck, 1974), but due to the high content of readily available silica and aluminium phases (Gutierrez et al., 1993; Chang and Shih, 1998) fly ash has been found to be particularly useful as a starting material for both zeolite and geopolymer synthesis.

### **6.1.2 Types of Zeolites**

Zeolites are crystalline natural volcanic material consisting of hydrated aluminosilicates of group I and group II elements. The zeolite framework is structurally aluminosilicates that consist of infinitely extending three-dimensional networks of  $\text{AlO}_4$  and  $\text{SiO}_4$  tetrahedrally linked to each other by sharing all of the oxygen atoms. There are 34 species of zeolite minerals and about 100 types of synthetic zeolites (Breck, 1974), but only a few have practical significance at the present time. Many unsolved problems still exist in the characterisation and identification of zeolites due to the absence of chemical nomenclature. The classification presented by Breck (1974) is based on the framework topology of the zeolites for which the structures are known. The classification consists of seven groups. Zeolites have a common subunit of structure, which is a specific array of  $\text{AlO}_4$  and  $\text{SiO}_4$  tetrahedra. In the classification the Si-Al distribution is neglected. For example, the two simplest units are the ring of four tetrahedral (4-ring) and six tetrahedral (6-ring) as found in many other framework aluminosilicates (Breck, 1974). These subunits have been called secondary building units (SBU) by Meier (1971). The primary units are the  $\text{AlO}_4$  and  $\text{SiO}_4$  tetrahedra. The seven groups are listed in Table 6.1. Following the classification procedure of Breck (1974), the synthesised

zeolite, zeolite NaP1, is topologically similar to that of gismondine and is therefore a group 1 zeolite. Clinoptilolite is listed as a group 7 zeolite.

### **6.1.3 Inorganic/Organic Adsorption by Zeolites**

Zeolites, due to their uniform pore sizes and large surface areas, are very useful materials for a wide range of applications such as ion exchange, molecular sieves, adsorbents and catalysts. One gram of zeolite provides up to several hundred square metres of surface area for chemical reactions to take place. This characteristic of zeolites gives them enormous adsorbing power. Zeolites are able to absorb up to 30% of their dry weight in gases such as nitrogen and ammonia, over 70% of water and up to 90% of certain hydrocarbons (AmZorb). Zeolites also have the ability to exchange ions. This substitution of ions enables zeolites to selectively adsorb certain toxic elements from soil, water, and air. An example of this unique ability is the removal of calcium from hard water. Zeolites exchange sodium ions for calcium ions, which result in soft water. Zeolites also have a strong affinity for certain harmful heavy metals such as mercury, chromium and lead.

The adsorption of organics from aqueous streams depends not only on the pore structure, but also on the competition between the organic and the water for the adsorption site. For effective organic removal a hydrophobic zeolite is required. Higher Si:Al ratios correspond to higher hydrophobicity and a higher adsorption capacity of the zeolite towards the organic. This accounts for the dealumination process, which is explained in Chapter 4. It should, however, be noted that if the organic molecule is larger than the pore opening of the zeolite, adsorption can only occur on the external surface of the zeolite, and is therefore adsorbed with greatly diminished capacity. As a result of its considerable properties and abilities, industrial, and environmental applications of zeolites are numerous. Applications in the fields of engineering and industrial chemistry include air-purification systems, adsorption of heavy metals, absorbent linings in landfills, removal of radioactive elements from

contaminated waste water, gas absorption and separation and clean-up of oil rig leakages.

## **6.2 ZEOLITE SYNTHESIS**

### **6.2.1 Zeolite Synthesis**

The zeolitisation process in its simplest form is a hydrothermal synthesis of zeolites in aqueous sodium alkaline solutions. The term hydrothermal is used in a broad sense and includes the crystallisation of zeolites from aqueous solutions, which contain the necessary reagents. According to Yang et al. (1997), hydrothermal synthesis is a naturally occurring process that produces several classes of inorganic natural minerals such as smectites, feldspars and micas. The hydrothermal synthesis of zeolites can be described (Yang et al., 1997) by the chemical changes depicted in Figure 6.1. Chang and Shih, (1998); and Querol et al. (1995) have reported on the low-temperature conversion of fly ash into zeolites, namely zeolite A and P and faujasites. General conditions used in the synthesis of zeolites (Breck, 1974) are:

1. Reactive starting materials such as freshly coprecipitated gels, or amorphous solids.
2. Relatively high pH introduced in the form of an alkali metal hydroxide or other strong base.
3. Low temperature hydrothermal conditions with concurrent low autogenous pressure at saturated water vapour pressure.
4. A high degree of supersaturation of the components of the gel leading to the nucleation of a large number of crystals.

Synthesis and modifications of zeolite NaP1 and clinoptilolite are detailed in Chapter 4.

## 6.2.2 Influence of Synthesis Factors

Previous research has shown that various synthesis (especially alkalinity, Si:Al ratio and temperature) factors influence the structural formation of zeolites (Breck, 1974; Barrer, 1982). These differences greatly influence the chemical and physical properties of the final zeolitic product. The synthesis factors that affect zeolite synthesis are reported in the thesis of Van Jaarsveld (2000). These chemical and physical parameters are:

### 6.2.2.1. Temperature and Pressure

According to Breck (1974) early hydrothermal synthesis was confined to temperatures above 200°C and correspondingly elevated pressures (200 MPa). Querol et al. (1995) and Chang and Shih, (1998) reported on the low temperature (38°C) conversion of fly ash into zeolites, namely zeolite A and P and faujasites. Yang et al., (1997) investigated the synthesis of the stable structure gismondine at crystallisation temperatures of 100°C. The investigations of Yang et al. (1997) support the general rule that the more stable zeolite phases are favoured by crystallisation at high temperatures.

### 6.2.2.2. Alkalinity

The monographs of Querol et al. (1997a) and Singer and Bergaut (1995) detail the heat treatment of fly ash in an alkali environment to synthesise zeolites. Yang et al. (1997) observed that the most stable structure, analcime, is dominant at high alkalinity values, while the less stable structure of mordenite is observed for low alkalinity gels. The stable structure of gismondine is dominant at alkalinity values in the range of 0.9-2.0. Woolard et al. (2000) reported on the formation of zeolite NaP1 in solutions of 1M NaOH and 3M NaOH. Similar observations were made by Querol et al. (1997b) and Singer and Bergaut (1995) who found that zeolite NaP1 formed at base concentrations <3.5M. According to Singer and Bergaut (1995) zeolite NaP1 is the first zeolite to form, but with increasing reaction time is gradually replaced by a NaP1 derivative, hydroxysodalite. It can therefore, be concluded that the solid reagents

dissolve rapidly in the alkaline solution to form soluble active species for zeolite formation.

#### **6.2.2.3. Ageing/Crystallisation Times**

The crystallisation times of zeolites have been shown to range from 12-16 hours to anything between 24 hours to 60 days (Yang et al., 1997; Barrer, 1982). According to Breck (1974) an ageing reaction mixture prepared from colloidal silica sols adds an equilibration step in order to promote depolymerisation of the solid colloidal silica particles. The formation of zeolite nuclei occurs by the solubilisation of silicate anions from the colloidal silica product and interaction with the aluminate anions already present in the solution. It should be noted that temperature greatly influences crystallisation times, for example zeolite X can be synthesised at 50°C for 60 hours, as compared to 3 hours at 100°C. Zeolite NaP1 was synthesised using an ageing time of 72 hours.

#### **6.2.2.4. Alkali Cations**

The fundamental unit of a zeolite is a tetrahedral complex consisting of  $\text{Si}^{4+}$  coordinated with four oxygen atoms. The  $\text{Al}^{3+}$  ion commonly coordinates tetrahedrally as well as octahedrally with oxygen in silicates. The substitution of aluminium for silicon produces an electrical charge deficiency that must be neutralised by the addition of a positive charge, generally one of the alkali metals or alkaline earth metals. Different types of zeolites result from the different types of ions that substitute within the interstices.

#### **6.2.2.5. Si:Al Ratios**

The ratio of Si:Al greatly influences the final structure of zeolites. As illustrated by Breck (1974) the growth steps in zeolites indicate that the species in solution contribute to crystal growth. To produce the high purity synthetic type of mordenite a

SiO<sub>2</sub>:Al<sub>2</sub>O<sub>3</sub> ratio of 12:13 was required. Clinoptilolite has a relatively high silica content (Si:Al = 3.85) while zeolite NaP1 was synthesised from fly ash, which generally has low Si:Al ratio thereby producing low-Si zeolites with high ion exchange capacities.

#### **6.2.2.6. Starting Reagents**

Generally zeolites have been synthesised using laboratory reagents such as soluble silicates, aluminates and alkali solutions (Breck, 1974; Barrer, 1982). Stricter environmental regulations catalysed research into the synthesis of zeolites from various fly ashes. This led to a number of successful investigations. Zeolite NaP1 was synthesised utilising Eskom fly ash and clinoptilolite was commercially synthesised by Pratley.

The three compositional molar ratios that are important in determining the synthesis and structural formation of zeolites are Na<sub>2</sub>O:H<sub>2</sub>O, Na<sub>2</sub>O:SiO<sub>2</sub> and SiO<sub>2</sub>:Al<sub>2</sub>O<sub>3</sub> (Breck, 1974; Yang et al., 1997). These ratios are used widely in research to denote the compositions of the reaction mixtures for zeolite synthesis.

## **6.3 PHYSICAL/CHEMICAL PROPERTIES OF ZEOLITES**

### **6.3.1 Physical Properties**

#### **6.3.1.1 Particle Size**

Zeolite minerals occur in igneous rocks as well developed, single crystals, which may be as large as several millimetres (Breck, 1974). Synthetic zeolites that are crystallised from hydrogels or by the conversion of other aluminium silicates such as kaolin are produced as crystalline powders with a typical particle size of a few microns. The crystallites formed during the zeolitisation process of zeolite NaP1 are



small, mostly  $<1\mu\text{m}$  (Woolard et al., 2000). The very small particle size of most synthetic zeolites is not suitable for use in most applications and as a result, the crystals must be formed into polycrystalline aggregates in order to be packed into columns for use in adsorption or catalytic processes (Breck, 1974).

#### **6.3.1.2 Surface Morphology**

SEM is used extensively to study the surface topography of zeolites. SEM analysis of zeolite NaP1 indicates that the unmodified fly ash consists of spherical particles (Figure 6.2) but alkaline treatment gives rise to polycrystalline spherulites with an irregular surface exhibiting needle-like outwardly radiating crystals (Figure 6.3). These observations are in accordance with Woolard et al. (2000) and Querol et al. (1997a).

#### **6.3.1.3 Density**

The density of the zeolite depends on the openness of the zeolite structure and the cation. Cation exchange with heavy ions increases the density of the zeolite (Breck, 1974). According to Breck (1974) the density of zeolites is low, generally ranging from about 1.9 to 2.3 g/cc. Clinoptilolite and gismondine have a framework density of 2.2 g/cc and 1.52 g/cc respectively. Structures of increased density are less soluble, and from a physio-chemical point of view the denser structure is more stable (Yang et al., 1997).

#### **6.3.1.4 Zeolite Structure**

Zeolite Na-P1 has a topology similar to that of gismondine (Figure 6.4). In view of the absence of specific structural data, clinoptilolite is listed as a distinct zeolite (Breck, 1974), and may even structurally resemble mordenite.

### **6.3.1.5 Colour**

Zeolites in a pure state are colourless. If the alkaline or alkaline earth metals present in the zeolite are exchanged by transition metal ions, the zeolite may have a colour. Clinoptilolite has a reflection whiteness of 80%. Zeolite NaP1, because of impurities (not pure quartz or mullite) and due to the fact that the crystals of zeolite NaP1 nucleate on the surface of the fly ash particles, has the same greyish colour as that of the fly ash.

## **6.3.2 Chemical Properties**

Zeolites are microporous solids with high specific surface areas, an unusual crystal structure and a unique ability to exchange ions. Zeolites are composed primarily of hydrogen, oxygen, aluminium and silicon. The arrangement of these elements within the zeolite gives the crystal a honeycomb framework of channels and cavities. A summary of the chemical compositions of clinoptilolite and gismondine is listed in Table 6.2 and Table 6.3, respectively.

### **6.3.2.1 Zeolite Chemical Reactions**

The chemical reactions of zeolites may be classified in the following categories (Breck, 1974):

1. Reactions which involve:
  - 1.1 water as a volatile reacting phase – dehydration and hydrolysis.
  - 1.2 volatile phases other than water.
  - 1.3 ionic species in solution.
  
2. Recrystallisation reactions after dehydration.

3. Formation of structural defects by:
  - 3.1 decationisation and dehydroxylation.
  - 3.2 dealumination, that is removal of framework aluminium atoms.
  - 3.3 hydrothermal stabilisation.
  - 3.4 metal cation reduction.

Adsorption of organics onto zeolite NaP1 and clinoptilolite occurred only on the external surface of the zeolite since the microporosity of the zeolite is not accessible to the organic. The ultimate base exchange capacity of a zeolite depends on the chemical composition; a higher exchange capacity is observed with zeolites of low SiO<sub>2</sub>:Al<sub>2</sub>O<sub>3</sub> ratio (Breck, 1974).

### **6.3.2.2 Zeolite Reactions in Solutions**

Previous research (Breck, 1974) has shown that zeolite minerals are decomposed by acids, with the subsequent formation of gels. The general rule, according to Breck (1974) is that those zeolites with a Si/Al ratio < 1.5 gelatinize, whilst zeolites with a Si:Al ratio > 1.5 generally decompose and form precipitates of hydrous silica. The disintegration of zeolite structures by strong acids is related to the number of aluminium atoms in the tetrahedral positions in the framework since they appear to be the site of acid attack (Breck, 1974).

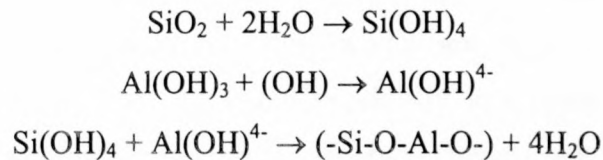
Zeolites are generally stable under the conditions of their synthesis, but may undergo conversion to different species with time. As reported by Breck (1974), zeolite A when exposed to dilute sodium hydroxide solutions for prolonged periods of time, converts to the zeolite P phase, and in more concentrated solutions, it converts further to the hydroxysodalite hydrate.

The use of chelating reagents for the removal of aluminium has also been reported (Breck, 1974). Aluminium can be removed from the framework structure of clinoptilolite and mordenite (Breck, 1974) by treatment with strong acids such as hydrochloric acid, other zeolites are, however, destroyed.

## 6.4 DIFFERENCES/SIMILARITIES BETWEEN ZEOLITES AND GEOPOLYMERS

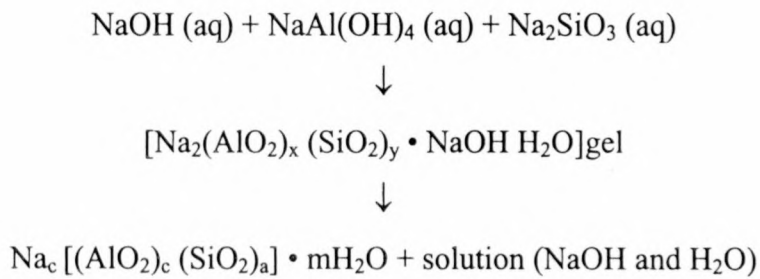
Geopolymeric binders are the synthetic analogues of natural zeolites and require similar hydrothermal synthesis conditions. In a geopolymeric system reaction times are, however, faster which results in amorphous to semi-crystalline matrices, whilst zeolites crystallise from dilute solutions and have enough time to form lower density, cage like crystalline structures.

**The polycondensation into a zeolite may be schematically represented as follows:**



The geopolymer condensation reaction can be schematically represented in the following way:

**Geopolymer polycondensation reaction:**



It should be noted that zeolites usually form in closed hydrothermal systems while geopolymers can be cured at room temperature. Geopolymer reactions are analogous to zeolite formation. Yang et al. (1997) reported on the tendency of zeolite systems to form amorphous structures at low temperatures, with a more crystalline product being formed at higher temperatures. Another difference between zeolite synthesis and

geopolymerisation is that the concentration of precursor species before solidification in geopolymerisation is far greater than in the case of zeolite formation. In zeolite synthesis the compositional ratios  $\text{SiO}_2:\text{Al}_2\text{O}_3$  and  $(\text{Na}_2\text{O} + \text{K}_2\text{O}):\text{SiO}_2$  determine the final crystal structure of different zeolites. It is believed that these ratios also structurally influence geopolymer formation. This work supports the idea that geopolymers are the amorphous equivalents of crystalline zeolites.

## **6.5 SUMMARY**

Chapter 6 provides a detailed explanation on zeolite types, synthesis and properties. It is these zeolite characteristics/properties, which are utilised in Chapter 7 for maximum organic adsorption. As stated previously in Chapter 6, studies on the adsorption of organic molecules from aqueous streams are rare. Modification procedures were therefore necessary to ensure maximum organic adsorption. These modification procedures are detailed in Chapter 4. The results of these modification procedures are reported in Chapter 7.

**Table 6.1: 7 Groups of zeolites (Breck, 1974)**

Group	Secondary Building Unit (SBU)	Examples
1	Single 4-ring, S4R	Analcime, Gismondine
2	Single 6-ring, S6R	Erionite
3	Double 4-ring, D4R	Zeolite A
4	Double 6-ring, D6R	Chabazite
5	Complex 4-1, T <sub>5</sub> O <sub>10</sub> unit	Edingtonite
6	Complex 5-1, T <sub>8</sub> O <sub>16</sub> unit	Bikitaite
7	Complex 4-4-1, T <sub>10</sub> O <sub>20</sub> unit	Clinoptilolite, Brewsterite

**Table 6.2: Chemical composition of clinoptilolite (Breck, 1974)**

Chemical Composition	Data
Oxide Formula	(Na <sub>2</sub> ,K <sub>2</sub> )O • Al <sub>2</sub> O <sub>3</sub> • 10SiO <sub>2</sub> • 8 H <sub>2</sub> O
Unit Cell Contents	Na <sub>6</sub> [(AlO <sub>2</sub> ) <sub>6</sub> (SiO <sub>2</sub> ) <sub>30</sub> ] • 24 H <sub>2</sub> O
Crystallography	Data
Symmetry	Monoclinic
Unit Cell Volume	2100 Å <sup>3</sup>
Structure	Properties
Cage Type	No Data
Free Apertures (Hydrated)	No Data
Cation Locations	Possibly related to heulandite but not determined.
Effect of Dehydration	Stable to 700°C
Largest Molecule Adsorbed	O <sub>2</sub>

**Table 6.3: Chemical composition of gismondine (Breck, 1974)**

<b>Chemical Composition</b>	<b>Data</b>
Oxide Formula	CaO • Al <sub>2</sub> O <sub>3</sub> • 2SiO <sub>2</sub> • 4 H <sub>2</sub> O
Unit Cell Contents	Ca <sub>4</sub> [(AlO <sub>2</sub> ) <sub>8</sub> (SiO <sub>2</sub> ) <sub>8</sub> ] • 16 H <sub>2</sub> O
<b>Crystallography</b>	<b>Data</b>
Symmetry	Monoclinic
Unit Cell Volume	1046 Å <sup>3</sup>
<b>Structure</b>	<b>Properties</b>
Cage Type	Non-Specific
Free Apertures (Hydrated)	8-rings
Cation Locations	At channel intersection coordinated to 4 H <sub>2</sub> O and 2 cations
Effect of Dehydration	Stable to 250°C
Largest Molecule Adsorbed	H <sub>2</sub> O

**Figure 6.1: Hydrothermal synthesis of zeolites**

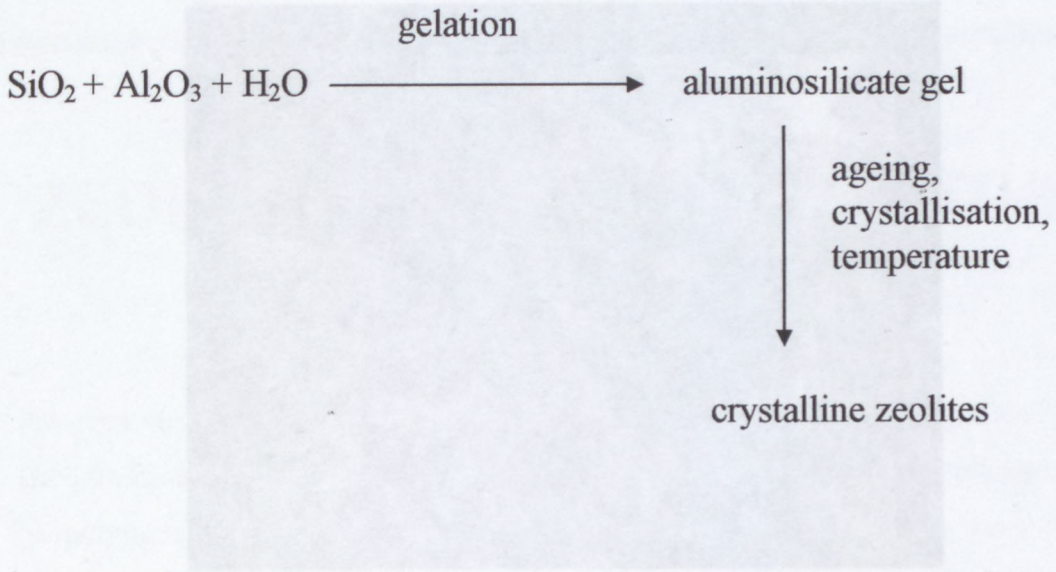


**Figure 6.2: SEM image of fly ash**

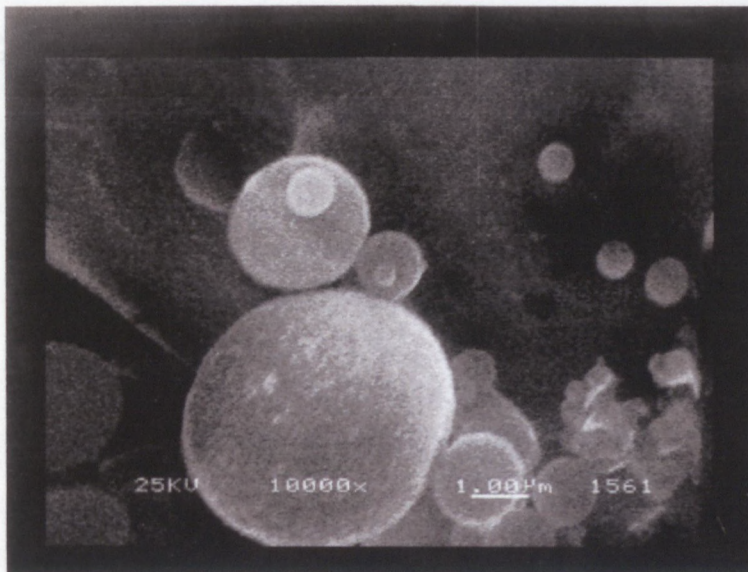
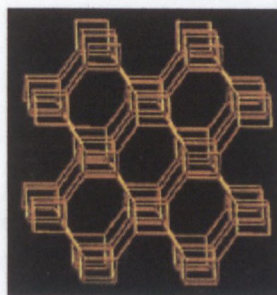




**Figure 6.3: SEM image of zeolite NaP1**



**Figure 6.4: Gismondine structure**



**Structure of zeolite NaP1**

# Chapter 7

## ZEOLITE INCORPORATION WITHIN GEOPOLYMERS

Previous studies by Van Jaarsveld et al. (1997); Van Jaarsveld et al. (1998) and Davidovits and Comrie (1990) have reported on the numerous applications of geopolymers in the immobilisation of toxic metals. Research into the possible utilisation of geopolymers as an encapsulation media for organic waste has, however, been rare. Chapter 7 provides an insight into the possible utilisation of geopolymers as binder for hazardous organic materials, specifically phenol and 4-chlorophenol. Leaching tests were performed on the geopolymer matrices containing the hazardous organic matter as an indication of the durability of the solid monolith. The leaching data also provide a quantitative measurement of the relative immobilisation efficiency of the geopolymer matrices. Chapter 7 reports on the leaching data obtained and a possible explanation for the trends observed.

### 7.1 INTRODUCTION

The brittle nature of ordinary Portland Cement (OPC) has necessitated the incorporation of an additional reinforcing phase. The use of mineral admixtures to prevent the deleterious effects of the alkali-silica reaction (ASR) and hence prevent the brittleness of OPC has been known for a long time (Chen et al., 1993; Thomas et al., 1996; Xu et al., 1995). LaRosa et al. (1992) investigated the alternative to mineral admixture, that is the feasibility of forming self-generating composites in which the reinforcing phase develops within the matrix during curing. LaRosa et al. (1992) have shown in their investigations that zeolites may serve in this capacity since they readily precipitate in matrices containing cement. Feng and Hao (1998) also reported on the

use of natural zeolites as a new kind of mineral admixture, which is capable of suppressing ASR expansion in concrete. The industrial application of zeolites in cement is their use as pozzolans in blended cement. In cement chemistry, pozzolans are highly reactive silicates, which are added to cement to reduce the free lime, content and aid in controlling the ASR reaction. According to LaRosa et al. (1992) zeolites can be more reactive, that is have a higher pozzolanic activity compared to nonzeolitic pozzolans; in addition zeolitic pozzolans can produce higher compressive strengths in cement as compared to OPC and nonzeolitic-pozzolan cements. Grutzeck et al. (1989) presented data suggesting that zeolites developed in the presence of calcium silicate hydrate. This evidence provides an indication of the potential for zeolites to be synthesised within cement paste. Chapter 7 will provide a discussion on the incorporation of zeolites within geopolymers and the effect on the physical/chemical properties of the geopolymer compared to that of OPC.

## **7.2 ORGANIC ADSORPTION BY ZEOLITES**

### **7.2.1 Introduction**

Adsorption is one of the most common control technologies used in the reduction of volatile organic compounds emission from industries. Two kinds of challenges exist (Bottero et al., 1994) when selecting any solid for the adsorption of organics from a waste water stream. These are: 1. Finding adsorbents with high specific surface areas, 2. Finding adsorbents, which adsorb large quantities of specific contaminants in the presence of background organics. Taking these two challenges into consideration, high surface area zeolitic material (zeolite NaP1 and clinoptilolite) was utilised in the adsorption of organics from aqueous solutions.

### **7.2.2 Zeolite Synthesis**

X-ray diffraction patterns and SEM images were utilised as the characterisation methods for the synthesised zeolite, zeolite NaP1. A detailed discussion on the

physical and chemical characteristics of zeolite NaP1 and clinoptilolite is reported in Chapter 6.

### 7.2.2.1: XRD Analysis

The XRD patterns for the untreated fly ash sample and the treated 3M NaOH fly ash sample can be seen in Figures 7.1 and 7.2 respectively. The crystalline phases identified are mullite ( $\text{Al}_6\text{Si}_2\text{O}_{13}$ ) and quartz ( $\text{SiO}_2$ ). There is a large proportion of amorphous material (glass phase) present in the samples. It is this amorphous glassy phase, which causes an increase in background counts. This can be clearly observed as a “hump” between  $\sim 15^\circ$  and  $35^\circ$ ,  $2\theta$  on the diffractograms. There are two minor peaks present at  $\sim 32.5^\circ$  and  $37.5^\circ$   $2\theta$ , probably of another minor component present that could not be identified at this stage. Apart from mullite and quartz present, a third phase was identified as sodium aluminium silicate ( $\text{Na}_6\text{Al}_6\text{Si}_{10}\text{O}_{32}$ ) commonly called zeolite NaP1. A minor unidentified peak is present at  $\sim 6^\circ$   $2\theta$ .

### 7.2.2.2: Surface Area Changes

Analysis of the scanning electron images of the untreated and treated fly ash samples show a significant change in the surface morphology. The untreated fly ash is composed of smooth spherical fly ash particles (Figure 6.2). After alkaline treatment the spherical particles of fly ash are covered with polycrystalline spherulites, exhibiting needle-like outwardly radiating crystals (Figure 6.3). The crystals formed during the zeolitisation process were found to be relatively small  $< 1\mu\text{m}$ .

Hydrothermal treatment of fly ash increased the surface area of the fly ash from  $5\text{m}^2/\text{g}$  to  $62.04\text{m}^2/\text{g}$ . Observations show that acid treatment of zeolite NaP1 increases the surface area of the zeolite by a factor of almost 4 (Table 7.1). The increase in surface area is primarily due to the removal of cementitious materials such as  $\text{CaCO}_3$ , which promotes agglomeration of particles.

### **7.2.2.3: Cation exchange capacity**

CEC's for zeolite NaP1 were determined using the procedure detailed in Chapter 3. The CEC value rose from 25 mmol/100g for untreated fly ash to 165 mmol/100g for the 3M NaOH treated fly ash. The calculation of CEC values was obtained from analysis of the concentration of Na being displaced from 1g of zeolitic material. This indicates that the zeolitic fly ash is activated with respect to ion exchange. Indeed Woolard et al. (2000) reported that the lead adsorption capacity of synthesised zeolite NaP1 was higher than that observed for the natural zeolite clinoptilolite. CEC values obtained from Pratley illustrate that typical CEC's vary from 1.2-1.5 meq/g that is 22-27 grams of ammonium ion per kg of clinoptilolite.

## **7.2.3 Adsorbed Organics on Zeolites**

### **7.2.3.1 Types of zeolites**

Zeolites NaP1 and clinoptilolite were used as the solid adsorbents for the removal of organics from aqueous solutions. Zeolite NaP1 was synthesised from Eskom fly ash according to the method detailed in Chapter 3. XRD analysis confirms the presence of zeolite NaP1 (Figure 7.2). The natural zeolite clinoptilolite was obtained from Pratley. Modification treatments to the zeolites were conducted (detailed in Chapter 3) to maximise organic adsorption by zeolites. The results/discussion of the modification treatments are reported in Section 7.2.3.3.

### **7.2.3.2 Organic adsorption experiments**

The adsorption capacities of the zeolites were measured by adding 5g of the adsorbent to a 200ml solution containing a known concentration of the adsorbate. The suspensions were shaken for 48 hours at 25°C, before making the equilibrium measurements. After centrifugation, the concentration of the supernatant was determined from the analysis of the DIONEX data. Adsorption was determined by

measuring the difference between the initial and final concentration of organic in solution.

### 7.2.3.3 Adsorption Data

A commercially available zeolite, clinoptilolite and the synthesised zeolite, NaP1, were the solid adsorbents used. Adsorption data are reported in Figure 7.3. Analysis of the data shows adsorption results of 13.9ppm for phenol and 38.5ppm for chlorophenol for the modified acid zeolite NaP1 [Zeolite 2 (3M)]. The dealuminated zeolite NaP1 [Zeolite 2 (3M-Deal)] however has higher adsorption results than the modified acid zeolite NaP1 [Zeolite 2 (3M)]. The adsorption values of Zeolite 2 (3M-deal) are 14.7ppm for phenol and 61.0ppm for chlorophenol. A similar trend is observed for Fine Zeolite and Fine Zeolite (Deal). Fine Zeolite (Deal) has higher adsorption values for phenol and chlorophenol than Fine Zeolite. This can be attributed to 2 reasons: 1. The organic molecules are larger than the pore sizes of the zeolite and can only be adsorbed on the external surface of the zeolite, hence larger surface areas equate to greater adsorption capacities. 2. The dealumination process causes an increase in the Si:Al ratio of the zeolite, which corresponds to higher hydrophobicity and hence higher adsorption capacities towards the organic molecules. The adsorption capacity of clinoptilolite (Fine Zeolite, Coarse Zeolite and fine Zeolite (Deal)) is much higher than that of zeolite NaP1 [Zeolite 2 (3M) and Zeolite 2 (3M-Deal)]. A possible explanation for this trend is that aluminium can be removed from the framework structure of clinoptilolite (Breck, 1974) without being completely destroyed, unlike other zeolites. The Fine Zeolite also has higher adsorption results than the Coarse Zeolite. This could be due to the higher external surface area of the fine zeolite. Higher adsorption values were also obtained for 4-chlorophenol. The adsorption for chlorophenols is higher than that for phenols, probably because of the higher solubility of phenol in water (Table 7.2). Another point of interest is the zeta potential data that were obtained. Zeta potential analysis shows that for optimum organic adsorption, experiments should be carried out at a pH of 5 or below. It is at this pH that a positive charge exists on the surface of the zeolite, thus allowing for the attraction of the negatively charged phenoxide ion. The data obtained by Woolard et al. (2000) support this general trend, where the equilibrium data of zeolite NaP1 lie far to the right at all pH's.

## **7.3 ZEOLITE ENCAPSULATION**

The zeolite samples containing the adsorbed organic were coated with a thin layer of geopolymer (utilising recipe 36), and dried for 2 hours at 100°C. The zeolite coated with a thin layer of geopolymer was then crushed, thereafter the crushed zeolite was mixed with the standard geopolymeric matrix (Table 7.3) and cured for 7 days at 30°C. Coating of the zeolite with a layer of geopolymer served a twofold function: firstly to prevent desorption of the organic from the zeolite, and secondly to provide an additional protective layer to the zeolite. The mass percentage of zeolite added to the geopolymeric matrix is reported in Table 7.3. The effect of zeolite addition on the chemical and physical properties of the geopolymer will be discussed in the following subsection.

## **7.4 THE EFFECT OF ZEOLITE ENCAPSULATION ON GEOPOLYMERISATION**

Zeolite incorporation within geopolymers affects both the physical and chemical properties of the geopolymer matrices. To test the effect of zeolite incorporation within geopolymers a variety of analytical tools were utilised; these included compressive strength tests, infrared data, XRD analysis and specific area determinations.

### **7.4.1 Compressive Strength Results and Specific Surface Area Analysis**

Compressive strength analysis was utilised to measure the strength of the geopolymeric matrix. Compressive strength values for the various matrices are reported in Table 7.4. A natural zeolite (clinoptilolite) was added to the matrix, to investigate the effect of zeolites on matrix stability. The strength of the matrices increases with an increase in zeolitic material from 1% to 5%. The increased strength

is expected due to increased crystallization contacts between zeolite and amorphous phases. The matrices containing coarse zeolitic (czeo) material have higher compressive strength values than the matrices containing fine zeolitic (fzeo) material, because the coarse aggregates mechanically interlock with the matrix thereby reducing porosity and increasing strength. However, an increase in crystallinity may lead to the formation of macro-cracks, which negatively affects the mechanical properties of the geopolymer. Research has shown that the maximum amount (g) of zeolitic material that the geopolymer matrix can encapsulate should not exceed 15% of the total mass of the geopolymer system. Zeolite addition exceeding this amount will serve to weaken the geopolymer structure. Encapsulation of the coated zeolite samples in the geopolymer matrix increases the compressive strength values to a maximum value of 40.79 MPa. As stated above, the increased compressive strength values could be attributed to the decreased porosity of the matrix as the coated zeolitic material performs a function similar to that of a filler.

Specific surface area measurements (Table 7.5) show no significant changes in surface area measurements of the geopolymer matrices containing zeolitic material. One would expect that the addition of high internal surface area zeolite materials to the geopolymer matrix would decrease the compressive strength of the matrix; this however is not observed. Addition of the coated zeolitic material has the opposite effect, actually increasing compressive strength of the matrix.

#### **7.4.2 X-Ray Diffraction Analysis**

Geopolymer structures are generally amorphous to semi-amorphous. Due to their amorphous nature a detailed study of geopolymers utilising XRD analysis is not feasible. There are no significant changes between the XRD graphs of the standard geopolymer matrix (Figure 7.3) and the matrices containing zeolites (Figures 7.4-7.7). It is also worth noting that the crystalline phases present in fly ash (quartz and mullite) are also present in the geopolymer matrices. These crystalline phases do not seem to be affected by the geopolymerisation reaction, therefore it can be concluded that fly ash particles are only partially dissolved and therefore a degree of crystallinity is retained in the final geopolymer matrix. The prominent peak at  $26.7^\circ$   $2\theta$  can be



attributed to the quartz component of the fly ash, while the hump in the diffractogram starting at about  $20^\circ 2\theta$  and extending through to  $40^\circ 2\theta$  is due to the significant quantities of amorphous silica present in the sample. Zeolite addition appears to have no significant affect on the size of the hump observed. XRD analysis therefore supports the idea that any new phases that were formed, were largely amorphous and thereby not possible to detect.

### 7.4.3 Infrared Analysis

The bending and stretching modes of the Si-O and Al-O bonds (T-O bonds, where T is either Si or Al) form the basis of all aluminosilicate structures. The peaks as well as the type of bending and stretching modes for geopolymers are listed in Table 7.6 For zeolitic structures the bending and stretching modes of vibrations are listed in Table 7.7. Analysis of the infrared spectra shows that the peaks between  $950$  and  $1050\text{ cm}^{-1}$  are not present for the 36 Sasol geopolymer matrix (Figure 7.8). The matrices containing zeolitic material (Figures 7.9-7.11) and coated zeolitic material (Figures 7.12-7.14) encapsulated within 36 Sasol show peaks in the  $950$ - $1050\text{ cm}^{-1}$  region. These peaks are asymmetric stretching of T-O-bonds. From Table 7.8 it can be seen that in zeolitic structures the strongest stretching vibrations occur in the region  $950$ - $1250\text{ cm}^{-1}$ . This could be a possible explanation for the appearance of peaks in the region  $950$ - $1050\text{ cm}^{-1}$  for matrices containing zeolitic material. Also of interest is the peak appearing at  $1049\text{ cm}^{-1}$ . The ordinary geopolymer (36 Sasol) and matrices containing zeolitic material have this prominent peak at  $1049\text{ cm}^{-1}$ . This peak could be attributed to the stretching of the primary T-O bond and can therefore be viewed as originating from within a Si or Al tetrahedron. Analysis of the infrared spectra shows that the peak at  $1049\text{ cm}^{-1}$  does not shift significantly, therefore the addition of zeolitic material to geopolymers does not significantly affect tetrahedral formation.

## **7.5 LEACHING**

### **7.5.1 Introduction**

Solidification is a common practice for the treatment of wastes before it can be disposed of in a landfill. Hazardous wastes produced as aqueous solutions are being isolated from the environment by incorporation into cement based monolithic solids, where the waste is physically contained and /or chemically bound. Leaching tests were introduced in order to evaluate the long-term leachability of solidified wastes. Geopolymer systems provide an attractive possibility as an immobilisation system for toxic waste. According to Davidovits (1999) immobilisation technologies with geopolymeric materials have three goals. The first goal is to seal the materials into an impermeable monolith. This prevents direct contact of potential leachates, like ground water and percolating rain. The second goal is to design a solid matrix that binds the specific hazardous elements. This reduces the mobility of the hazards within the monoliths. The third goal is to make a durable monolith that weathers environmental stresses.

### **7.5.2 Previous Studies**

Leaching of inorganic metal contaminants from geopolymer matrices has been investigated and discussed by Van Jaarsveld et al. (1997). Davidovits and Comrie (1988) also discussed the efficiency of geopolymer matrices in the stabilisation of waste materials containing various heavy metals. Davidovits (1994) presented leaching data on the immobilisation efficiency of geopolymer matrices for the solidification of waste. Pienaar (1999) performed laboratory scale leaching tests to test the stability of various pozzolanic and geopolymeric matrices. Also of interest were studies conducted by Alberts (1996) and Van Zyl (1997) on the immobilisation and leaching of various toxic metals from fly ash-based immobilisation systems.

### 7.5.3 Factors Affecting Leaching

According to Conner (1990) two sets of factors determine the leachability of a material:

- those that originate with the material itself
- those that are a function of the leaching test (external factors)

The discussion that follows is aimed mainly at the external factors that affect leaching. The discussion is also aimed at batch leaching tests such as the TCLP test (Table 4.4).

#### 7.5.3.1 External Factors

##### (a) Temperature:

Leaching tests are a function of the solubility of the species being investigated and solubility of constituents is a function of temperature. In order to eliminate any errors that may result due to temperature, all leaching tests were conducted at a constant temperature of 25°C. The TCLP standard test is normally 22°C ± 3°C.

##### (b) pH

The control of pH is a very important factor in evaluating the leachability of a species since the solubility of metal hydroxides is very much pH dependent. An acetic acid buffer solution was used to attain pH control in the leaching test. The acetic acid solution causes the geopolymer matrix to break down to a certain extent. This will affect the number of metal ions being released from the matrix.

##### (c) Equipment and Agitation Technique

A vertical stirred impeller system was used to contact the solid and liquid phases. All batch methods use some form of agitation to permit a more rapid attainment of equilibrium. Mixing speeds of 245 rpm were used. Van Jaarsveld (2000) showed that mixing speeds around 200 rpm were optimal because particles were kept suspended

without resulting in an excessive amount of breakage. In the TCLP test a zero headspace extractor (ZHE) is used for leaching of organic constituents.

#### (d) Ratio of Leachant to Waste

It is obvious that no ratio can be selected that would represent real conditions in any given landfill at all times (Conner, 1990). Previous research has shown that higher ratios are more appropriate, resulting in more particle breakdown and also high concentrations of species in solution. When the ratios are low the non-toxic components generate common ion and total ionic strength effects that can reduce the solubility of certain hazardous species. Van Jaarsveld (2000) found that a solid/liquid ratio of 1:25 would be adequate. This leaching ratio was used throughout all the leaching tests.

#### (e) Contact Time

Leaching procedures are normally conducted to achieve or approach equilibrium in reasonable test times. A contact time of 48 hours was chosen since it was found to be adequate for equilibrium to be attained. Most tests use 24 hours as a standard time as it was found to be a compromise in most situations. The TCLP test is normally conducted for 18 hours due to practical scheduling. According to Conner (1990), it is believed that this time change does not substantially affect the results, compared with other uncontrolled variables.

#### (f) Nature of Leachant

The general trend is to use an aggressive leaching medium with a moderately low pH. An acetic acid buffered solution (pH 3.3) is used in this study because it is an ordinary laboratory reagent; preparation is simple, reproducible and useable at atmospheric pressure in air. The acetic acid buffer solution is also used in the standard TCLP tests.

#### (g) Particle Size / Surface Area

A maximum particle size for most test methods, such as TCLP, is specified. Research done by Van Zyl (1997), Alberts (1996), Van Jaarsveld (2000) makes mention of the importance of particle size when performing leaching tests. In order to create a worst case scenario the surface area of the waste is increased by grinding or crushing. When the physical structure is destroyed, the surface area is increased and the leachability of the waste increases. In this study leaching tests were conducted using particle sizes of 3350 $\mu\text{m}$  and 250 $\mu\text{m}$ .

### 7.5.4 Leaching Data

The immobilisation efficiencies of the various geopolymer matrices were evaluated by analysing silicon, aluminium and organic leaching data. Since silica and aluminium are reported to be the basic building blocks of geopolymer systems, analysis of these two species provides information on the matrix breakdown of the various geopolymer samples. Organic leaching data provided an indication of the immobilisation efficiency of the geopolymer systems for organic material. To avoid any discrepancies that may arise due to particle size, the geopolymer samples were crushed and sieved into two particle size fractions, 3350 and 250  $\mu\text{m}$ . Silicon and aluminium leaching data are contained in Figures 7.15–7.28. Leaching experiments were performed on matrices made from a standard geopolymer recipe (36 Sasol) which contained various encapsulated coated zeolitic material (Figures 7.15-7.24). As a point of comparison, leaching experiments were also conducted on the standard geopolymer matrix (Figure 7.25) and geopolymer matrices containing zeolitic material (Figures 7.26-7.28).

#### 7.5.4.1 Silicon Leaching

Silica is generally found to be unstable in the pH region 3-4. Since leaching experiments were conducted in this region a greater concentration of silicon species

was expected to be leached than aluminium species. Another possible reason for a greater silicon species concentration being leached from the system stems from the fact that additional silicon is added to the system in the form of sodium silicate, hence increasing the amount of unreacted silicon in the system. It is interesting to note that silicon leaching data for the geopolymer systems containing coated zeolitic material (Figures 7.15-7.24) show a marked increase in the concentration of silicon species being leached followed by a sharp decrease. The system shows no equilibrium stage being reached like that observed by Van Jaarsveld (2000). Also of interest is the leaching data for the standard geopolymer matrix (Figure 7.25) and the matrices containing uncoated zeolitic material (Figures 7.26-7.28). Analysis of the data shows a continuous increase in the concentration of silicon species being leached from the system, with no maximum value being reached.

#### 7.5.4.2 Aluminium Leaching

As stated above the system should leach a greater concentration of silicon species than aluminium species, however, this pattern is not observed. Analysis of the various geopolymer systems shows the same trend, i.e. a greater concentration of aluminium species being leached from the system than silicon. Zeolite encapsulation within geopolymers does have a significant effect on the levels of silicon and aluminium being leached from the system. A possible explanation for the difference in silicon and aluminium leaching rates is that zeolitic phases tend to form nucleation sites thereby crystallising silica on the zeolitic surface. This is less likely to happen to aluminium, as aluminium tends to polymerise and gives rise to amorphous phases. Hence the silica is fixed in crystals and the aluminium in amorphous phases. Products in amorphous phases are significantly more soluble than crystalline products, hence greater aluminium being leached from the system than silica. The difference between leaching rates for coated and uncoated zeolitic materials as observed for silicon leaching is also observed for aluminium leaching.

### 7.5.4.3 Organic Leaching

Analysis of the organic leachant shows no phenol and 4-chlorophenol present. If any organic had leached from the geopolymer the concentration would have been <2ppm. This concentration would be too low for the DIONEX to detect. A concentration of phenol and chlorophenol <2ppm in a waste water stream is acceptable as detailed by the SABS. No organics being leached from the system is possible, as zeolites are generally stable in an acidic medium. Coating of the zeolite and then encapsulation of the coated zeolite within a geopolymeric structure, significantly retards the leaching of organics from the geopolymer system.

It should be noted that even though large concentrations of silica and alumina had leached from the system, this was still not detrimental to the immobilisation capacity of the system, as no organics had leached from the system

## 7.6 SUMMARY

It is evident from the discussion detailed above that zeolite incorporation greatly influences the physical characteristics of the geopolymer matrices. This influence is prominently evident when one analyses compressive strength data. It can be seen that zeolitic encapsulation significantly increases the compressive strength of the ordinary geopolymer matrix (36 Sasol). Analysis of leaching data also shows that even though matrix breakdown in the various geopolymer matrices was significant, leaching of organics was minimal. Geopolymer systems, therefore provide attractive possibilities for organic encapsulation.

**Table 7.1: Surface area results for synthesised zeolites**

<b>Mineral</b>	<b>BET Surface Area (m<sup>2</sup>/g)</b>
Eskom fly ash	1.0850
Zeolite NaP1	62.0358
Zeolite NaP1 (deal)	220.1586
Zeolite NaP1 (acid)	241.8823

**Table 7.2: Solubility of phenol and 4-chlorophenol**

<b>Compound</b>	<b>PKa</b>	<b>Solubility (g l<sup>-1</sup>)</b>
Phenol	9.89	87
4-Chlorophenol	9.18	27

**Table 7.3: Geopolymer matrices**

<b>Ingredient</b>	<b>Composition (mass%)</b>
Fly ash	60.0
Kaolinite	6.7
KOH	8.0
Sodium Silicate soln	14.7
Water	10.7
Zeolite	11.25



**Table 7.4: Compressive strength data for geopolymers containing zeolites**

<b>Sample</b>	<b>Age (days)</b>	<b>Mass (kg)</b>	<b>Force (kN)</b>	<b>Strength (MPa)</b>
36 Sasol	7	0.40	61.18	28.80
36 Sasol (1%fzeo)	7	0.39	38.10	17.90
36 Sasol (1%czeo)	7	0.40	49.70	23.40
36 Sasol (5%czeo)	7	0.40	62.82	29.60
36 Sasol (5%fzeo)	7	0.40	56.67	26.70
36 Sasol (coated fzeo)	7	0.42	86.63	40.79
36 Sasol (coated czeo)	7	0.42	72.63	34.19

**Table 7.5: Geopolymer (with encapsulated zeolite) surface area results**

<b>Geopolymer</b>	<b>BET Surface Area (m<sup>2</sup>/g)</b>
36 Sasol	52.7369
36 Sasol (5% fzeo)	49.7435
36 Sasol (5% czeo)	52.8527
36 Sasol (11.25% coated fzeo)	53.5479

**Table 7.6: Infrared absorption bands for geopolymer systems**

Region (cm <sup>-1</sup> )	Description
460-470	Bending of T-O bonds
950-1050	Stretching of T-O bonds
913	-OH bending bands
543	Si-O-Al bending
1080	Presence of unreacted amorphous silicate.
460, 1010, 1033	Degree of polymerisation
1630	H <sub>2</sub> O adsorbed on polysialate

**Table 7.7: Infrared absorption bands for zeolites**

	Region (cm <sup>-1</sup> )	Description
Internal Tetrahedra	1250-950	Asymmetric stretch
	720-650	Symmetric stretch
	500-420	T-O bend
External Linkages	650-500	Double ring
	420-300	Pore opening
	750-820	Symmetric stretch
	1150-1050	Asymmetric stretch

Figure 7.1: XRD graph of untreated fly ash

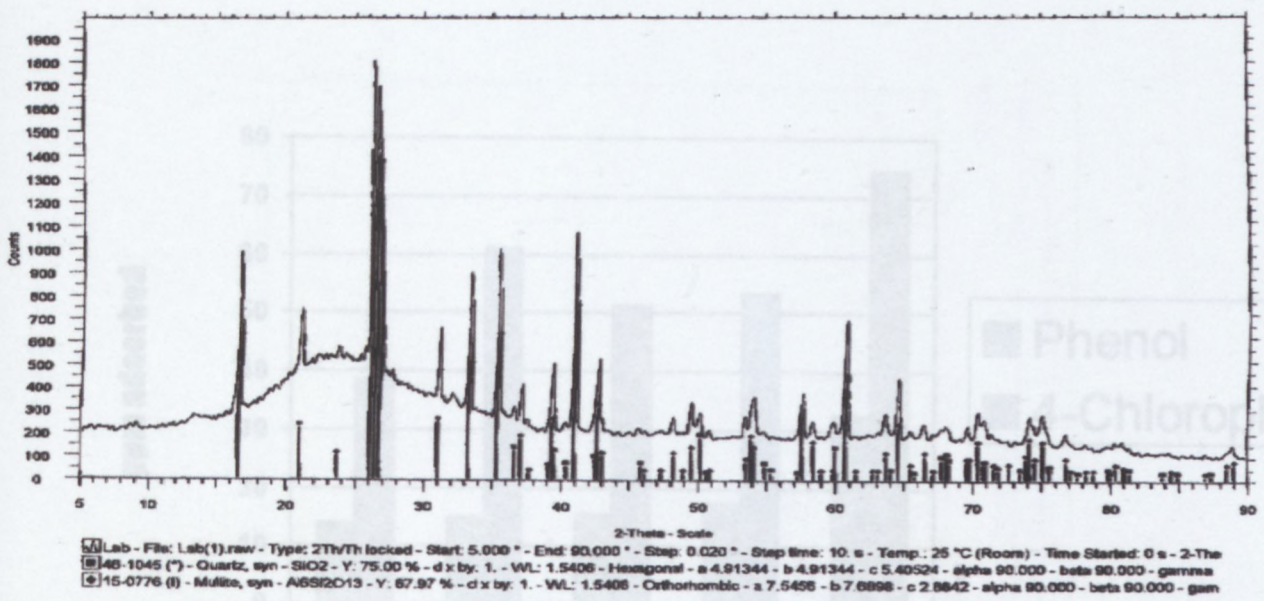


Figure 7.2: XRD graph of zeolite NaP1

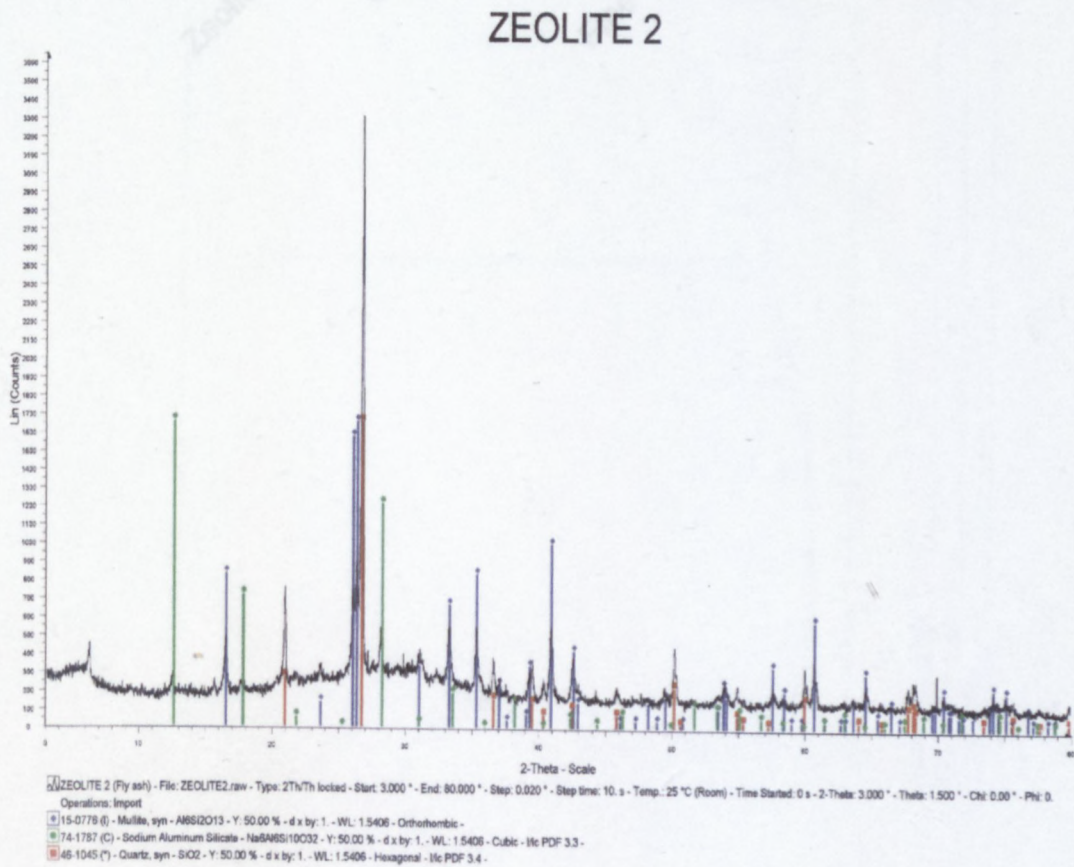


Figure 7.3: Organic adsorption data

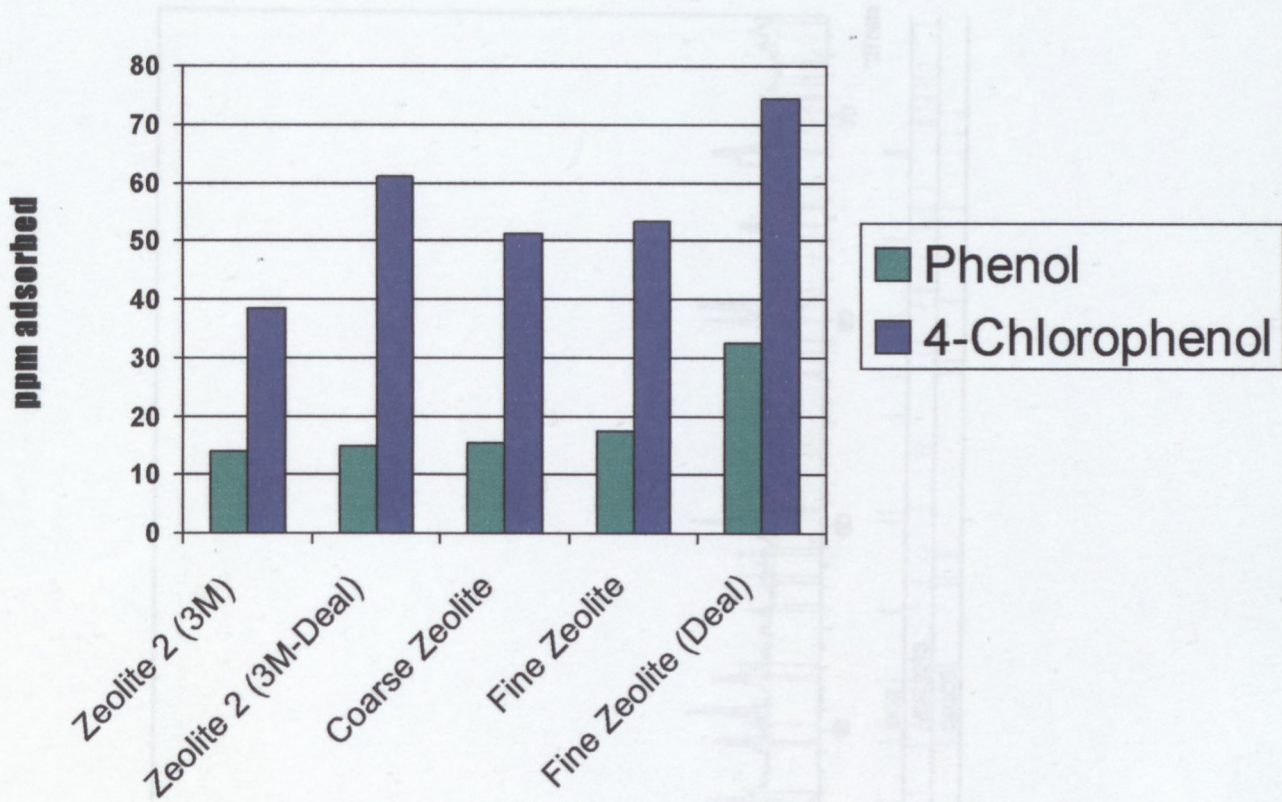


Figure 7.4: XRD graph of 36 Sasol (5% fzeo)

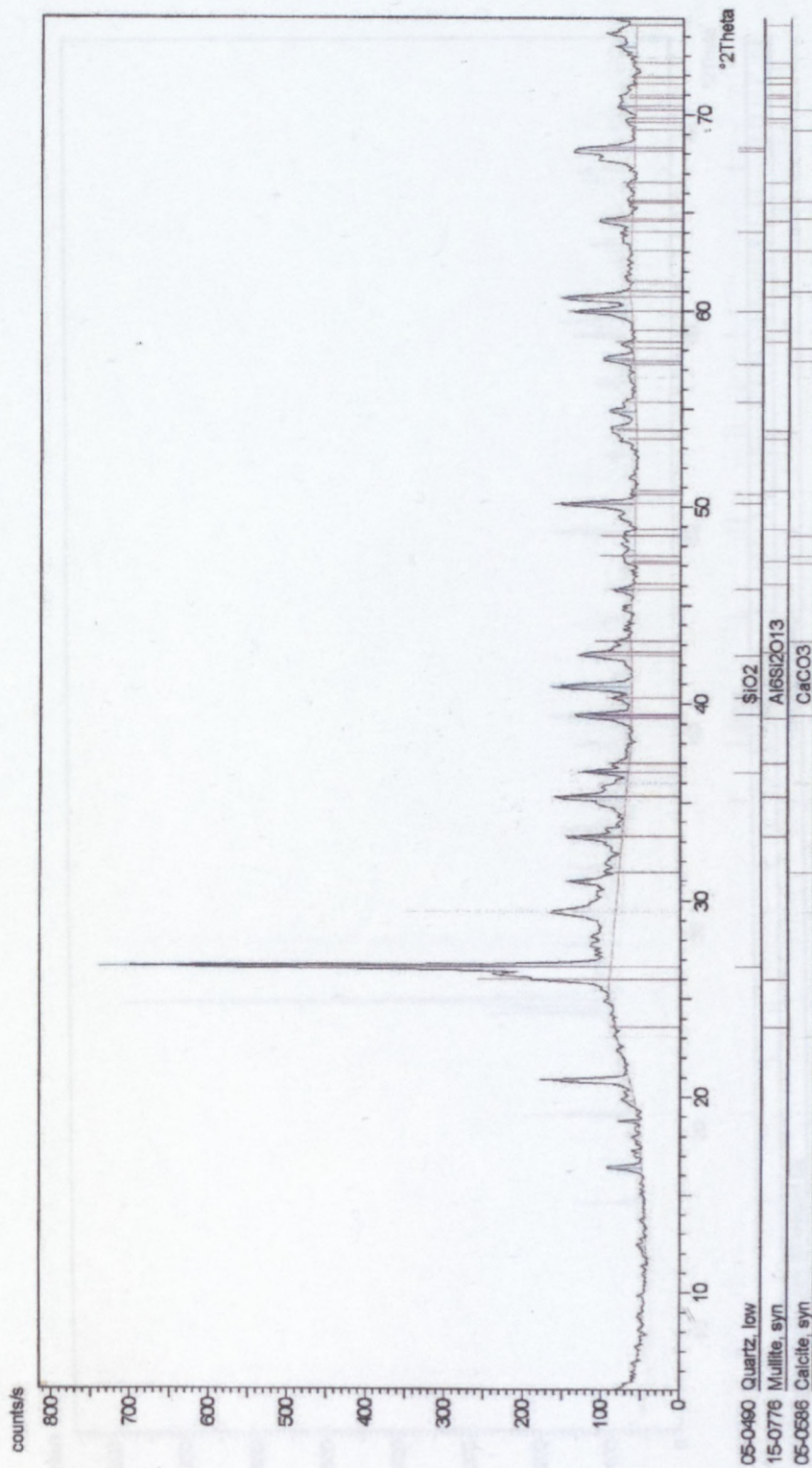


Figure 7.5: XRD graph of 36 Sasol (5% czeo)

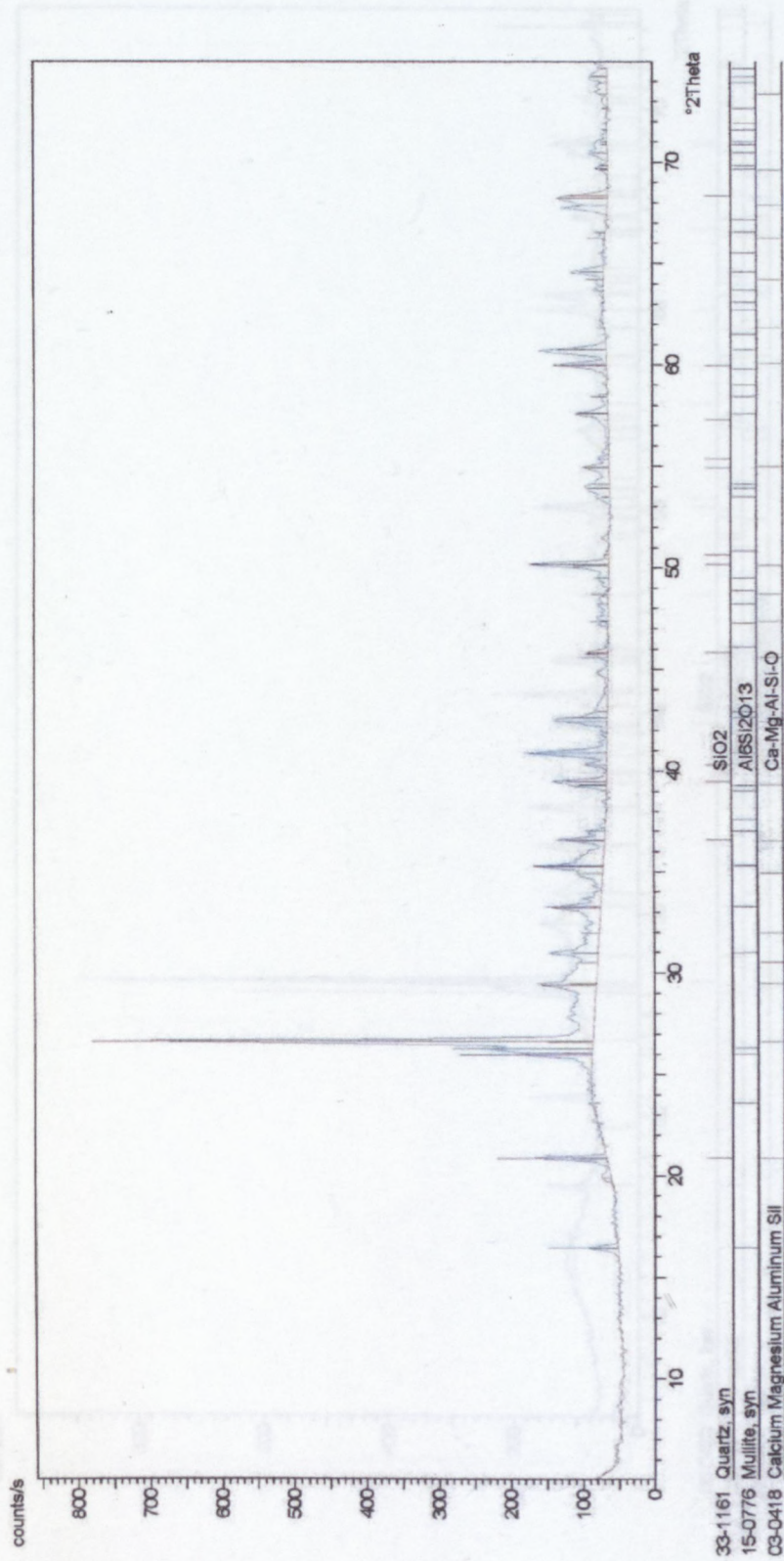


Figure 7.6: XRD graph of 36 Sasol (5% zeo NaP1)

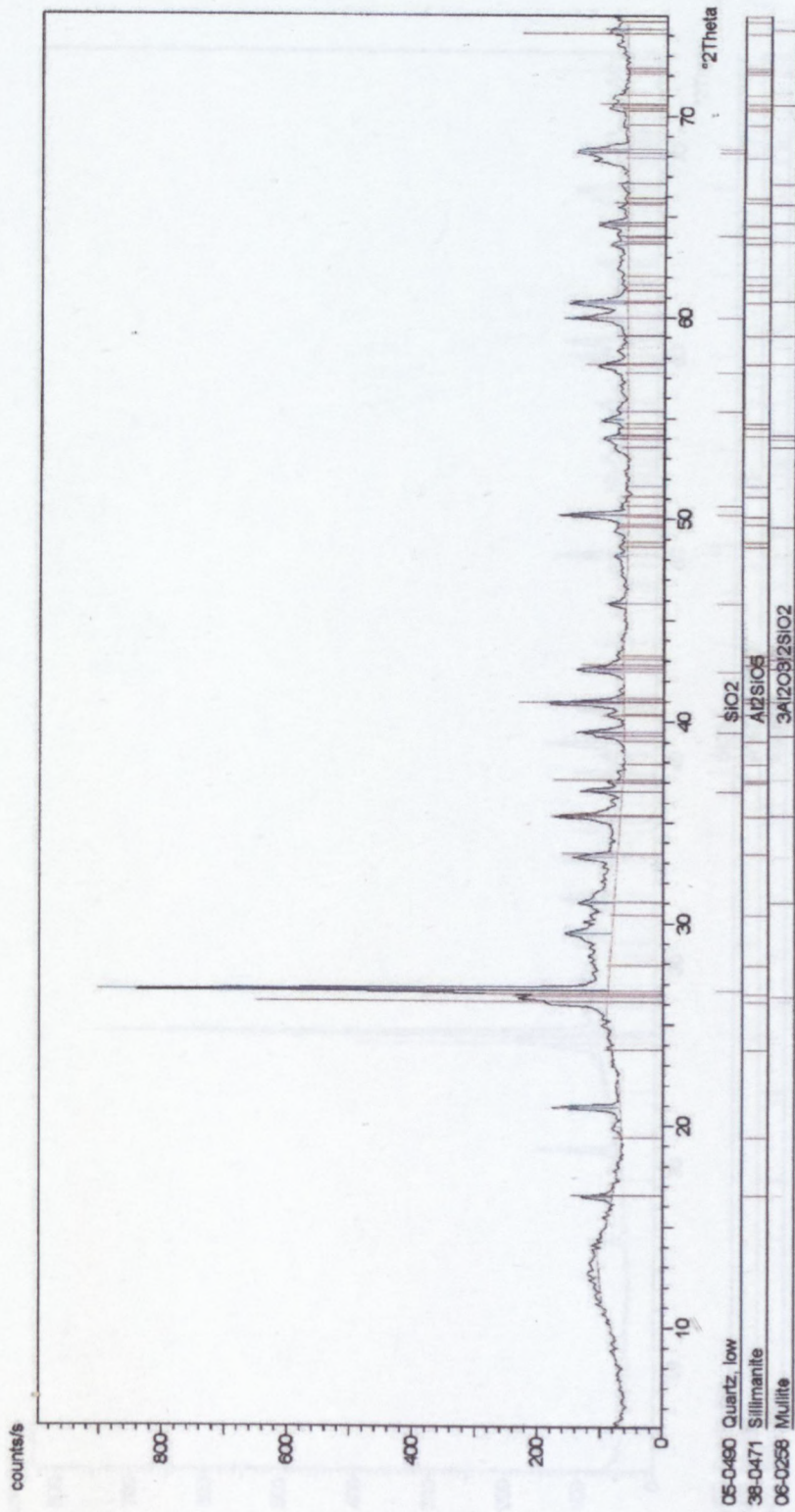


Figure 7.7: XRD graph of 36 Sasol (coated czeo)

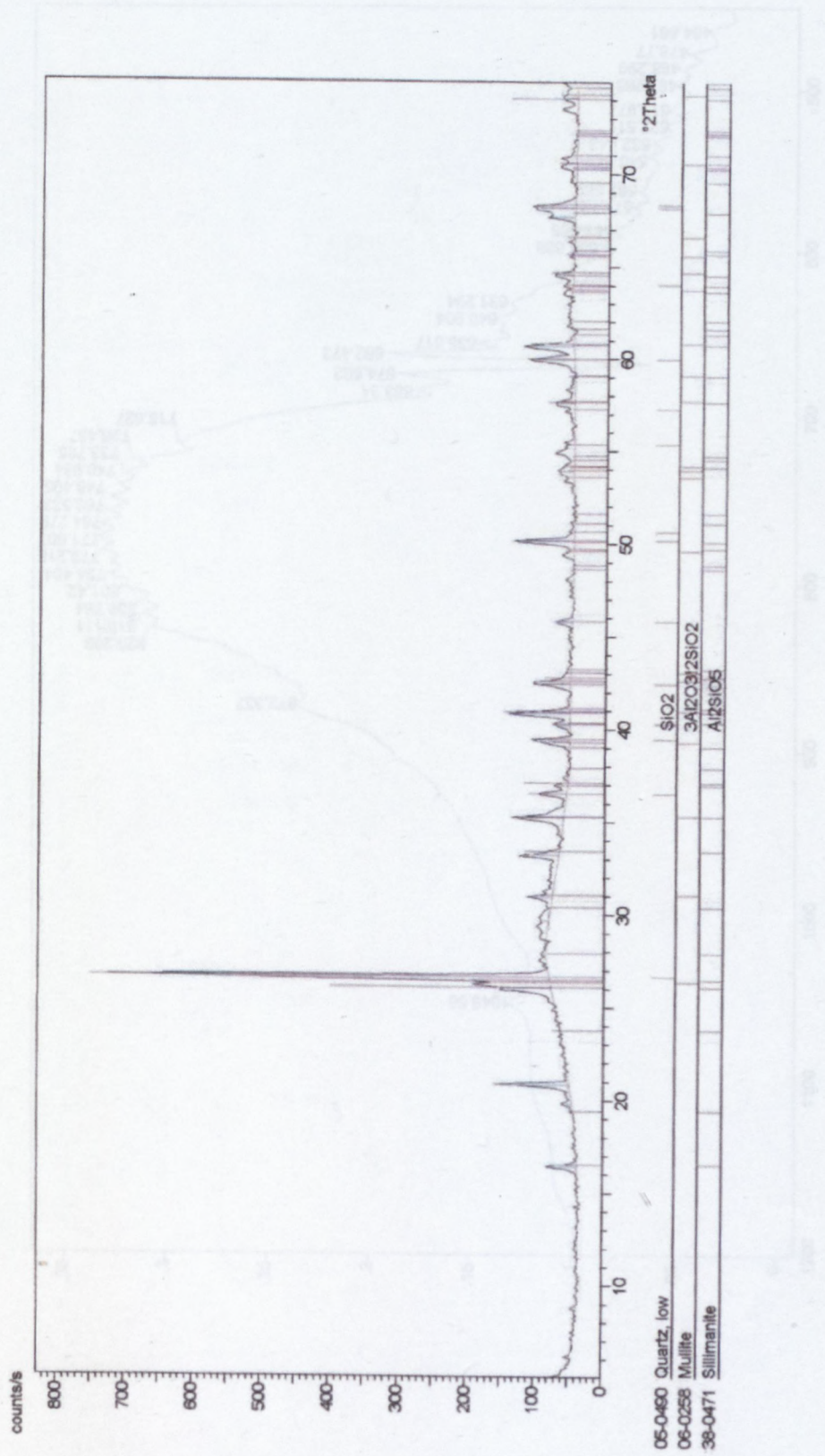




Figure 7.8: IR graph of 36 Sasol

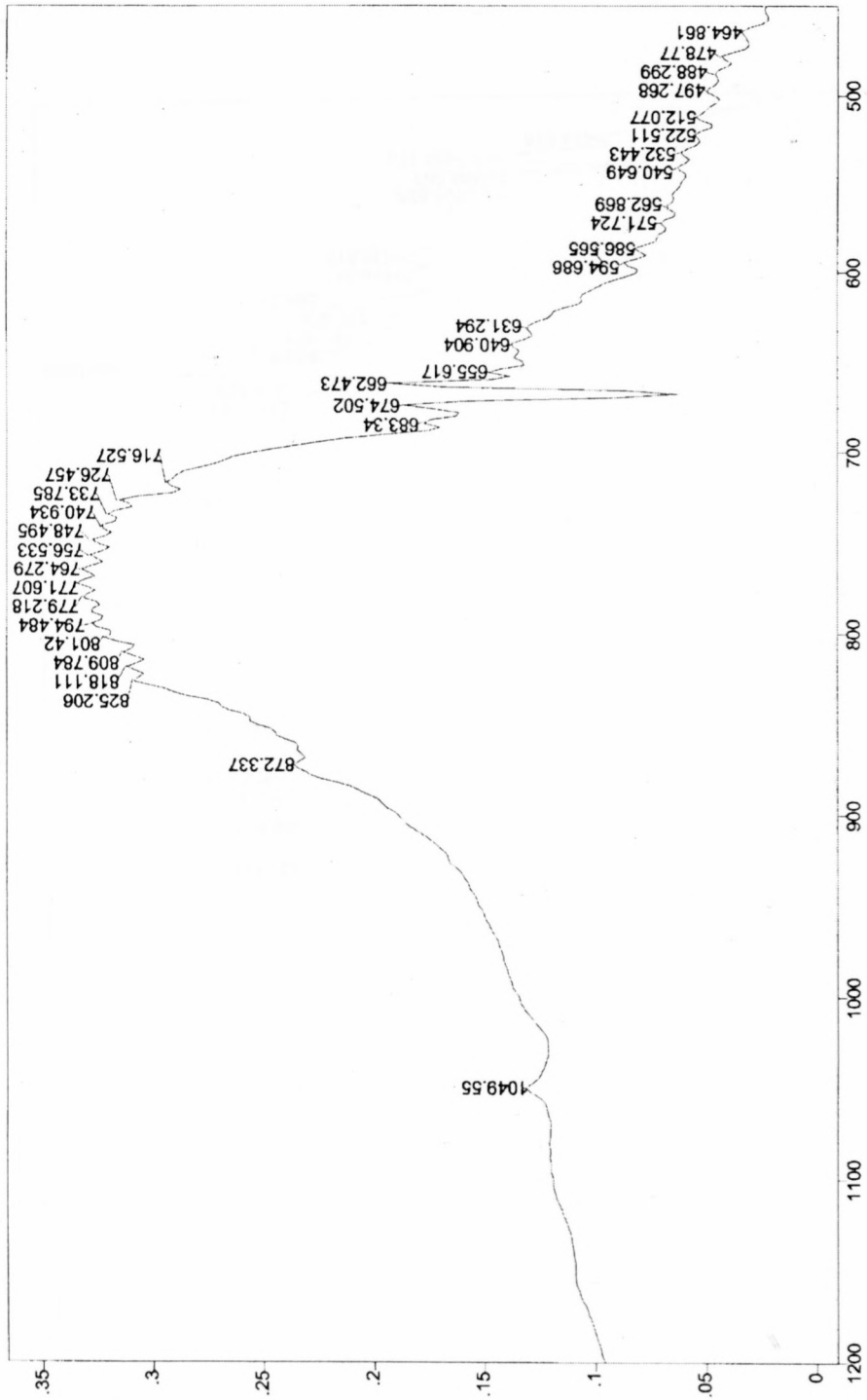


Figure 7.10: IR graph of 36 Sasol (5% zeo NaP1)

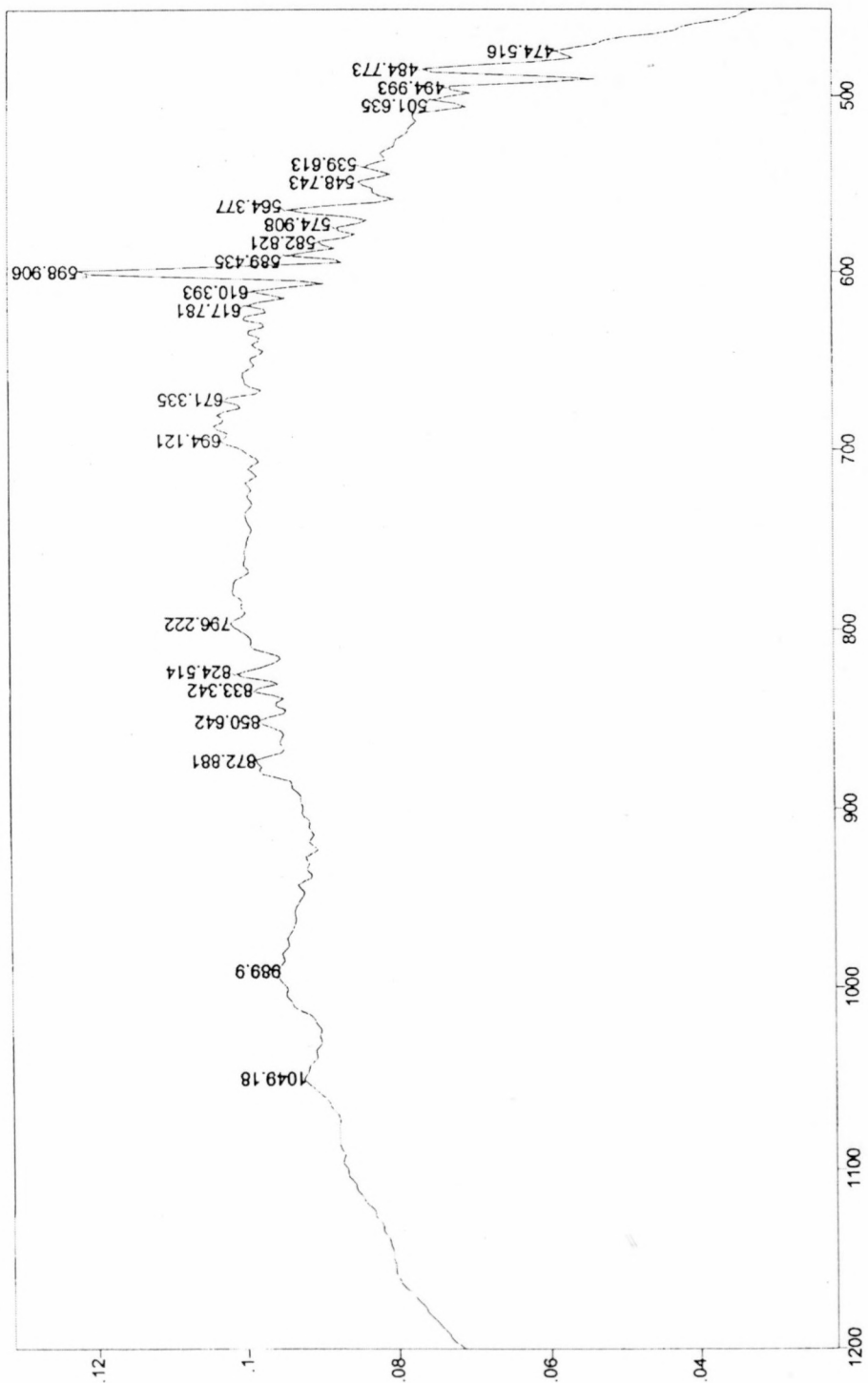


Figure 7.10: IR graph of 36 Sasol (5% zeo NaP1)

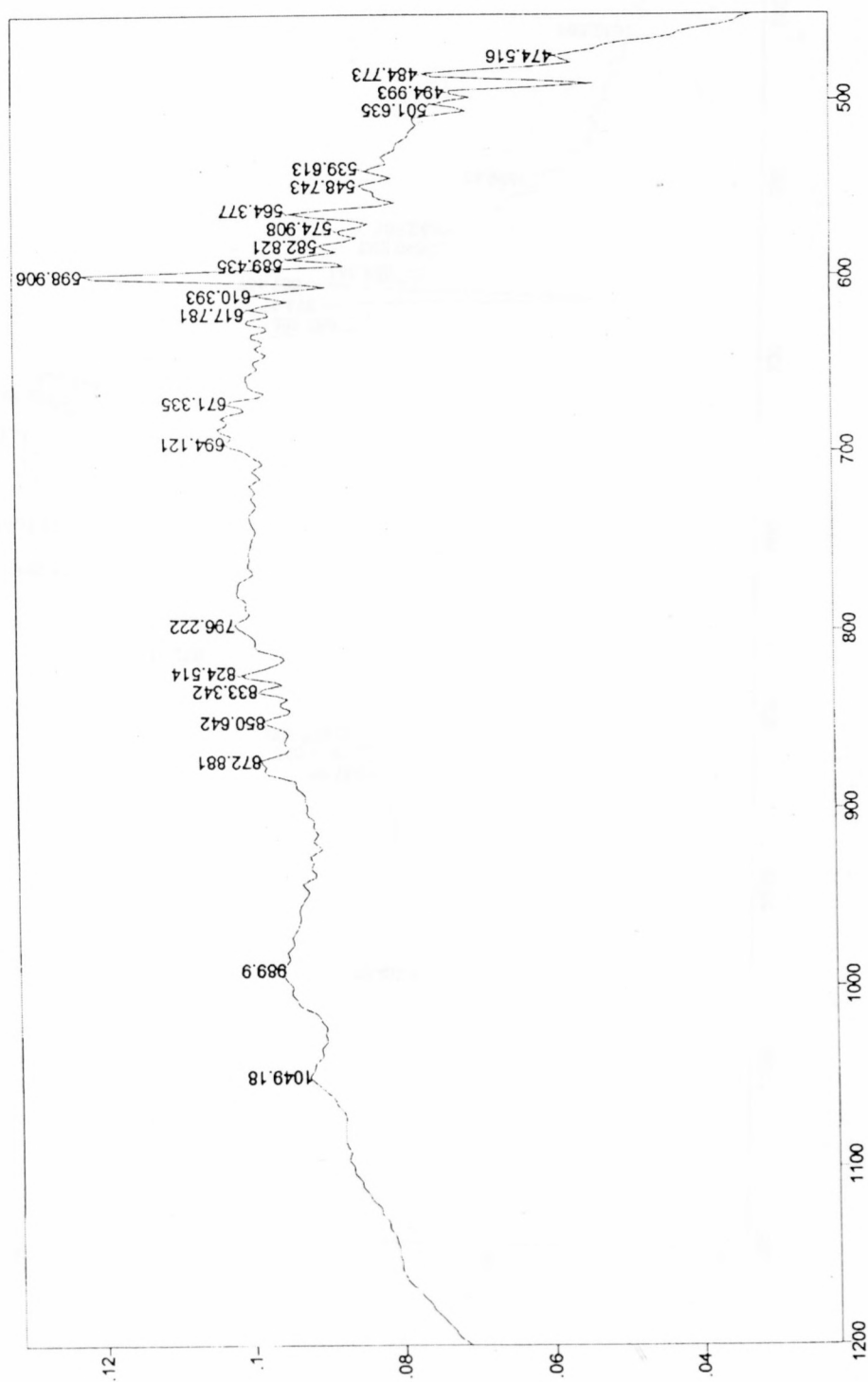


Figure 7.11: IR graph of 36 Sasol (5% czeo)

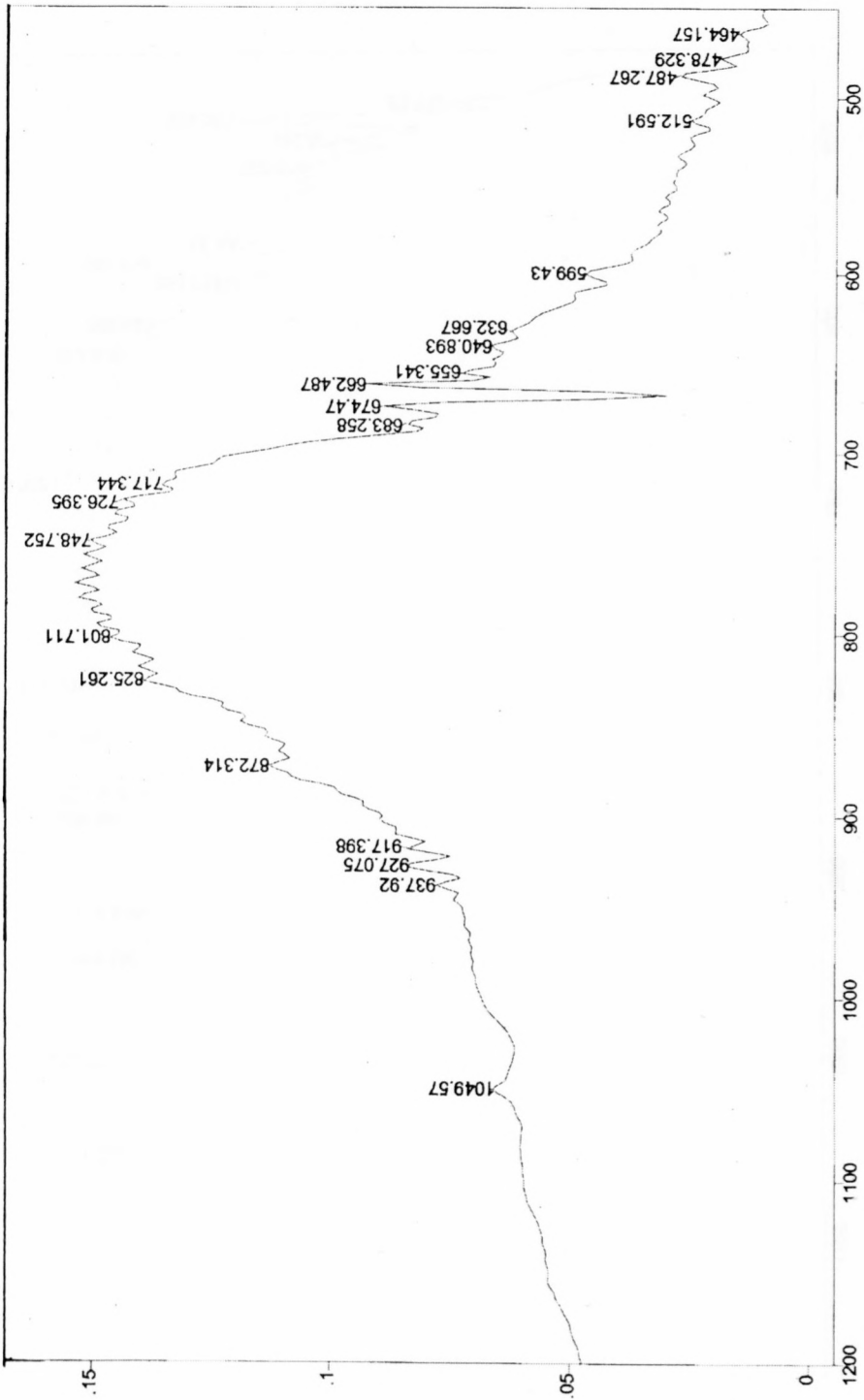


Figure 7.12: IR graph of 36 Sasol (coated fzeo)

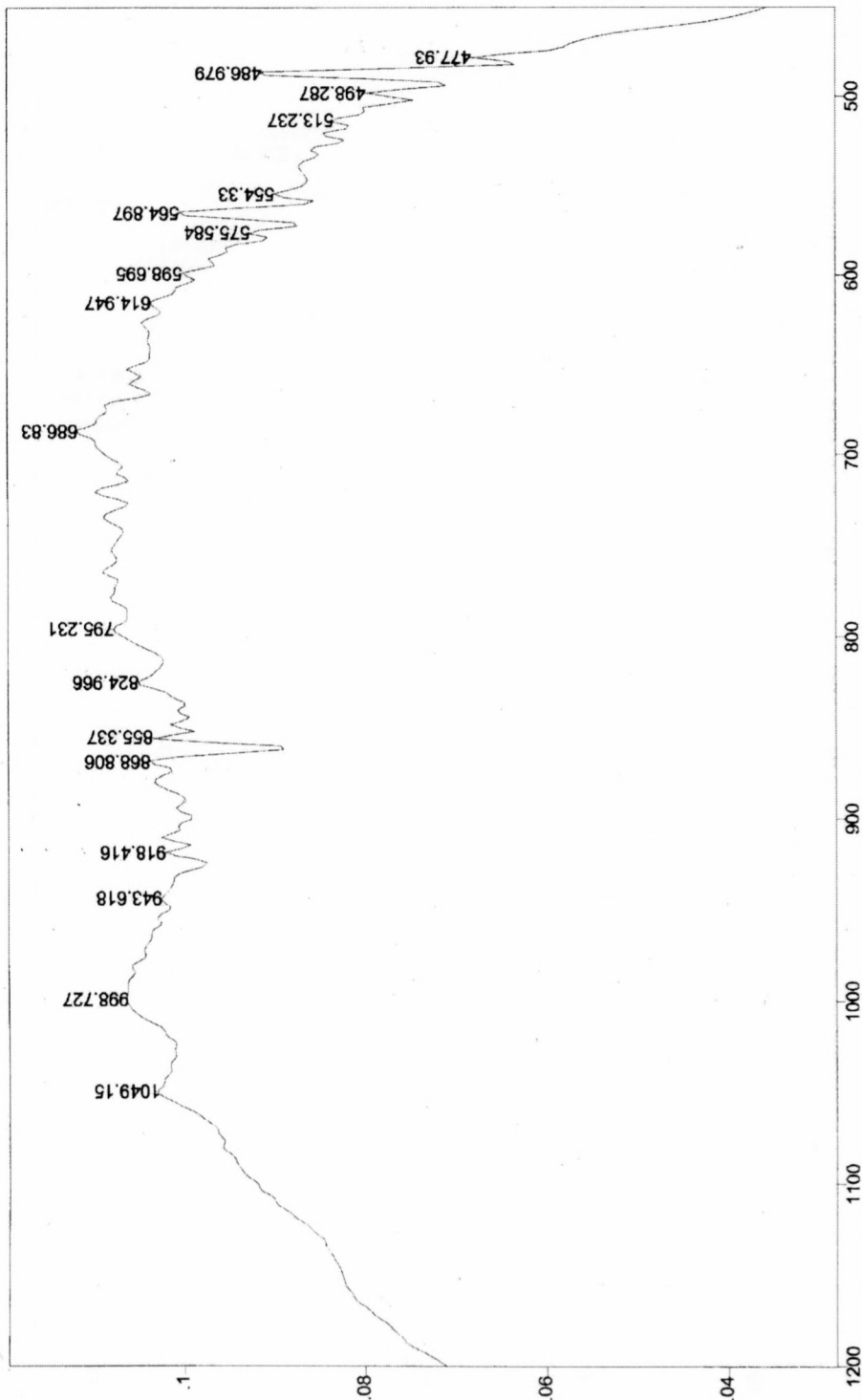


Figure 7.13: IR graph of 36 Sasol (coated czeo)

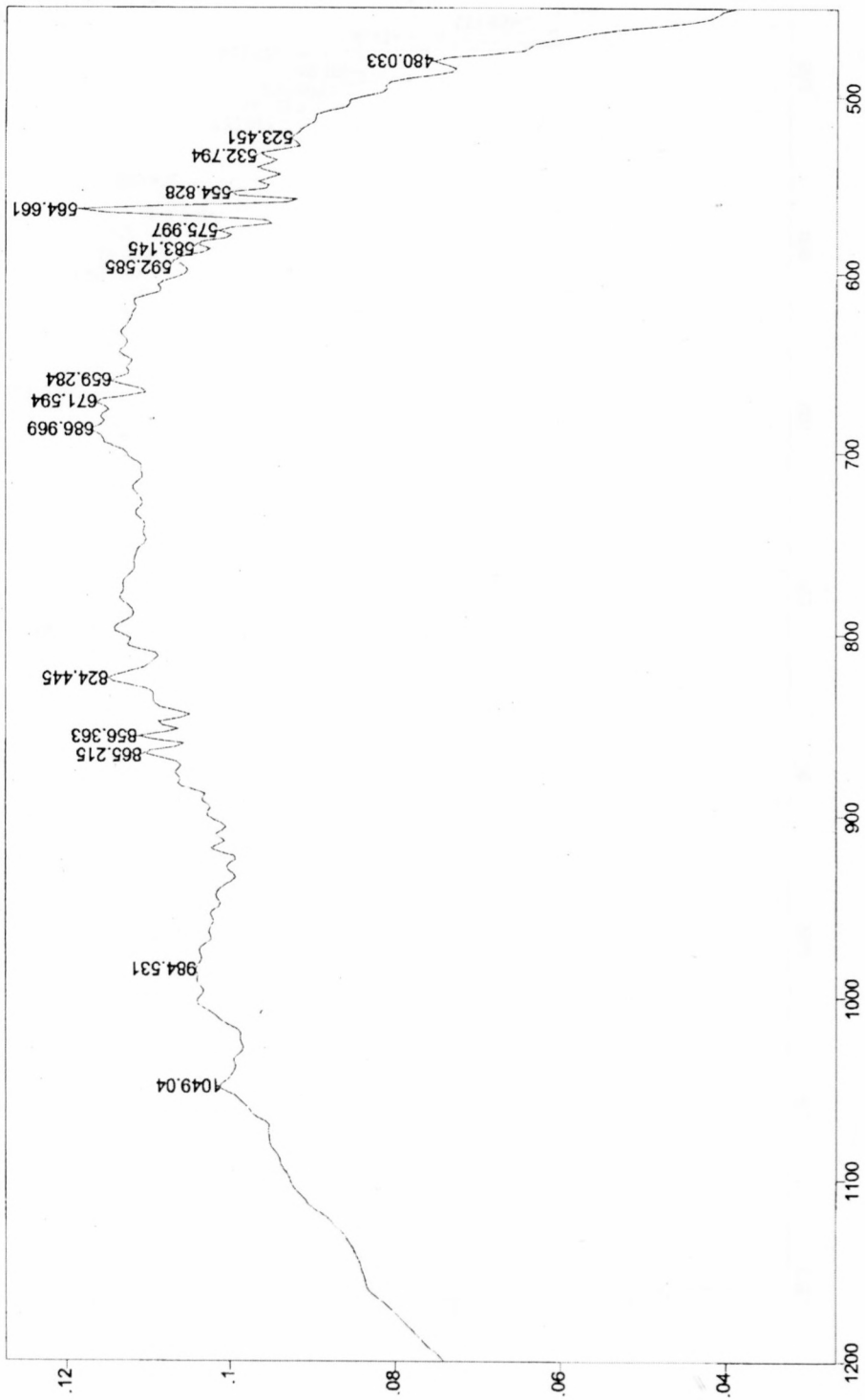


Figure 7.14: IR graph of 36 Sasol (coated zeo NaP1)

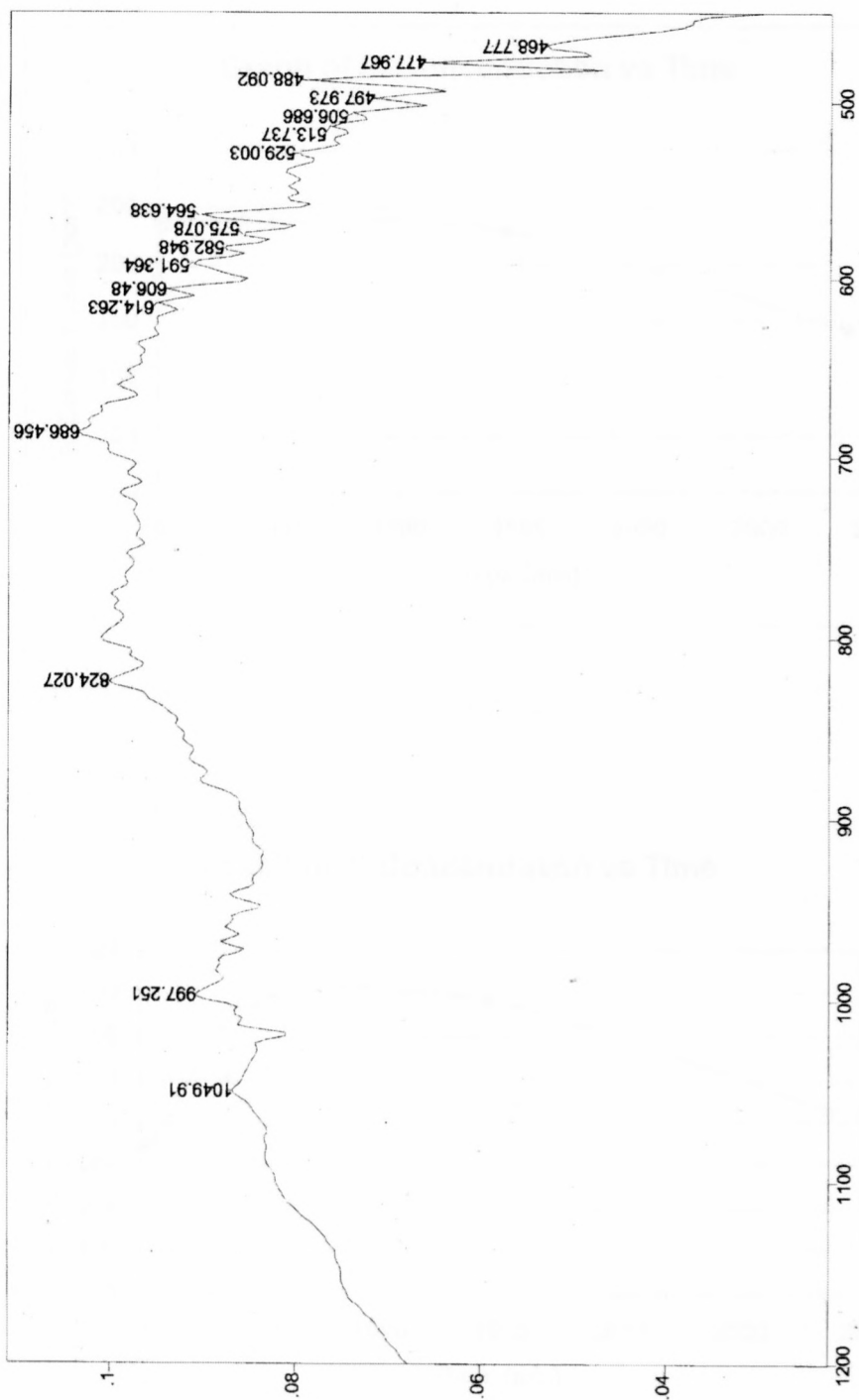


Figure 7.15: Leaching graphs of 36 Sasol [coated zeo NaP1 (PhOH)]

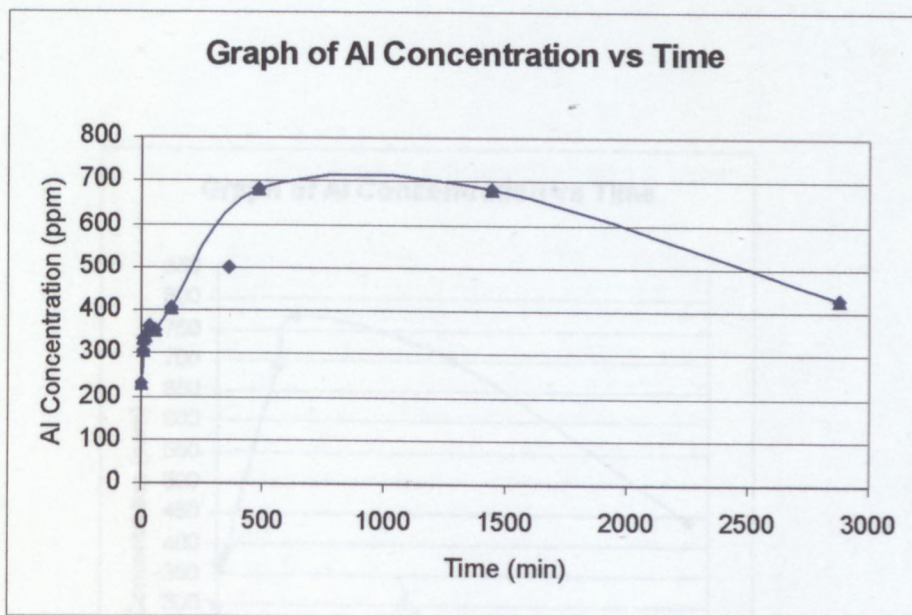
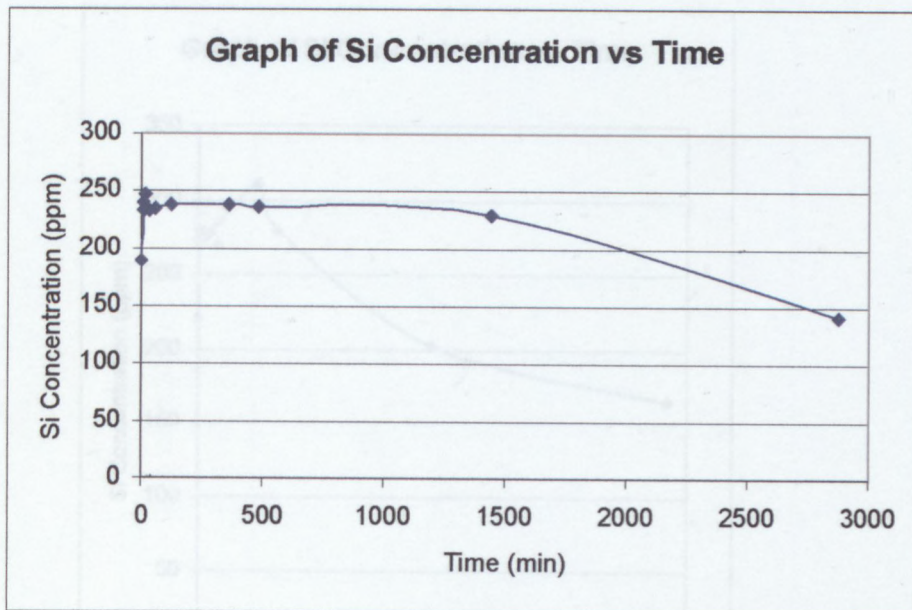




Figure 7.16: Leaching graphs of 36 Sasol [coated zeo NaP1 (Cl-PhOH)]

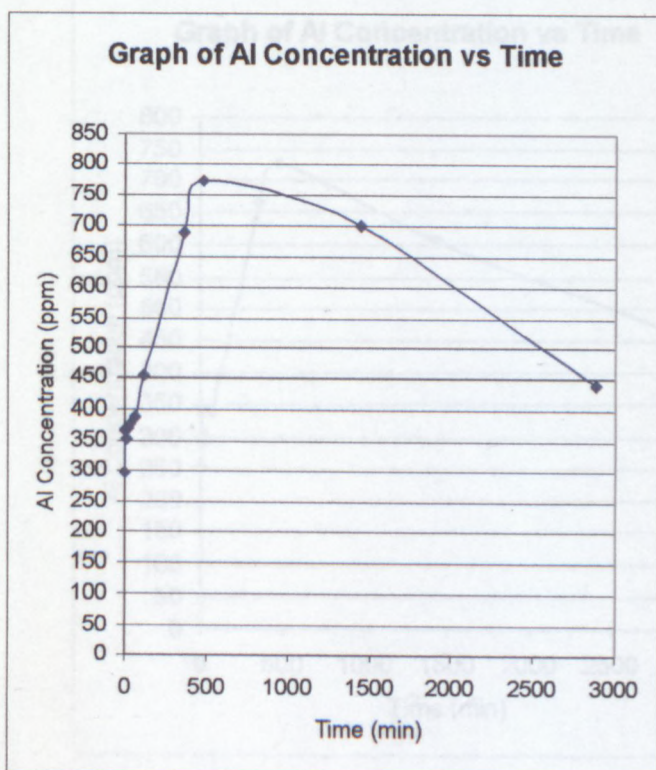
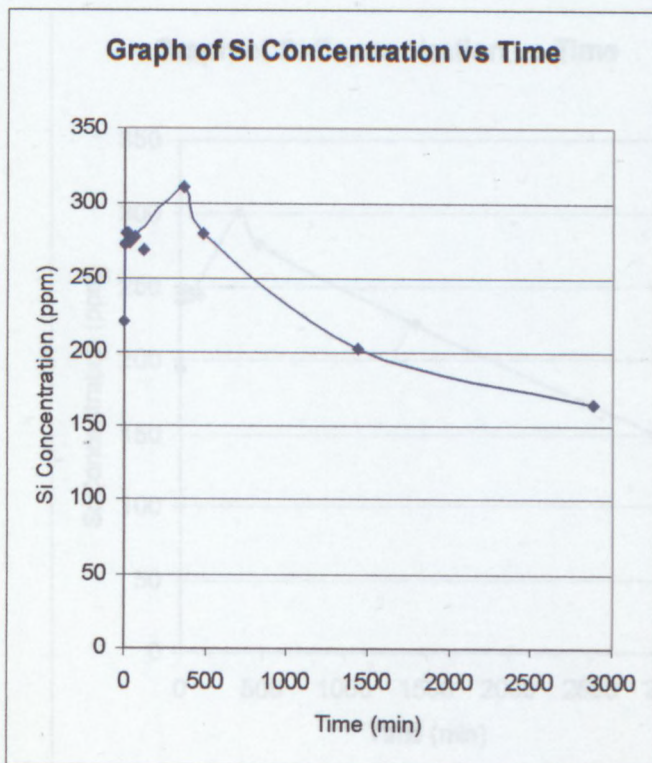


Figure 7.17: Leaching graphs of 36 Sasol [coated deal zeo NaP1 (Cl-PhOH)]

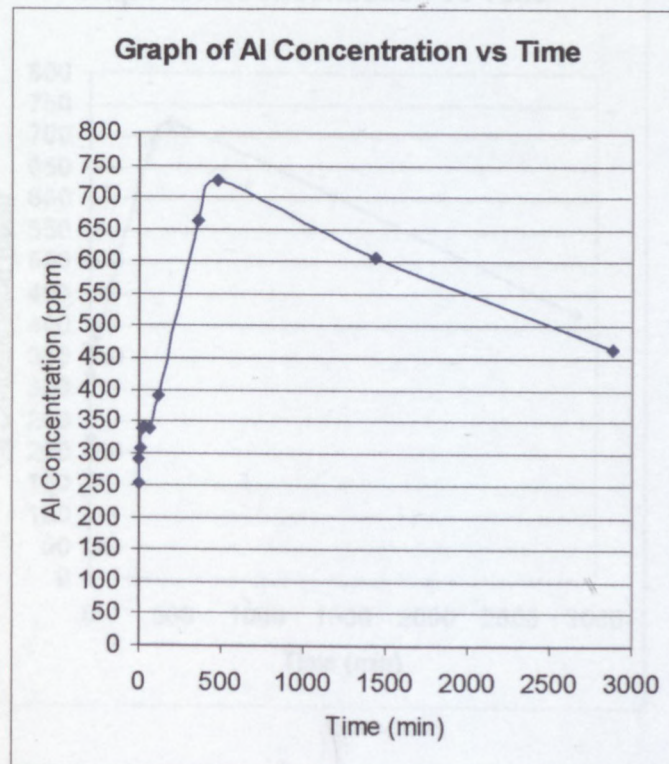
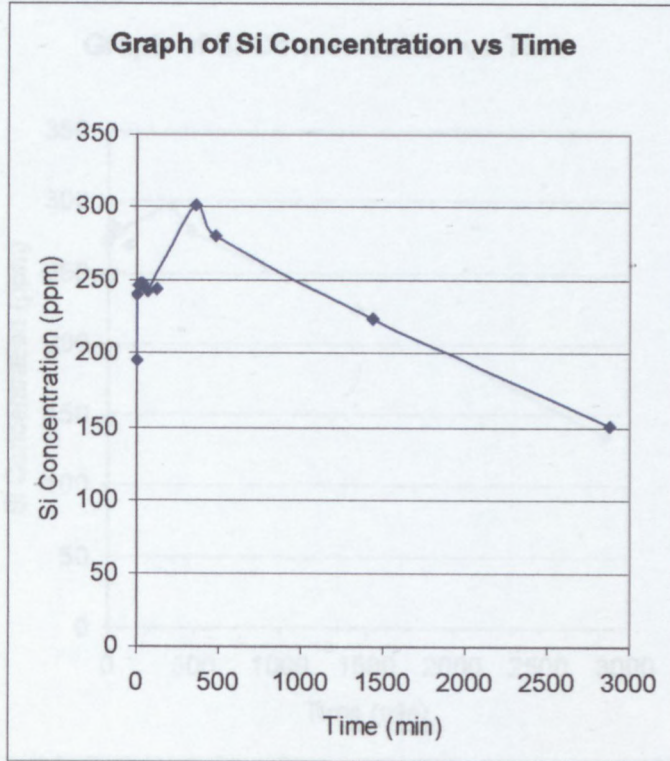
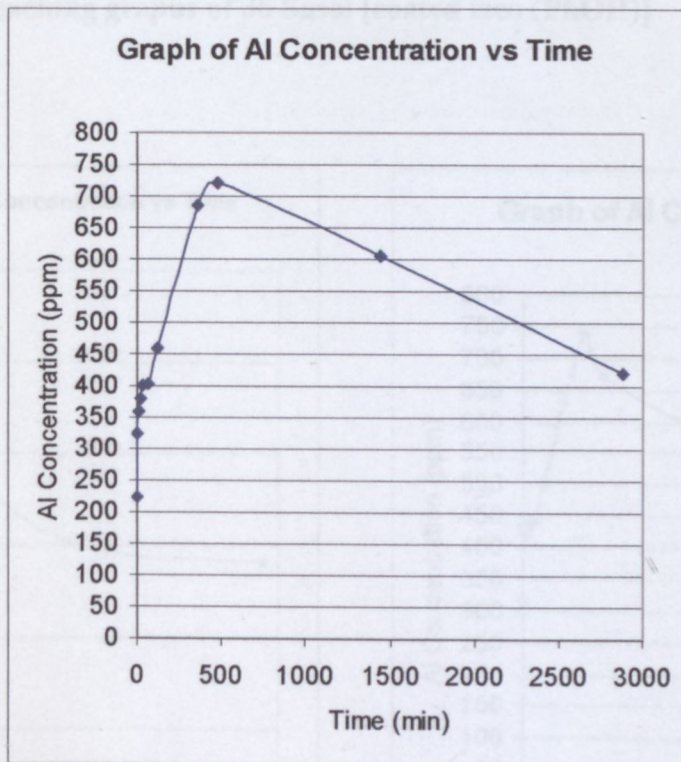
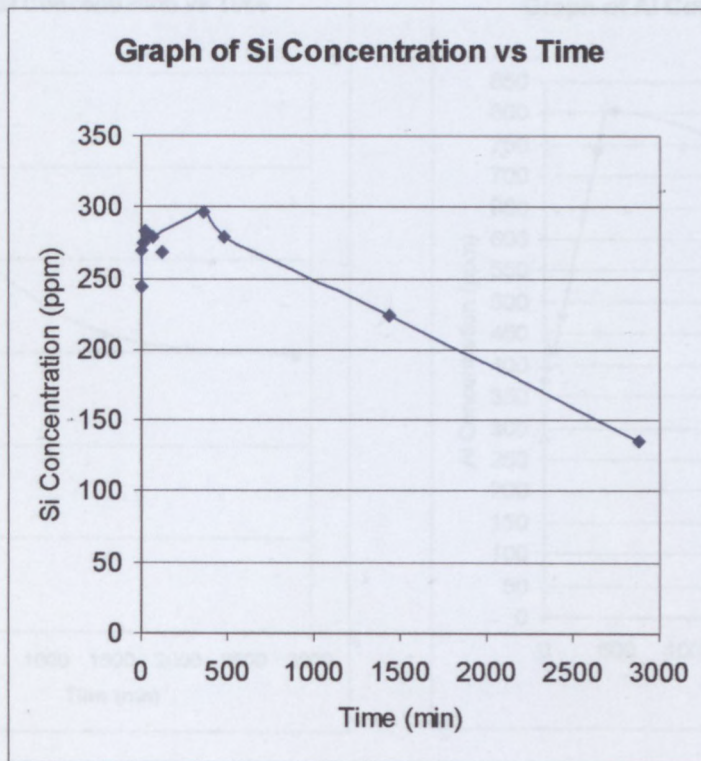
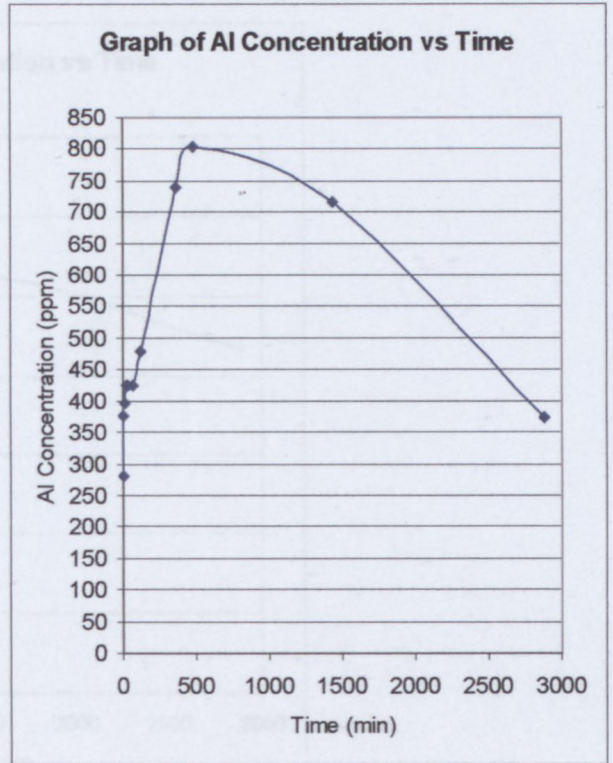
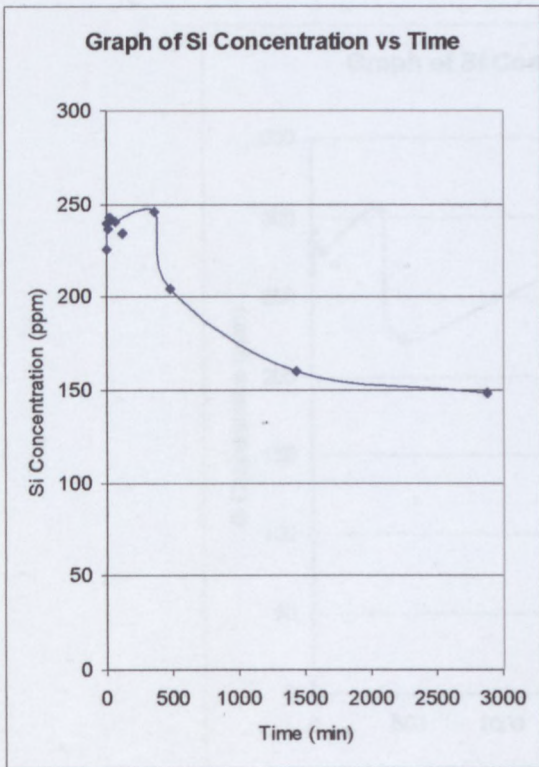


Figure 7.18: Leaching graphs of 36 Sasol [coated deal zeo NaP1 (PhOH)]



**Figure 7.19: Leaching graphs of 36 Sasol [coated fzeo (Cl-PhOH)]**



**Figure 7.20: Leaching graphs of 36 Sasol [coated fzeo (PhOH)]**

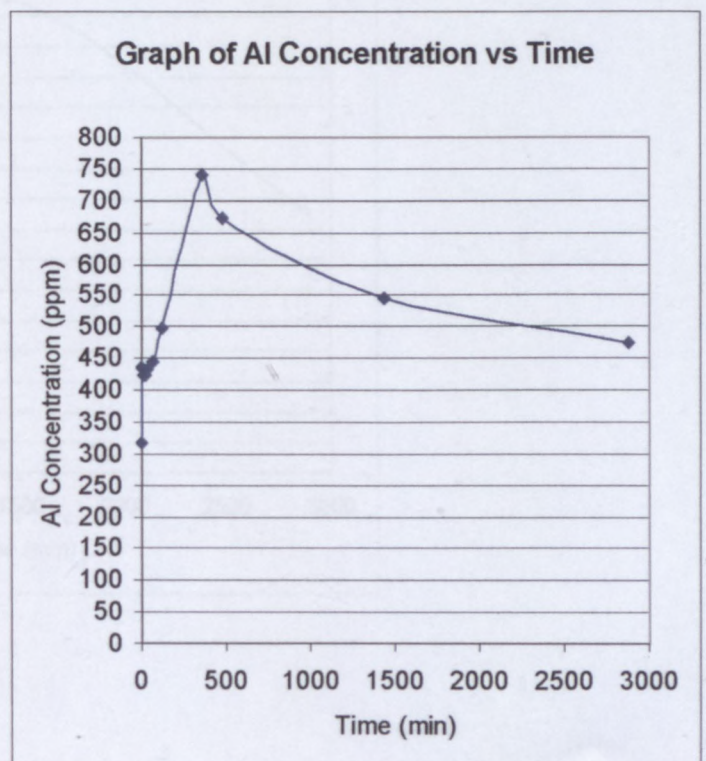
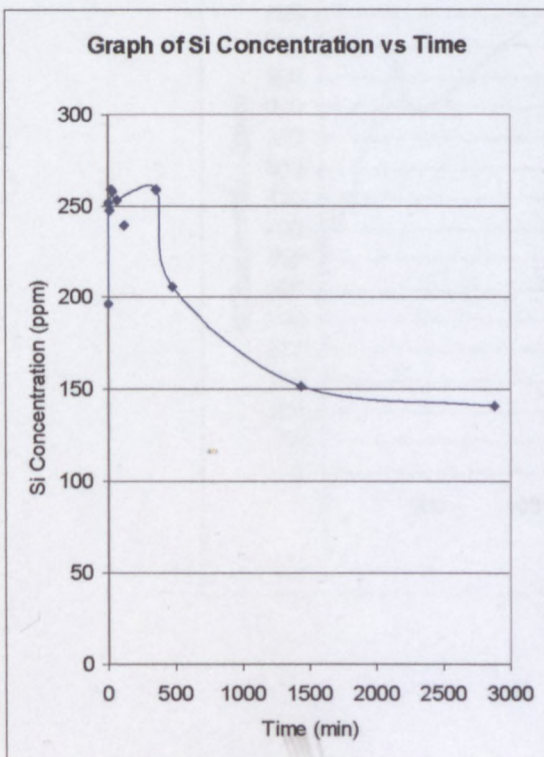


Figure 7.21: Leaching graphs of 36 Sasol [coated deal fzeo (Cl-PhOH)]

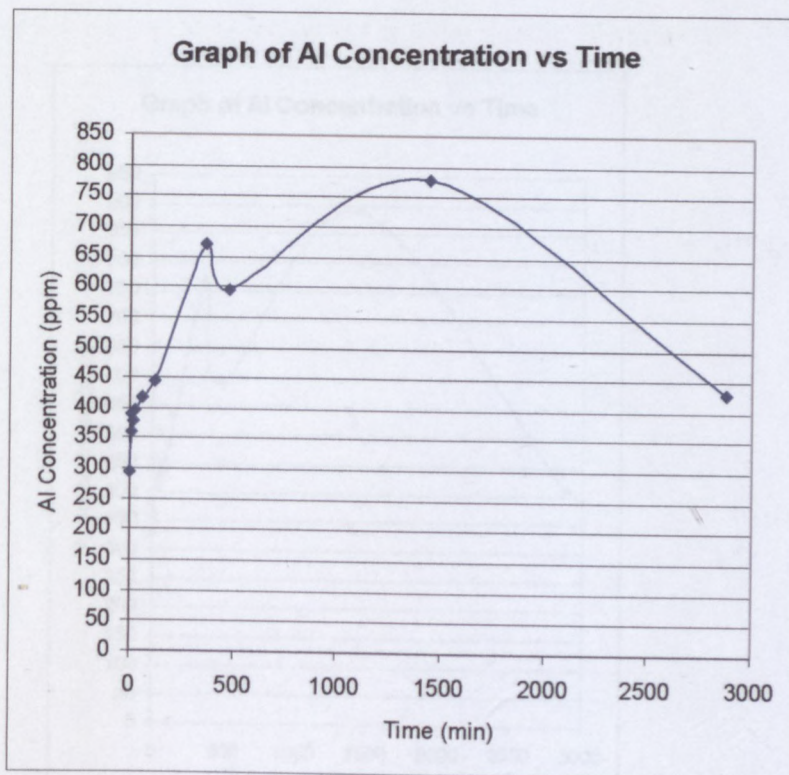
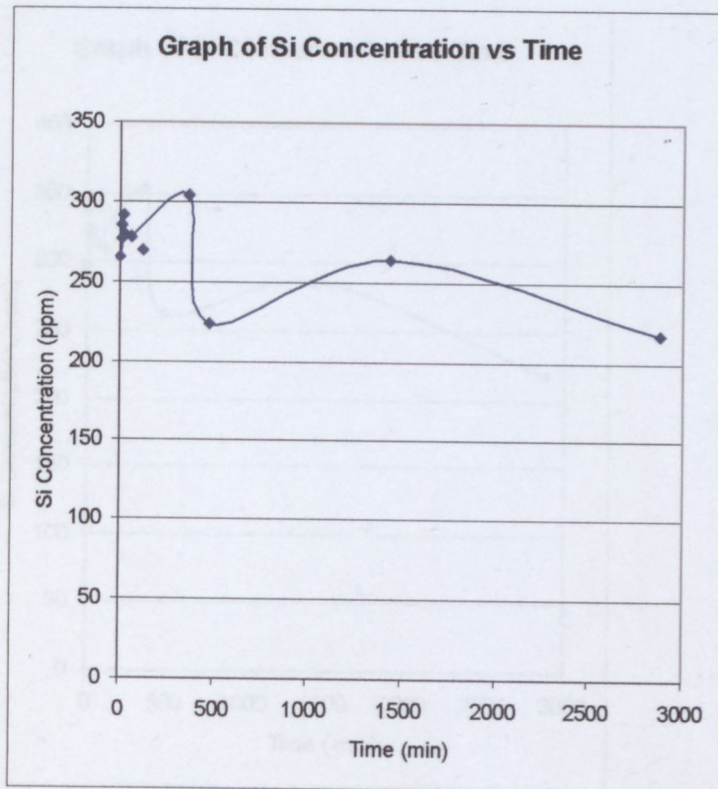


Figure 7.22: Leaching graphs of 36 Sasol [coated deal fzeo (PhOH)

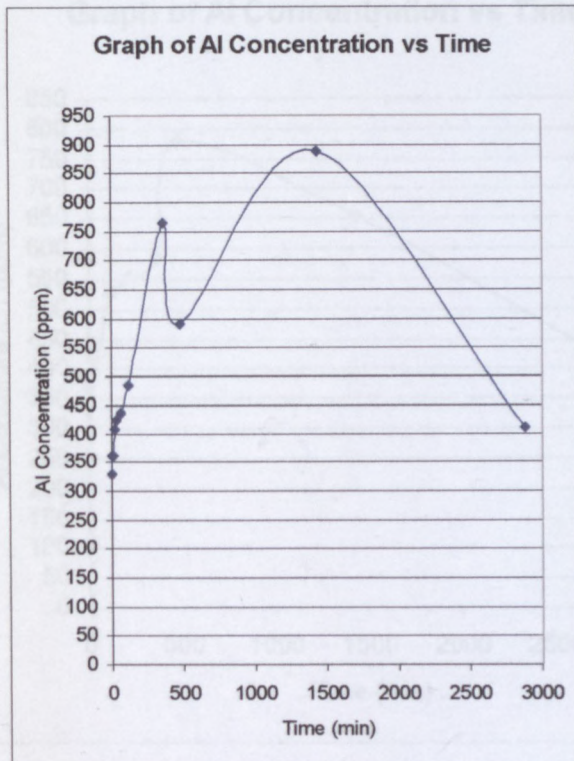
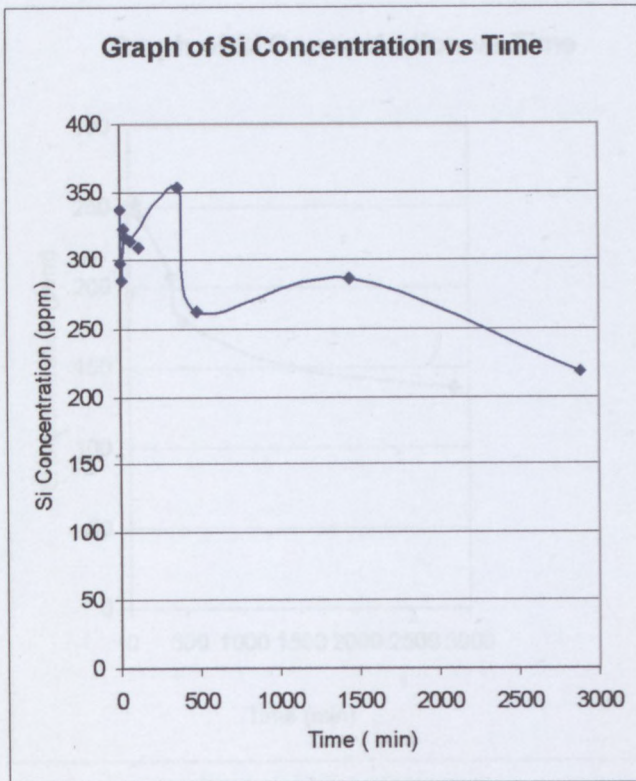


Figure 7.23: Leaching graphs of 36 Sasol [coated czeo (PhOH)]

Figure 7.24: Leaching graphs of 36 Sasol [coated czeo (C<sub>2</sub>-PhOH)]

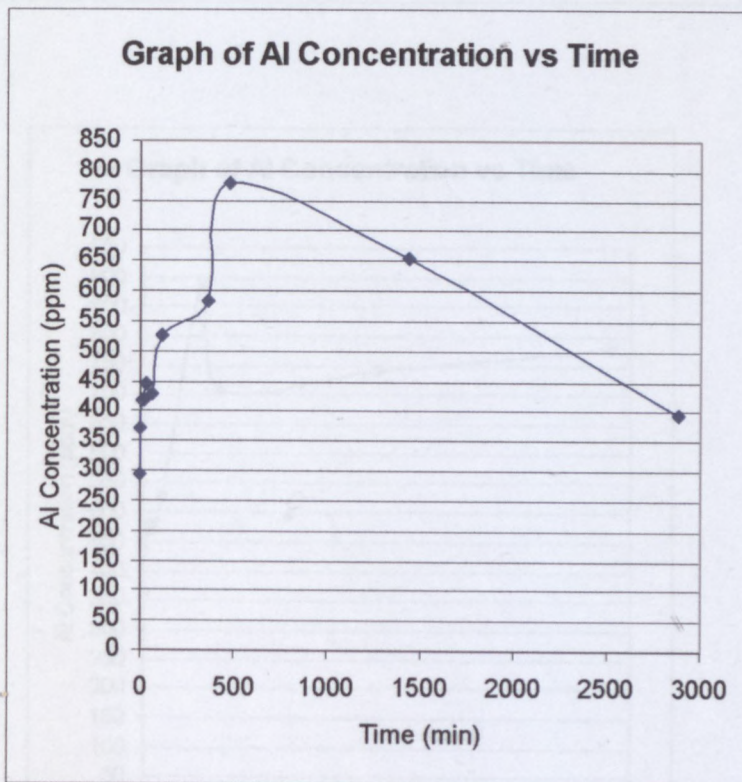
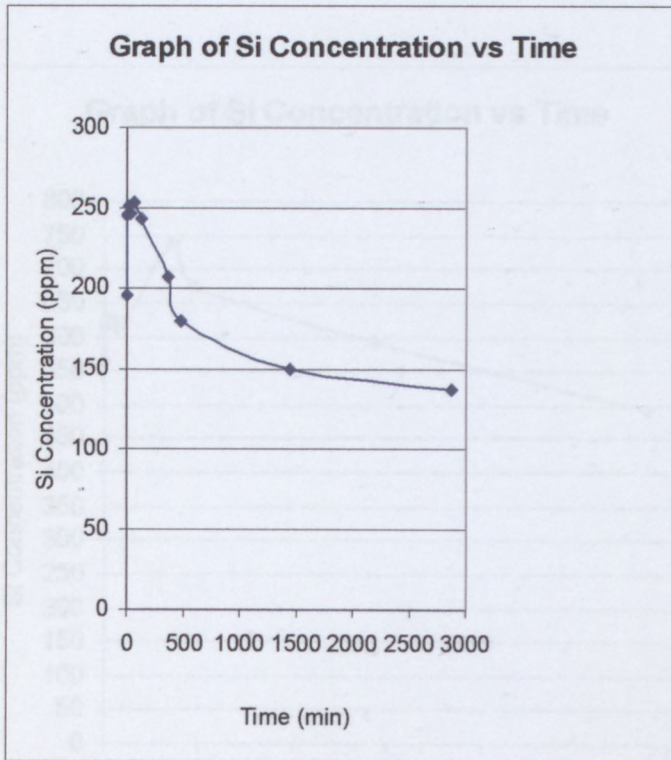


Figure 7.25: Leaching graphs of 36 Sasol

Figure 7.24: Leaching graphs of 36 Sasol [coated czeo (Cl-PhOH)]

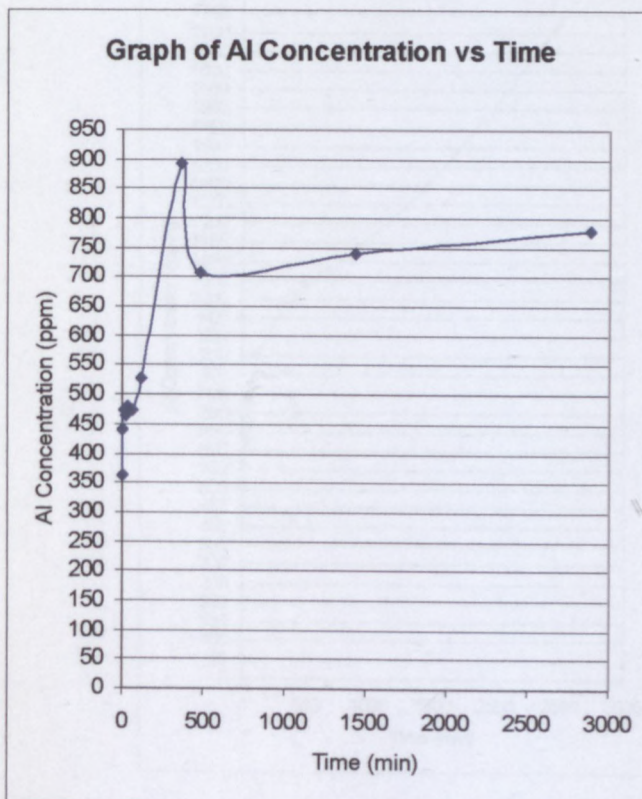
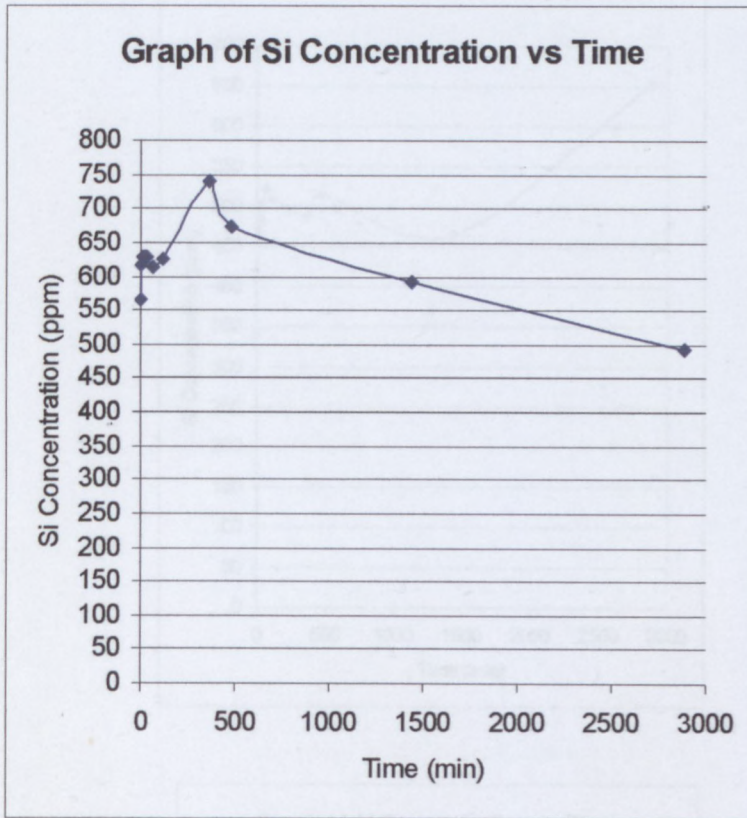




Figure 7.25: Leaching graphs of 36 Sasol

Figure 7.26: Leaching graphs of 36 Sasol (5% farm)

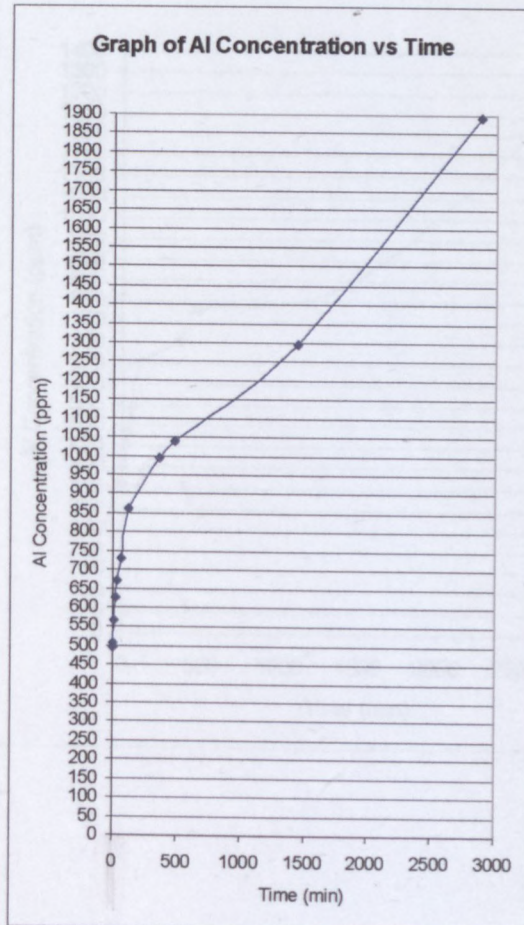
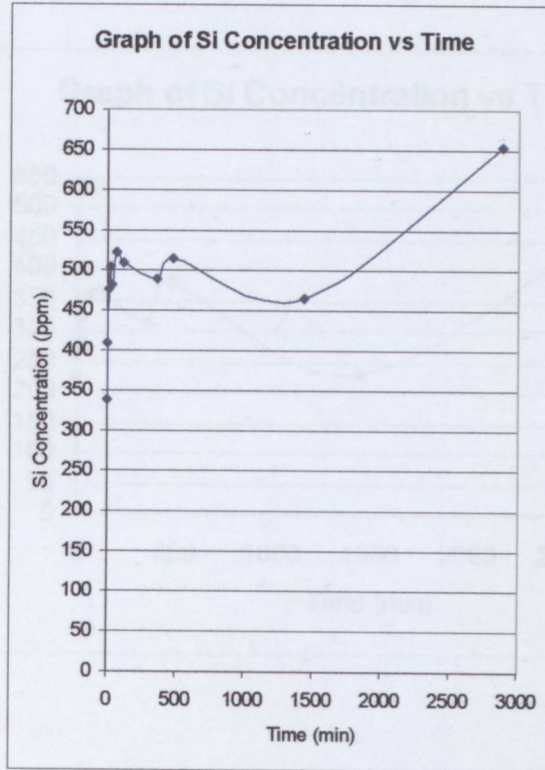


Figure 7.27: Leaching graphs of 36 Sasol (5% NaPi)

Figure 7.26: Leaching graphs of 36 Sasol (5% fzeo)

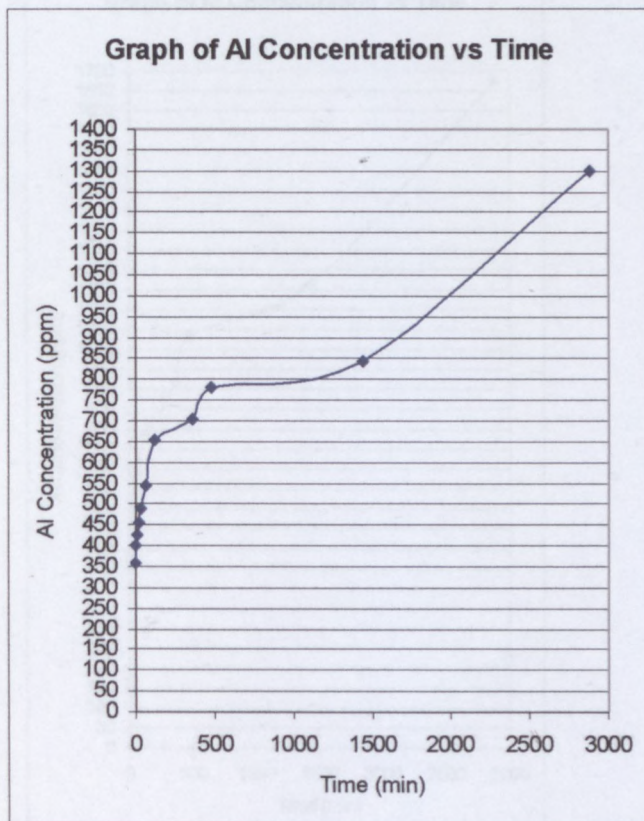
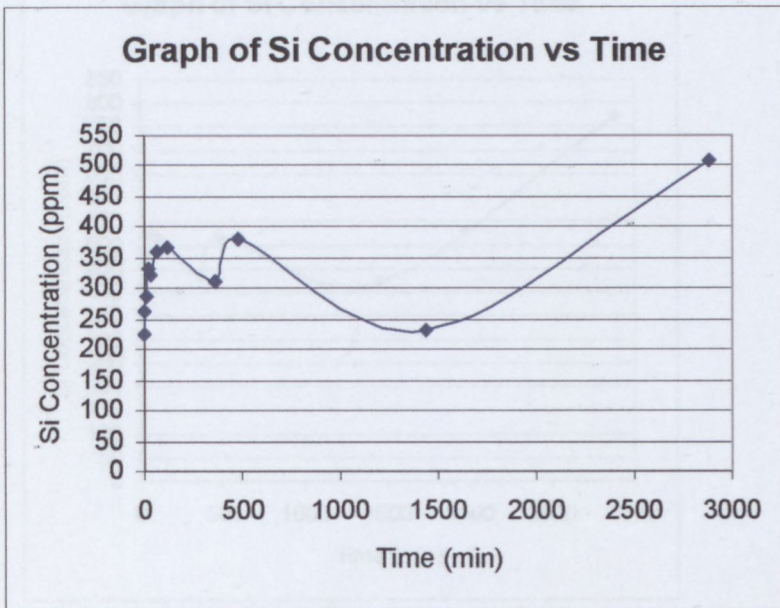


Figure 7.27: Leaching graphs of 36 Sasol (5% zeo NaP1)

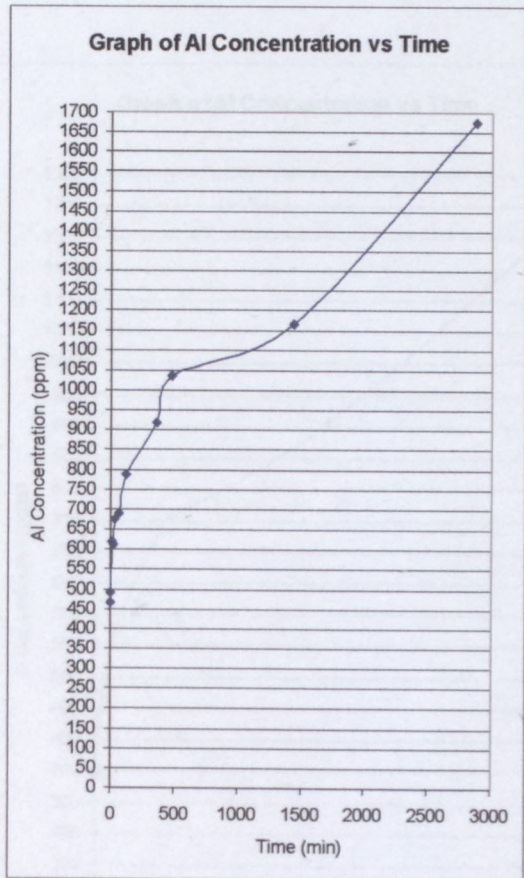
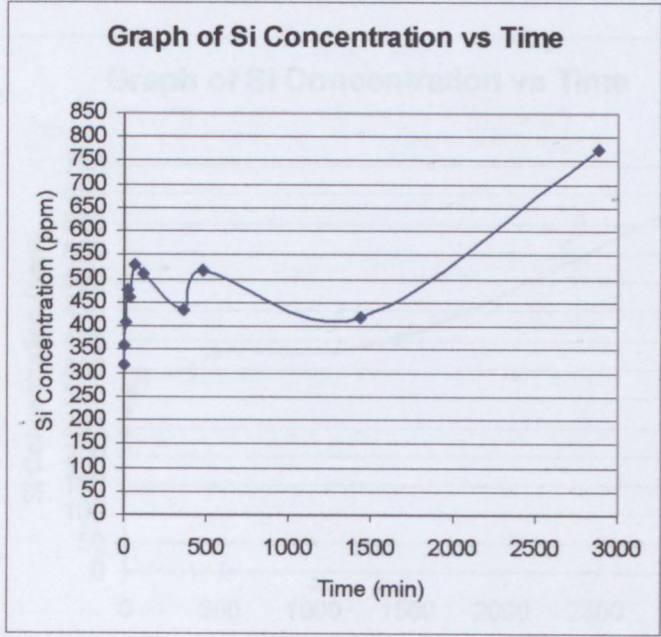
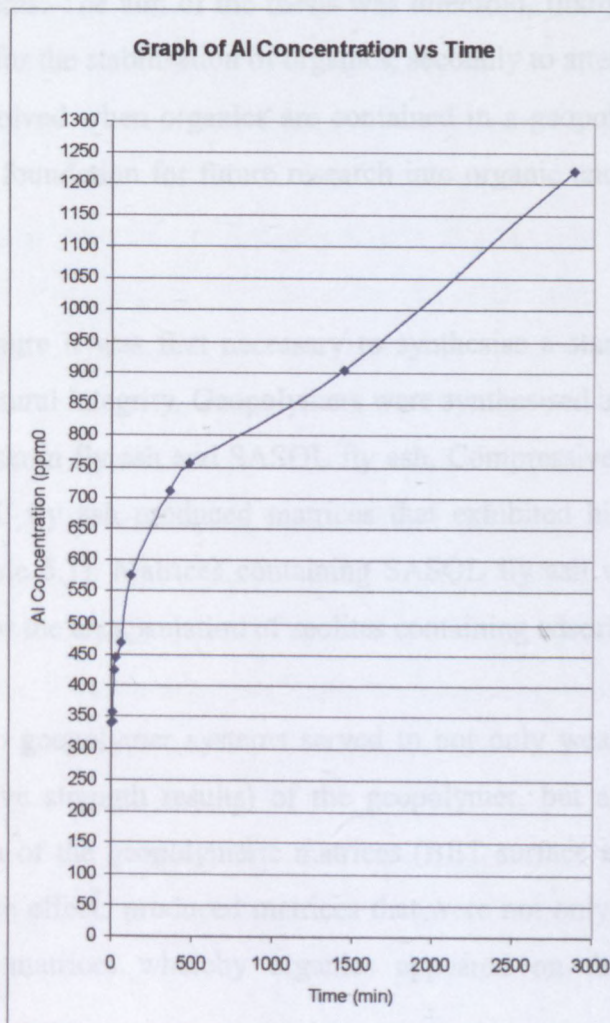
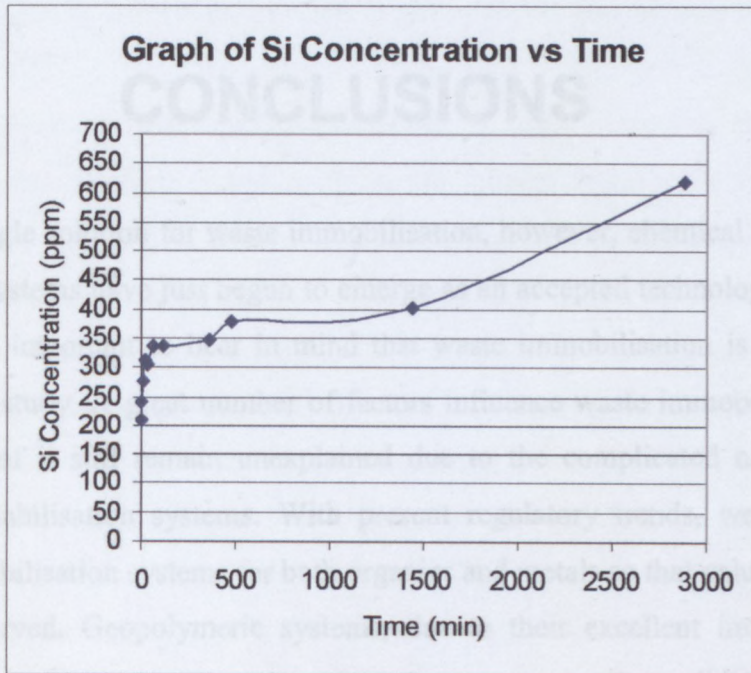


Figure 7.28: Leaching graphs of 36 Sasol (5% czeo)



# Chapter 8

## CONCLUSIONS

There is no single solution for waste immobilisation, however, chemical fixation and solidification systems have just begun to emerge as an accepted technology for waste treatment. It is important to bear in mind that waste immobilisation is a wide and varied field of study. A great number of factors influence waste immobilisation and many aspects of it still remain unexplained due to the complicated nature of the solidification/stabilisation systems. With present regulatory trends, we need even better waste stabilisation systems for both organics and metals so that valuable landfill space is conserved. Geopolymeric systems, due to their excellent immobilisation efficiencies, are gaining increasing attention as versatile solidification and immobilisation systems. The aim of the thesis was threefold, firstly to form a stable geopolymer system for the stabilisation of organics, secondly to attempt to understand the mechanisms involved when organics are contained in a geopolymer system and thirdly to provide a foundation for future research into organic encapsulation within geopolymers.

As a point of departure it was first necessary to synthesise a standard geopolymer matrix that had structural integrity. Geopolymers were synthesised using two different fly ashes, namely Eskom fly ash and SASOL fly ash. Compressive strength analysis showed that SASOL fly ash produced matrices that exhibited higher compressive strength values (Table 5.1). Matrices containing SASOL fly ash were therefore the matrices of choice for the encapsulation of zeolites containing adsorbed organics.

Organic additions to geopolymer systems served to not only weaken the structural integrity (compressive strength results) of the geopolymer, but also decreased the specific surface area of the geopolymeric matrices (BET surface area results, Table 5.11). These negative effects produced matrices that were not only soft and crumbly but also produced matrices whereby organics appeared on the surface of the

geopolymer thus indicating very low immobilisation efficiencies. Structural integrity of a matrix is extremely important as it ensures an extra barrier between the organic waste and the environment. In order to achieve structural integrity an alternative method was utilised in order to encapsulate organics within geopolymer systems.

Synthesised and commercial zeolites were used to adsorb organics from aqueous solutions (Chapter 6). The commercial zeolite, clinoptilolite adsorbed a greater concentration of organics than the synthesised zeolite, zeolite NaP1 (Figure 7.3). The main reason for the greater adsorption by clinoptilolite is that clinoptilolite can be dealuminated to increase its hydrophobicity. Compressive strength analysis of the geopolymer matrix containing 5% czeo shows a slight increase in the strength of the geopolymer matrix compared with that of the standard geopolymer matrix (Table 7.4). Analysis of the specific surface area results of the standard matrix and those containing zeolites, however, showed no significant changes in surface area measurements (Table 7.5).

Zeolites were coated with a layer of geopolymer to decrease the possibility of leaching of the organics from the system. Addition of the coated zeolite to the geopolymer matrix further increased compressive strength of the system (Table 7.4).

A study of the leaching behaviour of the geopolymer matrix containing zeolites with adsorbed organics showed higher concentrations of aluminium than silica being leached from the system (Figures 7.15-7.26). The high concentrations of silica and aluminium being leached from the system points to the fact that a certain degree of matrix breakdown had possibly occurred. The fact that no organics had been leached from the system (if any had leached it would have been <2ppm) indicates that the overall structural integrity of the matrices was still intact. Leaching procedures used in this study were an adaptation of a standard TCLP test. The adapted leaching test was more aggressive than the standard test, indicating that under environmental conditions geopolymers will be an effective medium for organic waste encapsulation.

Also of interest were the numerous analytical tools required to better identify and explain the phenomena that were occurring within the various geopolymer systems. These tools ranged from various fields such as chemistry (IR) to civil engineering

(compressive strength tests). Due to the complicated nature of the system, certain analytical tools had to be used in conjunction with other analytical tools (Chapter 4) to provide an explanation of the reactions that had possibly occurred.

The main objectives of the project were achieved to a certain extent; firstly a stable geopolymer matrix containing coated zeolites with adsorbed organics was synthesised. Secondly the geopolymer exhibited excellent immobilisation qualities when the process detailed in the thesis was followed. These two achievements thus make geopolymers a viable solution to the industrial problem of organic waste. However, it is necessary to point out that this is a complicated system and the mechanisms proposed with regard to organic encapsulation and leaching data were possible suggestions. Further research is therefore necessary to provide a more comprehensive explanation on these two aspects. It is, however, hoped that this project will serve as a foundation for future research into organic encapsulation within geopolymers.

# REFERENCES

- Alberts, C.J. (1996). The immobilisation of inorganic pollutants in fly-ash and other waste components, *M.Eng.-thesis, Department of Chemical Engineering*. Stellenbosch, University of Stellenbosch: 182.
- Barrer, R.M. (1982). *Hydrothermal chemistry of zeolites*, Academic Press.
- Bottero, J.Y., Khatib, F.T., Jucker, K., Bersillon, J.L. and Mallevalle, J. (1994). "Adsorption of atrazine onto zeolites and organoclays, in the presence of background organics." *Wat. Res.* 28: 483-490.
- Breck, D.W. (1974). *Zeolite Molecular Sieves*. London, John Wiley and Sons.
- Chang, H.L. and Shih, W.H. (1998). "A general method for the conversion of fly ash into zeolites as ion exchangers for cesium." *Ind. Eng. Chem. Res.* 37: 71-78.
- Chapman, P.M., Romberg, G.P. and Mortland, M.M. (1982). "Design of monitoring studies of priority pollutants." *J. Water Pollution Control Federation* 36: 125-130.
- Chen, H., Soles, J.A. and Malhotra, V.M. (1993). "Investigations of supplementary cementing material for reducing alkali-aggregate reaction." *Cement and Concrete Composites* 15: 75-83.
- Chestnut, R., Colussi, J.J., Frost, D.J., Keen Jr., W.E. and Raduta, M.C. (1985). U.S. Patent No. 4,514,307.
- Chou, A.C., Eaton, H.C., Cartledge, F.W. and Tittlebaum, M.E. (1988). "A transmission electron microscope study of solidified/stabilized organics." *Hazardous Waste Hazardous Mater.* 5: 145-153.
- Conner, J.R. (1990). *Chemical fixation and solidification of hazardous wastes*. New York, Van Nostrand Reinhold.



- Côte, P.L. (1986). Contaminant leaching from cement-based waste forms under acidic conditions. Ontario, McMaster University.
- Cotton, F.A., Wilkinson, G. and Gaus, P. (1986). *Basic inorganic chemistry*. New York, John Wiley and Sons.
- Cullinane, M.J., Bricka, R.M. and Francingues Jr., N.R. (1987). *An assessment of materials that interfere with stabilisation/solidification processes*. Proc. 13th Annual research Symposium, Cincinnati.
- Davidovits, J. (1994a). "Geopolymers: Inorganic polymeric new materials." *J. Materials Education* 16: 91-139.
- Davidovits, J. (1994b). *Properties of geopolymer cements*. Proceedings First International Conference on Alkaline Cements and Concretes, Ukraine.
- Davidovits, J. (1999a). *Chemistry of geopolymer systems terminology*. Proceedings of the Second International Conference on Geopolymers, France.
- Davidovits, J. (1999b). *Geopolymeric reactions in the economic future of cements and concretes. World-wide mitigation of carbon dioxide emission*. Proceedings of the Second International Conference on Geopolymers, France.
- Davidovits, J., Comrie, D.C., Paterson, J.H. and Ritcey, D.J. (1990). "Geopolymeric concretes for environmental protection." : 30-40.
- Davidovits, J. and Davidovics, J. (1991). "Geopolymer: Ultra-high temperature cooling material for the manufacture of advanced composites." *36th International SAMPE Symposium* 36: 1939-1949.
- Davidovits, J. and Davidovics, M. (1988). "Low temperature geopolymeric setting (LTGS) and archaeometry." *Ceram. Eng. Sci. Proc.* 9: 835-842.

- Dragun, J. (1988). "The fate of hazardous materials in soil." *Hazardous Mater. Control*: 24-43.
- Dragun, J. and Helling, C.S. (1985). *Soil Sci.* 139(2): 100-111.
- Feng, N. and Hao, T. (1998). "Mechanism of natural zeolite powder in preventing alkali-silica reaction in concrete." *Advances in Cement research* 10: 101-108.
- Flaig, W., Beutelspacher, H. and Reitz, E. (1975). *Chemical composition and physical properties of humic substances: in Soil Components*. New York.
- Flanigan, E.M., Khatami, H. and Szymanski, H.A. (1971). *Infrared structural studies of zeolite frameworks*.
- Forss, B. (1983). *Experiences from the use of F - cement - a binder based on alkali - activated blast furnace slag*. Proc. 6th Int. Conf. Alkaline Concr.
- Franklin, K.R., Hunt, R.R. and Williams, C.D. (1988). "Sorption of butan-1-ol from aqueous solution by silica molecular sieves." *Zeolites* 8: 432-435.
- Grutzeck, M.W. and Hoyle, S.L. (1989). "Incorporation of cesium by hydrating calcium aluminosilicates." *J. Am. Ceram. Soc.* 72: 1938-1947.
- Gutierrez, B., Pazos, C. and Coca, J. (1993). "Characterisation and leaching of coal fly ash." *Waste Manag. Res.* 11: 279-286.
- Hesse, P.R. (1972). *A textbook of soil chemical analysis*. New York, Chemical Publishing Company.
- Iler, R.K. (1979). *The chemistry of silica*. New York, John Wiley and Sons.
- Kruger, R.A. (1990). "The chemistry of fly ash and the pozzolanic reaction." *ChemSA* 16(11): 16-19.

- Kuwahara, M., Shindo, N. and Munakata, K. (1970). "The photochemical reaction of pentachlorophenol." *J. Agric. Chem. Soc. Jpn.* 44: 169-174.
- LaRosa, J.L., Kwan, S. and Grutzeck, W. (1992). "Zeolite formation in Class F fly ash blended cement pastes." *J. Am. Ceram. Soc.* 75: 1574-1580.
- Lyon, R.E., Foden, A.J., Balaguru, P., Davidovits, J. and Davidovics, M. (1999). *Properties of GEOPOLYMER-MATRIX-Carbon Fiber Composites*. Proceedings of the Second International Conference on Geopolymers, France.
- Mabey, W. and Mill, T.J. (1978). "Data." *J. Phys. Chem. Ref.* 17: 383.
- Meier, W.M. and Olson, D.M. (1971). "Zeolite frameworks. Molecular sieve zeolites." *Advan. Chem. Ser.* 101: 155-170.
- Milestone, N.B. and Bibby, D.M. (1981). "Concentration of alcohol on silicalite." *J. Chem. Technol. Biotechnol.* 31: 732-736.
- Narita, E., Horiguchi, N. and Okabe, T. (1985). "Adsorption of phenol benzyl alcohol from aqueous solutions by silicalite." *Chem Lett.* xxx: 787.
- Pienaar, J. (1999). Degradation characterisation of various geo-chemical matrices during leaching, *M.Eng.-thesis, Department of Chemical Engineering*. Stellenbosch, Univeristy of Stellenbosch: 192.
- Querol, X., Alastuey, A., Fernandez-Turiel, J. and Lopez-Solar, A. (1995). "Synthesis of zeolites by alkaline activation of ferro-aluminous fly ash." *Fuel* 74: 1226.
- Querol, X., Alastuey, A., Lopez-Solar, A., Andres, J.M., Juan, R., Ferrer, P. and Ruiz, C.R. (1997b). "A fast method for recycling fly ash: microwave-assisted zeolite synthesis." *Environ. Sci. Technol.* 31: 2527-2533.
- Querol, X., Plana, F., Alastuey, A. and Lopez-Solar, A. (1997a). "Synthesis of Na-zeolites from fly ash." *Fuel* 76: 793-798.

- Rahier, H., Simons, B., Biesemans, M. and Van Mele, B. (1997). "Low-temperature synthesized aluminosilicate glasses: Part III Influence of the composition of the silicate solution production, structure and properties." *J. Mat. Sci.* 32: 2237-2247.
- Shriver, D.F., Atkins, P.W. and Langford, C.H. (1990). *Inorganic chemistry*, Oxford University Press.
- Shu, H.-T., Li, D., Scala, A.A. and Ma, Y.H. (1997). "Adsorption of small organic pollutants from aqueous streams by aluminosilicate-based microporous materials." *Separation and Purification Technology* 11: 27-36.
- Singer, A. and Bergaut, V. (1995). "Cation exchange properties of hydrothermally treated coal fly ash." *Environ. Sci. Technol* 29: 1748-1753.
- Swamy, R.N. (1986). *Cement replacement materials*, Blackie and Son Ltd.
- Theng, B.K.G. (1974). *The chemistry of clay-organo reactions*. London, Adam Hilger.
- Thomas, M.D., Blackwell, B.Q. and Nixon, P.J. (1996). "Estimating the alkali contribution from fly ash to expansion due to alkali-aggregate reaction in concrete." *Magazine of Concrete Research* 48: 251-264.
- U.S.Government (1990). Toxicity characteristic leaching procedure (TCLP). *Federal Register*. United States. 55: 11798 - 11877.
- Van Jaarsveld, J.G.S. (2000). The physical and chemical characterisation of fly ash based geopolymers, *Ph.D. thesis, Department of Chemical Engineering*. Melbourne, Australia, University of Melbourne, Australia: 381.
- Van Jaarsveld, J.G.S., Van Deventer, J.S.J. and Lorenzen, L. (1996). *Immobilisation of toxic metals in geopolymers*. Proceedings of Chemeca 96: 24th Australian and New Zealand Chemical Engineering Conference., Sydney, Australia.

- Van Jaarsveld, J.G.S., Van Deventer, J.S.J. and Lorenzen, L. (1997). "The potential use of geopolymeric materials to immobilise toxic metals: Part I Theory and Applications." *Min. Eng.* 10(7): 659-669.
- Van Jaarsveld, J.G.S., Van Deventer, J.S.J. and Lorenzen, L. (1998). "Factors affecting the immobilisation of metals in geopolymerised fly ash." *Met. Mat. Trans. B* 29: 283 - 291.
- Van Zyl, R.L. (1997). The immobilisation of heavy metal ions in metallurgical waste, *M.Eng.-thesis, Department of Chemical Engineering*. Stellenbosch, University of Stellenbosch: 260.
- Wang, T.S., Li, S.W. and Ferng, Y.L. (1978). "Catalytic polymerisation of phenolic compounds by clay minerals." *Soil Sci* 126: 15-21.
- Woolard, C.D., Petrus, K. and Van der Horst, M. (2000). The use of a modified fly ash as an adsorbent for lead. Port Elizabeth, Department of Chemistry, University of Port Elizabeth.
- Xu, G.J., Watt, D.F. and Hudec, P.P. (1995). "Effectiveness of mineral admixtures in reducing ASR expansion." *Cement and Concrete Research* 25: 1225-1235.
- Xu, H. and Van Deventer, J.S.J. (2000). "The geopolymerisation of aluminosilicate minerals." *Int. J. Miner. Process* 59: 247-266.
- Yang, S., Vlessidis, A.G. and Evmiridis, N.P. (1997). "Influence of gel composition and crystallisation conditions on the conventional synthesis zeolites." *Ind. Eng. Chem. Res.* 36: 1622-1631.